AN EXPLICIT METHOD FOR THE ANALYSIS OF TRANSIENT COMPRESSIBLE FLOW IN PIPE NETWORKS

Frederick Botha

B.Eng. (Mechanical)

B.Sc. (Mathematics and Applied Mathematics)

Thesis submitted in partial fulfilment of the requirements for the degree

Magister Scientiae (Engineering)

School of Mechanical and Materials Engineering

at

Potchefstroom University for Christian Higher Education

Supervisor: Prof. GP Greyvenstein

Potchefstroom

2003

Abstract

This thesis deals with the development of an explicit pipe network analysis code for the benchmarking of Flownet. Flownet is a general-purpose thermal-fluid network analysis code used as a tool in the design of the Pebble Bed Modular Reactor. The National Nuclear Regulator (NNR) requires the use of benchmarks to verify and validate such a design code. RELAP5 was selected as an additional commercial code to benchmark Flownet.

Various benchmark cases were identified to determine the validity of specific models and components. Some of the models or components validated include pipes, boundary conditions, heat transfer, non-inertial elements and junctions. Comparisons were also done to validate the integrated use of these components in an arbitrary structured pipe network. For virtually all steady-state flow cases, Flownet compared very well with analytical results. Only for isothermal flow at high Mach numbers were some differences noted. Some anomalies were identified with the use of RELAP5.

Comparisons between the three codes for transient flow were very favourable, except for cases were the anomalies in RELAP5 came into play. For these cases Flownet and Lax-Wendroff still compared very well. The only noteworthy anomaly for transient flow was found when solving total temperature at pipe boundaries. This anomaly was only found at boundaries with a combination of little or no flow and sharp pressure transients. A difference in boundary modelling between Flownet and Lax-Wendroff is most likely the cause of this difference. This localized effect had virtually no impact on the solution elsewhere in the network.

Upon successful completion of the selected benchmark cases, one can conclude that Flownet uses a valid implementation of the basic components tested. Further, these models are also integrated in a way that enables valid modelling of complex pipe networks.

Uittreksel

Hierdie tesis handel oor die ontwikkeling van 'n eksplisiete analisekode vir pypnetwerke wat gebruik is in 'n vergelykende studie met Flownet. Flownet is 'n meerdoelige analisekode vir termo-vloei netwerke wat aangewend word in die ontwerp van die PBMR (Pebble Bed Modular Reactor). Die NNR (National Nuclear Regulator) vereis dat ontwerpkodes soos Flownet met ander kodes vergelyk word om die ontwerpkode te verifieer en te valideer. RELAP5 is 'n kommersiële kode wat ook as deel van die studie met Flownet vergelyk is.

In hierdie vergelykende studie is verskeie toetsgevalle geïdentifiseer om verskeie modelle en komponente in Flownet te valideer. Pypmodelle, randwaardes, hitte-oordrag, nie-inersiële elemente en vloei-interseksies is van die aspekte wat gevalideer is. Die integrasie van hierdie komponente is gevalideer deur resultate van 'n arbitrêr gestruktueerde netwerk te vergelyk. Gestadigde resultate in Flownet het baie goed met analitiese resultate vergelyk. Verskille is wel gevind vir isotermiese vloei by hoë Mach-getalle. Vir gestadigde resultate is daar beduidende verskille tussen RELAP5 en analitiese resultate gevind.

Behalwe vir gevalle waar die anomalieë in RELAP5 'n invloed gehad het, het die drie kodes baie goed vergelyk vir transiënte vloei. In hierdie gevalle het Flownet en Lax-Wendroff steeds goed vergelyk. Die enigste beduidende verskille tussen die twee kodes is waargeneem in die temperatuuroplossing vir randwaardes. Hierdie verskille is slegs waargeneem by skerp druktransiënte tesame met lae massavloei op die rand van pypelemente. Die oorsaak is heel waarskynlik die verskillende wyses waarop randwaardes hanteer word in Flownet en Lax-Wendroff. Hierdie verskil het feitlik geen invloed op resultate elders in die netwerk gehad nie.

Uit die suksesvolle voltooiing van die geselekteerde toetsgevalle kan 'n mens aflei dat Flownet 'n geldige implementering van die basiese komponente gebruik. Verder is die wyse waarop hierdie modelle geïntegreer is, geldig vir die modellering van komplekse pypnetwerke.

Acknowledgements

I would not have been able to complete or even start this work without the assistance and encouragement of others. During this study my family and friends were tremendously supportive. I will be able to improve on a lot, but definitely not on my family and friends. Thank you, Gideon, for your patient guidance and the invaluable lessons learnt. You have contributed to me far more than required for this thesis. My colleagues at PBMR gave me sufficient time off, a definite necessity.

To the only wise God, our Saviour, be glory and majesty
and might and authority, even now and forever!
(Jude 25, Modern King James Version)

Table of Contents

Abstract ii

Uittreksel iii

Acknowledgements iv

Table of Contents v

List of Figures viii

List of Tables x

Nomenclature xi

Acronyms xii

CHAPTER ONE: INTRODUCTION 1

1.1 Introduction 1

1.2 Background 2

1.3 Modelling approaches 5

1.4 Objective of this study 7

1.5 Layout of this study 7

CHAPTER TWO: LITERATURE SURVEY 9

2.1 Introduction 9

2.2 Historical background 9

2.3 Characterization of methods 11

2.4 Explicit methods 12

2.5 Commercial codes 15

2.6 Conclusion 17

CHAPTER THREE: THE TWO-STEP LAX-WENDROFF METHOD 18

3.1 Introduction 18

3.2 Partial differential equations 18

3.3 The standard two-step Lax-Wendroff method 20

3.4 Method based on total pressures 23

3.5 Implementation of boundary conditions 25

3.6 Non-inertial elements 27

3.7 Junctions and tanks 29

3.8 Conclusion 32

CHAPTER FOUR: COMPARATIVE STUDY FOR DIFFERENT PIPE FLOW SCENARIOS 33

4.1 Introduction 33

4.2 Structure of the validation process 33

4.3 Steady-state flow in a pipe element 34

4.4 Steady-state flow through an orifice 44

4.5 Slow transients between tanks 48

4.6 Fast transients in a pipe 51

4.7 Fast transients through an orifice 57

4.8 Effect of discretization 60

4.9 Conclusion 64

CHAPTER FIVE: COMPARATIVE STUDY FOR ARBITRARY STRUCTURED NETWORKS ... 65

5.1 Introduction 65

5.2 Slow transient through a junction 65

5.3 Fast transient through a junction 68

5.4 Steady-state flow in a complex network 70

5.5 Transient flow in a complex network 73

5.6 Conclusion 79

CHAPTER SIX: CONCLUSION AND RECOMMENDATIONS 80

6.1 Introduction 80

6.2 Perspective on this study 80

6.3 Validation of individual models and components 81

6.4 Validation of model and component integration 81

6.5 Recommendations for further work 82

REFERENCES 83

APPENDIX A: DERIVATION OF DIFFERENTIAL EQUATIONS 87

A.1 Introduction 87

A.2 Continuity 87

A.3 Momentum conservation 89

A.4 Energy conservation 93

A.5 Proof of theorem for compressible gas flow 94

APPENDIX B: COMMERCIAL CODE QUESTIONNAIRE 97

B.1 Introduction 97
B.2 Information obtained from web sites and questionnaires 98
APPENDIX C: RELATIONS FOR TOTAL PRESSURE BOUNDARIES 111
C.1 Introduction 111
C.2 Total pressure as a function of ρV 111
APPENDIX D: ANALYTICAL METHOD FOR STEADY-STATE FLOW IN PIPES 114
D.1 Introduction 114
D.2 Solution methodology of the analytical method 114
D.3 EES implementation of the analytical method 116

List of Figures

Figure 1.1: *Schematic representation of the PBMR Brayton cycle.* 2

Figure 1.2: *PBMR network on Flownet.* 4

Figure 3.1: *Time space discretization of the Two-step Lax-Wendroff method.* 20

Figure 3.2: *Time space discretization at boundary node.* 25

Figure 3.3: *Junction with discretized and non-inertial elements in Flownet.* 29

Figure 3.4: *Effect of junction model on pipe transient – 20 increments.* 31

Figure 3.5: *Effect of junction model on pipe transient – 80 increments.* 32

Figure 4.1: *Mach number vs. pipe position for different L/D values.* 36

Figure 4.2: *Total pressure drop vs. mass flow for $L/D = 10$.* 38

Figure 4.3: *Total pressure drop vs. exit Mach number for $L/D = 10$.* 38

Figure 4.4: *Total pressure drop vs. mass flow for $L/D = 100$.* 40

Figure 4.5: *Total pressure drop vs. exit Mach number for $L/D = 100$ - Plot 1.* 41

Figure 4.6: *Total pressure drop vs. exit Mach number for $L/D = 100$ - Plot 2.* 41

Figure 4.7: *Total pressure drop vs. mass flow for $L/D = 1000$.* 43

Figure 4.8: *Total pressure drop vs. exit Mach number for $L/D = 1000$ - Plot 1.* 43

Figure 4.9: *Total pressure drop vs. exit Mach number for $L/D = 1000$ - Plot 2.* 44

Figure 4.10: *Pipe geometry for orifice validation.* 45

Figure 4.11: *Mach number at orifice inlet and outlet vs. loss factor.* 46

Figure 4.12: *RELAP5 total temperature at orifice inlet and outlet.* 47

Figure 4.13: *Total pressure at orifice inlet and outlet vs. loss factor.* 47

Figure 4.14: *Slow transient between two tanks.* 48

Figure 4.15: *Total pressure variation during slow transient.* 49

Figure 4.16: *Total temperature variation during slow transient.* 49

Figure 4.17: *Mach number variation during slow transient.* 50

Figure 4.18: *Fast transient for adiabatic flow in a pipe, result at $x = L$.* 52

Figure 4.19: *Fast transient for adiabatic flow in a pipe, results at $x = 0.5\,L$* 52

Figure 4.20: *Pipe fast transient with positive heat transfer, results at $x = 0.5\,L$.* 53

Figure 4.21: *Pipe fast transient with positive heat transfer, result at $x = L$.* 54

Figure 4.22: *Pipe fast transient with negative heat transfer, result at $x = L$.* 54

Figure 4.23: *Pipe fast transient with negative heat transfer, results at* $x = 0.5\,L$ 55
Figure 4.24: *Fast transient for isothermal flow in a pipe, result at* $x = L$ 56
Figure 4.25: *Fast transient for isothermal flow in a pipe, results at* $x = 0.5\,L$ 56
Figure 4.26: *Transient flow through an orifice, result at* $x = L$ 58
Figure 4.27: *Transient flow through an orifice, result at orifice outlet.* 58
Figure 4.28: *Transient flow through an orifice, result at orifice inlet.* 59
Figure 4.29: *Required discretization at different Mach numbers.* 61
Figure 4.30: *Deviation between grid independent and grid-sensible solutions.* 62
Figure 4.31: *A grid-sensible solution at different Mach numbers.* 63
Figure 5.1: *Flownet network for quasi-steady blow down.* 65
Figure 5.2: P_0 *vs. time for quasi-steady blow down.* 66
Figure 5.3: T_0 *vs. time for quasi-steady blow down.* 67
Figure 5.4: *Mass flow vs. time for quasi-steady blow down.* 67
Figure 5.5: *Flownet network for transient flow through a junction.* 68
Figure 5.6: P_0 *and* T_0 *vs. time for transient junction network – Node 3.* 69
Figure 5.7: P_0 *and* T_0 *vs. time for transient junction network – Node 4.* 69
Figure 5.8: *Mass flow vs. time for transient junction network.* 70
Figure 5.9: *Flownet arbitrary structured network.* 71
Figure 5.10: *Total pressure and total temperature at Node 11.* 74
Figure 5.11: *Total pressure and total temperature at Node 1.* 74
Figure 5.12: *Total pressure and total temperature at Node 12.* 75
Figure 5.13: *Total pressure and total temperature at Node 13.* 75
Figure 5.14: *Total pressure and total temperature at Node 14.* 76
Figure 5.15: *Total pressure and total temperature at Node 15.* 76
Figure 5.16: *Total pressure and total temperature at Node 16.* 77
Figure 5.17: *Total pressure and total temperature at Node 17.* 77
Figure 5.18: *Mass flow through Pipe 8.* 78
Figure 5.19: *Mass flow through orifice.* 78

List of Tables

Table 2.1: *List of software to model transient compressible flow.* 16
Table 4.1: *Components tested as part of validation.* 34
Table 4.2: *Steady-state input data for Mach number vs. pipe position plot.* 35
Table 4.3: *Steady-state input data for* $L/D = 10$. 39
Table 4.4: *Steady-state solution time for* $L/D = 10$. 39
Table 4.5: *Steady-state input data for* $L/D = 100$. 40
Table 4.6: *Steady-state solution time for* $L/D = 100$. 42
Table 4.7: *Steady-state input data for* $L/D = 1\,000$. 42
Table 4.8: *Steady-state solution time for* $L/D = 1\,000$. 44
Table 4.9: *Loss factors for validation of orifice model.* 45
Table 4.10: *Solution time for slow transient between tanks.* 50
Table 4.11: *Steady-state input data for transient flow in pipes.* 51
Table 4.12: *Solution time for transients in pipes.* 57
Table 4.13: *Solution time for transient flow through an orifice.* 60
Table 4.14: *Boundary conditions used in steady-state grid analysis.* 60
Table 4.15: *Nodes required to stay within 1% of analytical solution.* 61
Table 4.16: *Boundary conditions used in transient grid analysis.* 63
Table 5.1: *Input to quasi-steady blow down network.* 66
Table 5.2: *Steady-state initial results for quasi-steady blow down.* 66
Table 5.3: *Input to transient junction network.* 68
Table 5.4: *Steady-state initial results for transient junction network.* 68
Table 5.5: *Input to arbitrary structured network.* 72
Table 5.6: *Steady-state initial results for arbitrary structured network.* 72

Nomenclature

μ	Viscosity [kg/m.s]
ρ	Density [kg/m^3]
θ	Angle of the pipe with the horizontal
A	Area [m^2]
c	Acoustic velocity [m/s]
c_p	Constant pressure specific heat [J/kg.K]
c_v	Constant volume specific heat [J/kg.K]
D	Diameter [m]
e	Pipe roughness [μm]
f	Darcy Weisbach friction factor
g	Gravitational acceleration [kg.m/s^2]
G	Mass flow per unit area [kg/s.m^2]
h	Enthalpy [J/kg.K]
h_0	Total enthalpy [J/kg.K]
k	Loss factor
L	Pipe length [m]
m	Mass flow [kg/s]
M	Mach number
p	Static pressure [kPa]
p_0	Total pressure [kPa]
$\dot{q}$	Heat transfer per unit volume [W/m^3]
R	Gas constant [J/kg.K]
t	Time [s]
T	Static temperature [K] or [°C]
T_0	Total temperature [K] or [°C]
u	Internal energy [J/kg.K]
u_0	Total internal energy [J/kg.K]
V	Velocity [m/s]
x	Spatial coordinate in length of pipe
z	Vertical position [m]

Acronyms

Acronym	Description
CFD	Computational Fluid Dynamics
CHT	Convective Heat Transfer
CS	Control Surface
CV	Control Volume
EES	Engineering Equation Solver
ENO	Essentially Non-oscillatory
FCT	Flux Correct Transport
HPC	High-pressure Compressor
HPT	High-pressure Turbine
HTGR	High-temperature Gas-cooled Reactor
IPCM	Implicit Pressure Correction Method
L/D	Length/Diameter (ratio)
LPC	Low-pressure Compressor
LPT	Low-pressure Turbine
MOC	Method of Characteristics
MUSCL	Monotic Upstream-centred Scheme for Conservation Laws
n/a	Not Applicable,
NNR	National Nuclear Regulator
NR	Not Relevant
NRC	Nuclear Regulatory Commission (USA)
PBMR	Pebble Bed Modular Reactor
PCU	Power Conversion Unit
PPM	Piecewise Parabolic Method
PT	Power Turbine
PU for CHE	Potchefstroom University for Christian Higher Education
TVD	Total Variation Diminishing

CHAPTER ONE: INTRODUCTION

1.1 Introduction

Pipe networks are found in a wide variety of engineering applications, and play an important role in these applications. In general, a pipe network can be described as a number of pipes or flow conduits connected in an arbitrary manner. This field has, however, developed to far more than just the modelling of pipes connected in this fashion. Various other component models can now also be implemented in such a network.

Water distribution networks were one of the earliest applications that typified pipe networks. Modern day examples of such networks include air-conditioning systems, internal combustion engines, city gas pipe networks, and networks in the chemical processing industry. In some complex air-conditioning system, three separate pipe networks can be identified for the water, air and refrigerant parts of the system.

'Thermal-fluid networks' is probably a more descriptive term for such networks. The modelling of many additional components has been included to analyse the dynamic response of very complex systems. Fluid dynamic, thermal and control aspects of, for example, a complete power station, can now be modelled.

Numerical methods used to model pipe networks are still fundamental to the modelling of more general thermal-fluid networks. A vast amount of research has been done in this field and numerous modelling approaches have been developed. Research in this field is often focused at improving the speed, accuracy and stability of the modelling approach. Current techniques still leave room for improvement.

In this study, an explicit method is implemented to model transient compressible flow in such networks. This implementation is then used as part of the verification and validation process for a thermal-fluid network modelling tool used in the design of the PBMR.

1.2 Background

1.2.1 The Pebble Bed Modular Reactor (PBMR)

The PBMR is a new type of inherently safe nuclear reactor being developed by Eskom. It is a High-temperature Gas-cooled Reactor (HTGR) operating on a closed, recuperative Brayton cycle with helium as the working fluid. This system, with all its components interacting with the working fluid, is classified as a thermal-fluid network as defined in the context of this study.

Some of the components in the PBMR include compressors, turbines, heat exchangers, valves and the reactor. The use of a thermal-fluid network simulation code in the design of such a complex system holds definite advantages. With such as a simulation code, the dynamic response of the system can be analysed. Components can then be designed to attain the desired dynamic system response.

Figure 1.1 shows a basic representation of the PBMR Brayton cycle as described in PBMR Safety Analysis Report, Chapter 3.4 (Botha, 2001:7).

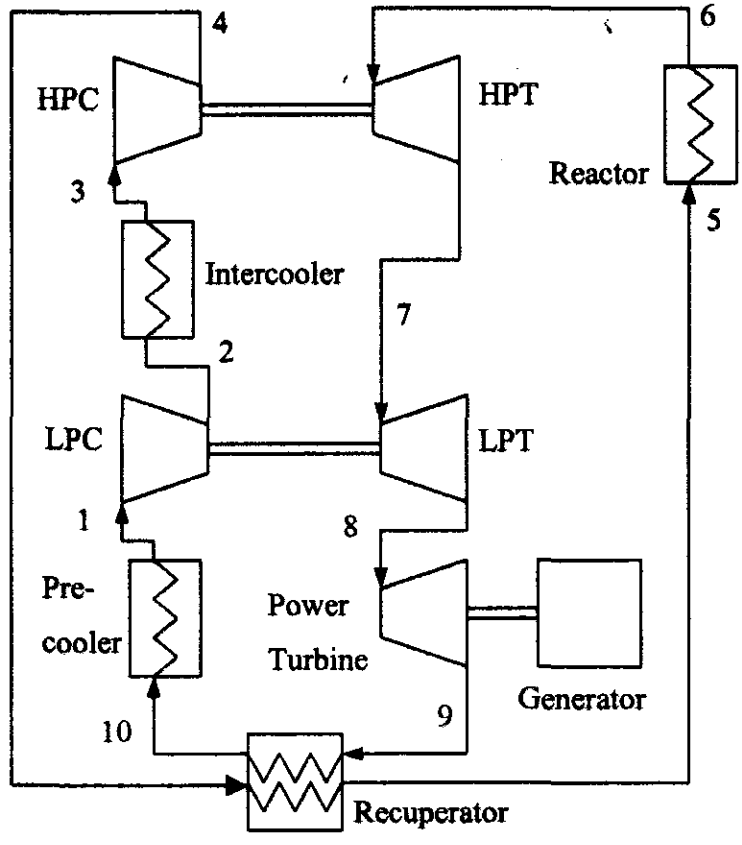


Figure 1.1: *Schematic representation of the PBMR Brayton cycle.*

Starting at 1 in Figure 1.1, helium at a relatively low pressure and temperature (1) is compressed by a Low-Pressure Compressor (LPC) to an intermediate pressure (2), after which it is cooled in an intercooler to state 3. A High-pressure Compressor (HPC) then compresses the helium to state 4. From 4 to 5, the helium is preheated in the recuperator before entering the reactor, which heats the helium to state 6. After the reactor, the hot high-pressure helium is expanded in a High-pressure Turbine (HPT) to state 7, after which it is further expanded in a Low-pressure Turbine (LPT) to state 8. The HPT drives the HPC while the LPT drives the LPC. After the LPT, the helium is further expanded in the Power Turbine (PT) to pressure 9, which is approximately the same as the pressure at 10 and 1. From 9 to 10, the still hot helium is cooled in the recuperator, after which it is further cooled in the pre-cooler to state 1. This completes the cycle. The heat rejected from 9 to 10 is equal to the heat transferred to the helium from 4 to 5.

At the end of 1998, a thermal-fluid network simulation code, Flownet, was selected for the thermo-hydraulic design of the PBMR's Power Conversion Unit (PCU). Since then, the software has been extended to include additional features needed as part of the design process.

1.2.2 Flownet

Flownet is a one-dimensional thermal-fluid network simulation code written in Visual C++. M-Tech Industrial developed the code in collaboration with the School of Mechanical and Materials Engineering at the Potchefstroom University for Christian Higher Education (PU for CHE). It uses an implicit solution method developed by Greyvenstein (2002:1127). This method is referred to as the Implicit Pressure Correction Method (IPCM), and is similar to the SIMPLE algorithm in Computational Fluid Dynamics (CFD). This method is suitable for steady-state and transient flow. A comprehensive description of Flownet can be found in the code manual (Coetzee et al., 2003)

Components such as pipes, ducts, orifices, pumps, fans, heat exchangers and free-running compressor-turbine pairs can all be modelled in Flownet. Other features in Flownet include the ability to solve pipe networks with compressible and incompressible flow, as well as the capability to model heat transfer.

Figure 1.2 shows the network representation of the PBMR in Flownet.

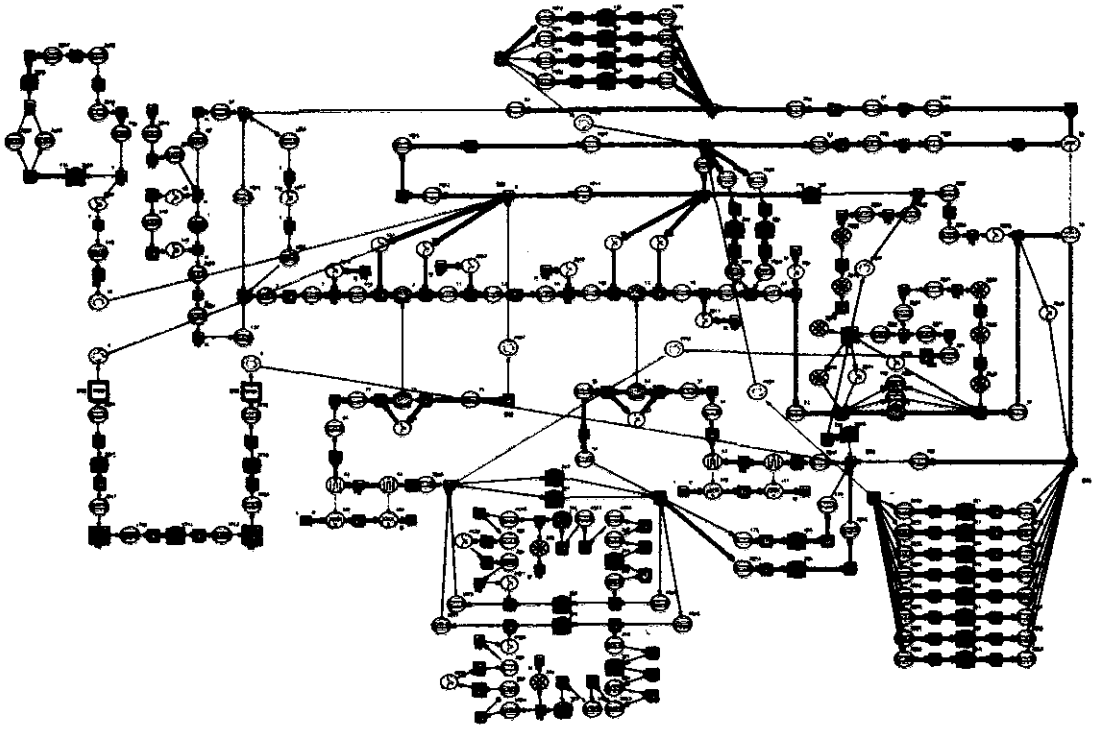


Figure 1.2: *PBMR network on Flownet.*

1.2.3 Verification and validation required for quality assurance

As part of its regulatory process, the National Nuclear Regulator (NNR) requires Eskom to show that the PBMR design is safe and feasible. This implies that prior to the construction of the prototype, Eskom must be able to show that the system will operate as it was designed to do. With Flownet as a major design tool in this process, the accuracy of the results produced by this code is imperative. Sufficient proof must therefore be presented to confirm this accuracy.

As with any software simulation code, verification and validation play a crucial role in the reliability of Flownet. In this context, validation can be seen as the evidence that demonstrates that the analysis tool is fit for its purpose (NNR, 2001:4). This implies showing that Flownet gives accurate results when modelling typical systems. Verification is defined as the process of ensuring that the governing physical equations have been correctly translated into computer code. Validation is of no consequence without verification. However, if the governing physical equations are applicable and their implementation verified, this implies some measure of validation.

In the context of this study, verification and validation will be called validation in short.

As part of validation, the NNR requires the use of benchmarks to validate a code (2001:4). Analytical solutions to benchmark problems are often used in this regard. However, only a restricted number of simple problems have analytical solutions. For more complex problems, other codes are used as benchmarks. These codes should use independently developed methods that differ from the code being validated.

1.3 Modelling approaches

Pipe networks are usually modelled assuming the flow is one-dimensional in a given pipe cross-section. This implies that the velocity, pressure and other fluid properties across a section of the pipe are equal to their respective average values. One might argue that necessary detail is then lost. However, when modelling the dynamics of large complex networks, such detail is of lesser importance. The interaction of the components and overall system characteristics are of far greater value. By only considering change in fluid properties in the flow direction, the method is known as a one-dimensional method.

Most of the one-dimensional modelling approaches can be classified as finite volume, finite difference or finite element methods. Ferziger and Peric (1999:35) give a good overview of these methods. In this study, only finite volume and finite difference methods are considered. For both methods the objective is to approximate partial differential conservation equation with algebraic equations. Variables in these algebraic equations describe the flow at discrete points in space and time (nodes).

Finite difference methods use the differential form of the conservation equations. The solution domain is covered with a grid of nodes. Differentials are approximated by the change in variables between adjacent nodes. For *finite volume methods*, an integral form of the conservation equations is used. The solution domain is subdivided into a finite number of volumes. At the centre of each volume lies a node at which flow variables are solved. By applying the conservations equations over each of these discrete volumes, a set of algebraic equations is derived.

For finite difference and volume methods, variables at a new time step are written as a function of variables at the previous time step and variables at adjacent nodes. If the adjacent conditions used in the algebraic function are the known values from the previous time step, an *explicit method* results. Because known values are used in the algebraic equation, next time step values are calculated directly. When the yet unknown adjacent conditions of the new time step are used in the algebraic equation, an *implicit method* results. For every unknown variable at the new time step, there then exists an algebraic equation with unknown adjacent variables. A set of non-linear equations with equal unknowns and equations is formed in this way. A solution is then obtained for each time step by solving this set of equations.

One can also use a weighted average of values at the current and next time step. A *semi-implicit* method then results, but a simultaneous solution of values at the next time step is still required. In Flownet, this weighted average is defined using a Crank-Nicolson parameter. A value of 1 implies a fully implicit scheme. The 0.5 value case implies an equally weighted average. Such a scheme is called a Crank-Nicolson scheme, and is second-order accurate in time (Versteeg & Malalasekera, 1998:173). Experience has shown that a value of 0.6 gives acceptable results in Flownet (Van Ravenswaay, 1998:119). Lower values can lead to spurious oscillations and even instability.

Explicit methods generally require less computational time per time step. This is useful when a transient solution is desired where a lot of small time steps are necessary. There is, however, a limitation on the size of a time step for these methods. A Courant number smaller than unity is required (Ferziger & Peric, 1999:138). Courant number is defined as the ratio of time step Δt to the characteristic convection time $|V \pm c|/\Delta x$ (Ferziger & Peric, 1999:136 & 310). Characteristic convection time is the time it takes for a disturbance to be convected a distance Δx. Implicit methods, on the other hand, have no inherent limitation on time step.

One way of obtaining a steady-state solution is by taking large time steps until the solution of consecutive time steps converges. Large time steps tend to smooth transient effects in implicit methods, but this is unimportant when a steady-state solution is the objective. This smoothing or smearing of transient flow is also known as dissipation. With larger time steps, implicit methods take fewer steps and generally

less time to obtain a steady-state solution. When a lot of small time steps are taken to calculate a transient solution, an explicit method will generally use less computational time. Such small time steps are only required when larger implicit time steps will result in unacceptable dissipation.

Using three-dimensional CFD codes is another approach that is used in the design of complex networks. A detail flow field is then solved in every part of the network. Modelling this additional detail is orders of magnitude more computationally intensive. This approach is therefore impractical for the modelling of the transient response of thermal-fluid systems such as the PBMR. CFD often plays a crucial role in the application of one-dimensional thermal network simulation codes. Components can be modelled more accurately in one dimension by characterization in three dimensions with the use of CFD.

1.4 Objective of this study

The objectives of this study are:

- To develop an explicit pipe network simulation code that can be used as a benchmark for Flownet.
- To identify basic test cases and use these to benchmark Flownet with the explicit code and another commercial code.

These goals form part of the programme to verify and validate Flownet as a simulation design and safety analysis tool on the PBMR. Landman et al. (2003) gave an overview of the verification and validation performed by the code developers.

1.5 Layout of this study

This study starts with a literature survey in Chapter 2, in which various explicit methods are reviewed. Commercial one-dimensional software codes that can be used for validation are also discussed in this chapter. Based on this information, a suitable explicit method and commercial code is selected. With an explicit method chosen, one needs to implement this method in a code to analyse transient flow in pipe networks.

The implementation of the basic method, boundary conditions, non-inertial elements, junctions, tanks, etc. is discussed in Chapter 3. For thorough validation using benchmarks, it is important to focus on specific aspects of a network before considering the results of more complex problems. In this manner, the cause of an anomaly can more easily be identified.

In Chapter 4, comparisons are performed on pipe elements, boundary conditions, loss factors, heat transfer, non-inertial elements and tanks. Consideration is also given to the effect of sub-incrementation of pipe elements for steady and transient flow.

Steady and transient flow through junctions is benchmarked in Chapter 5. Subsequently, all validated aspects or models are then used in an arbitrary structured network. This benchmark is also done for steady and transient flow. In Chapter 6, some concluding remarks and recommendations for further work are made.

CHAPTER TWO: LITERATURE SURVEY

2.1 Introduction

In keeping with the aim of this study, a literature survey was conducted primarily to:

- Select an explicit numerical method which will be used to develop an explicit pipe network simulation code.
- Select a commercial code that will be used with the explicit code to benchmark Flownet.

To aid in these decisions, some historical background is given in the next paragraph. Various explicit methods and their features are subsequently discussed. An extensive survey was also conducted to determine what commercial software is available. Based on the information gathered, decisions regarding an appropriate explicit method and commercial code are made.

2.2 Historical background

A vast amount of research and literature have been dedicated to numerical methods in fluid mechanics. Only a broad overview is given of the historical development of this field.

Initially, the focus in pipe network modelling was on solving steady-state flow. For many systems that were modelled, this approach was sufficient. When designing complex thermal-fluid systems, it is important to analyse the dynamic response of a system. Loads experienced by components are often larger during system transients. With such analysis, the transient response of a system can be optimized.

A first method to analyse transient flow was developed by Riemann in 1858 (Winterbone et al. 2000:2). In his Method of Characteristics (MOC), Riemann transformed the set of partial differential equations into a set of ordinary differential equations. By the 1950s, the graphical MOC was in widespread use. With the development of digital computers, the mesh MOC was developed by Hartree (1953). This method was widely used in industry for transient analysis by 1970. It is still used

today, but has largely been replaced by finite difference or finite volume techniques. It is interesting to note how long the MOC remained the preferred method after finite difference and finite volume techniques were already available.

In 1952, Courant introduced a first-order explicit finite difference method to solve the inviscid Euler equations. A large number of explicit finite difference schemes soon followed. One of these was a second-order method called the Lax-Wendroff method. Hirsch (1990) describes the work of Peter Lax and Burt Wendroff published from 1957 to 1964 as a milestone in the modern development of numerical schemes for time-dependent Euler and also compressible Navier-Stokes equations. It was found that second-order methods such as the Lax-Wendroff method produced oscillations in the vicinity of discontinuities such as shock waves. The occurrence of this type of oscillation is referred to as dispersion. Various second-order methods have been developed to limit dispersion in the region of discontinuities. For the purpose of this study, the occurrence of shocks is not considered.

Due to the Courant limitation on time step size, explicit transient methods use a large number of iterations to reach steady-state conditions. Very often the rate of change for a transient simulation is relative small, and larger time steps could be taken without losing resolution. This led to the development of implicit methods which do not have the same limit on time step size. Lerat (1979,1983) developed implicit formulations using the Lax-Wendroff scheme.

The implicit method used in Flownet (Greyvenstein, 2002) is based on the SIMPLE algorithm by Patankar (1980). Van Ravenswaay (1998) used the MOC and an implicit method by Kiuchi (1994) to benchmark Flownet. Comparisons were done on simple networks using rigid liquid column theory, transients in simple gas pipe networks and water hammer cases. Generally these methods compared well with water and steam as the working fluid. Additional aspects that need consideration for this study are the use of helium, and comparisons that include the use of non-inertial elements.

Besides the thesis of Van Ravenswaay, a few other papers have been published on Flownet (see Greyvenstein & Laurie, 1994. Greyvenstein, 2001. Greyvenstein & Rousseau, 2002. Rousseau & Greyvenstein, 2002. Du Toit et al.,

2003. Landman et al., 2003. Rousseau & Van Ravenswaay, 2002. Van Niekerk et al., 2003. Greyvenstein et al., 2003).

An industry that has attracted a lot of research in one-dimensional compressible flow is the internal combustion engine industry. Due to the fast transients in this application, small time steps are required. Explicit methods are therefore preferred in this field. Winterbone and Pearson (2000) published a book containing a historical background and short description of various methods used in the industry. The modelling of boundary conditions, junctions and non-inertial elements is also treated in detail. According to Winterbone and Pearson (2000:50), numerical methods for the simulation of flow in engine manifolds developed as follows.

Benson et al. (1963) introduced the mesh Method of Characteristics using digital computing for engine applications. This method became the dominant technique in the industry until the 1980s. Higher order finite difference techniques that were capable of modelling shocks were increasingly being used. Various workers used methods such as the two-step Lax-Wendroff and MacCormack schemes. All these methods offered higher resolution at discontinuities, but also introduced numerical oscillations at these discontinuities. A first attempt to solve this was to calculate the flux at 'control volume' boundaries using Riemann variables. This gave satisfactory results for first-order schemes. Dispersion, however, still occurred when using this approach for steep gradients in second-order schemes. Finite difference evaluation of steep gradients results in unrealistic flux values that cause these oscillations. One way to resolve this is to limit the flux calculated at steep gradients by using numerical damping. This use of 'flux limiters' has been applied to various methods including the two-step Lax-Wendroff method.

2.3 Characterization of methods

Different methods possess different properties in terms of the solutions they produce. Some of the more important criteria that are used to evaluate or characterize methods will now be discussed briefly. A complete description can be found in various texts on computational fluid dynamics (Ferziger & Peric, 1999).

Consistency: When the numerical solution approaches the exact solution as the grid spacing tends to zero.

Stability: Stable methods do not magnify errors that appear as part of the numerical solution.

Conservatism: Conservation of mass, energy and momentum should be satisfied locally and globally.

Accuracy: Three types of errors influence the accuracy of a solution.

- Modelling errors are due to the difference between the exact solution of the mathematical model used and the physical flow it attempts to model.
- Discretization errors are caused by a difference in the exact solution of the partial differential equations and the exact solution of the discretized form of these equations.
- Iteration errors are the difference between the exact solution of the discretized equations and the numerical solution of these equations.

Two discretization errors that have been mentioned are dissipation (paragraph 1.3) and dispersion (paragraph 2.2). Dissipation occurs typically when using first-order methods in the vicinity of steep gradients. The smoothing effect these methods have on these gradients is called dissipation. Dispersion is found when second-order methods are used in the vicinity of discontinuities. Oscillations then develop in these regions.

2.4 Explicit methods

To perform an extensive evaluation of explicit methods is a study in itself. Fortunately, this has been done repeatedly in the past. Recommendations and comments on such previous evaluations will therefore be used in selecting a suitable method for validation. In this paragraph, a short overview of some of the methods discussed in Winterbone and Pearson (2000) is given. Other studies on such methods include Sod (1978) and Liska & Wendroff (2001).

An important requirement for such a method is conservatism. When modelling closed cycles such as the PBMR, a non-conservative method will lead to a loss or gain of, for instance, mass.

2.4.1 Method of Characteristics (MOC) and the CIR scheme

In both these methods, the three partial differential equations describing mass, momentum and energy conservation are rewritten as two ordinary differential equations. These equations are only valid along characteristic lines (lines indicating propagation in time and space at the local speed of sound). When 'discretized' on these lines, conditions at the next time step are calculated at points where these lines intersect. The solution of these total differential equations does, however, not enforce conservatism. Both these methods are also first-order accurate in space and time.

2.4.2 Lax-Wendroff schemes

It can be shown that this family of finite difference schemes satisfies conservation of mass, momentum and energy over control volumes (Winterbone et al. 2000:91). Points where conservation quantities are calculated are taken to be at the centre of these control volumes. To calculate these quantities at a next time step, the flux term(s) for mass, momentum or energy conservation are integrated over time. This is done at the boundaries of each control volume. These methods differ in the way the control volume is defined, and the way the flux on the boundaries is calculated. In Winterbone et al. (2000:92-103), the following methods of this family are discussed.

The single-step Lax Friedrichs scheme is first-order accurate in space and time. This scheme is highly dissipative. For the single-step Lax-Wendroff method, fluxes are calculated using a Jacobian matrix. In a two-step version of the Lax-Wendroff method, these fluxes are calculated by solving conservation quantities on the control volume boundaries at an intermediate time step. For this method, evaluation of the Jacobian matrix is not required. The MacCormack method uses a predictor and then a corrector step. Fluxes on the boundaries are calculated using values of the predictor time step.

All three of the latter methods are second-order accurate in space and time. For all such higher order methods, oscillations occur in the vicinity of sharp gradients (discontinuities). A first attempt to resolve these oscillations was to use explicit artificial viscosity. When using artificial viscosity, a parameter that is problem specific needs to be specified. Only limited success was achieved with this solution.

2.4.3 Rieman solvers

Second-order methods discussed this far do not distinguish between the upstream and downstream propagation of information in calculation of the flux values on control volume boundaries. This is one of the factors that cause dispersion. Upwind schemes and Rieman solvers do take this directionality into account. Two generic types of Rieman solvers, namely Godunov type methods and flux vector splitting methods, have been developed. Flux vector splitting has been widely adopted for implicit methods. All the methods described in Winterbone et al. (2000:102-119) are Godunov type methods of first-order accuracy.

In Godunov's original method, the fluxes at the boundary of a control volume are determined using an exact solution to the Rieman problem. That is to say, the same total differential equations used for the MOC is used to solve these fluxes. Later variants using the same approach as Godunov made use of approximate solutions of the Rieman problem to calculate fluxes.

2.4.4 Flux limiters and rate limiters

It has been shown that the extension of Rieman solvers to second-order accurate methods still produces oscillations in the vicinity of discontinuities (Winterbone et al. 2000:120). This occurrence of oscillations for second-order methods suggests a fundamental underlying problem. Godunov's theorem explains why this will always occur for methods discussed thus far.

It was suggested that using non-linear methods to determine the flux at boundaries could circumvent this fundamental problem. This can be accomplished by using coefficients for flux calculation that are a function of the current solution. Explicit artificial viscosity falls in this class. More recent methods aim to limit the total variation of the solution for each time step. Two popular classes of these methods are discussed in Winterbone et al. (2000:121-161): flux limiters and slope limiters.

Some of the methods described include the Flux Corrected Transport (FCT) scheme, self-adjusting hybrid schemes, Monotonic Upstream-centred Scheme for Conservation Laws (MUSCL), Piecewise Parabolic Method (PPM) and Essentially Non-oscillatory (ENO) schemes. All of these methods are successful at removing

most or all evidence of oscillations. All these methods use a criterion called the Total Variation Diminishing (TVD) principle. According to Winterbone et al. (2000:157), methods based on this criterion resulted in conservation errors when source terms (area variations, heat transfer and friction) had a large effect on the solution. These errors are significantly reduced when utilizing the correct state variables to apply the TVD principle.

2.5 Commercial codes

In choosing a commercial code, the following factors should be considered:

- A detail description of the numerical method and the models should be available to resolve possible anomalies that will arise.
- The code chosen should be well validated.

An extensive survey was done to determine what commercial software is available. Generally, software that can simulate transient compressible pipe-flow was considered. Table 2.1 provides a list of the software that was considered. Some of the candidates in the list only have steady-state capabilities.

A questionnaire was sent to all the companies forming part of the survey. The questions in this questionnaire as well as the information for each code are given in Appendix B. Unfortunately, less than a third of the companies replied. Some of the information for companies that did not reply was obtained from their web sites. If a particular company replied, it was indicated by a 'responded' written in brackets.

While conducting the survey, a copy of the RELAP5 manuals was obtained (NUREG/CR-5535, 2001). RELAP5 has been developed for best-estimate transient simulation of light water reactor coolant systems during postulated accidents in the USA. It has been extensively validated and helium fluid data has recently been added. Due to its application to the nuclear industry, the numerical methods and models used have been documented thoroughly. In addition to this, the Fortran source code is also made available when distributing the code. Bearing this in mind, the USA Nuclear Regulatory Commission (NRC) was contacted to obtain a copy of the code.

Software Title	Company	Site
	Engineering Dynamics Incorporated	www.engdyn.com
AFT Arrow	Applied Flow Technology	www.aft.com
BOS Fluids	Paulin Research	www.paulin.com
C-MAX	UNICADE Inc.	www.unicade.com
Delta-Q	Helix Technologies Pty Ltd	www.helixtech.com.au
DESIGN II	ChemShare Corporation	www.winsim.com
DFS DesigNet	ABZ, Incorporated	www.abzinc.com
D-SPICE™	Fantoft Process Technologies AS	www.fantoft.com
EASY5	Boeing	www.boeing.com
Flow Net	Engineering Design System Technology	www.edstech.com
Flownet	M-Tech Industrial (Pty.) Ltd.	www.flownet.net
FLOWMASTER	Flowmaster international Ltd	www.flowmaster.com
FlowTran	William J Turner Pty Ltd	www.users.bigpond.com/wjturner
FluidFlow	Flite Software Ltd	www.fluidflowinfo.com
GASWorkS	Accutech 2000 Pty Ltd	www.accutech2000.com.au
GENNET	Fluid Flow Consultants	www.fluidflow.tulsa.net
MELCOR	USNRC	www.nrc.gov
OLGA 2000	Scandpower AS	www.olga2000.com
PIPE2000	University of Kentucky	www.kypipe.com
PIPEFLO	Neotechnology Consultants Ltd.	www.neotec.com
PIPE-FLO	Engineered Software	www.eng-software.com
Pipeline Studio	Energy Solutions International	www.energy-solutions.com
PIPENET™	Sunrise Systems Limited	www.sunrise-sys.com
PIPESIM suite/2000	Baker Jardine	www.bakerjardine.com
PULS & PlantFLOW	Rebis	www.rebis.com
RELAP5	USNRC	www.nrc.gov/RES/RELAP5
SIMONE	LIWACOM	www.liwacom.de
SIMOTTO	Jodocy & Schmitz AG	www.euregio.net/simotto
SINDA/FLUINT	Cullimore and Ring Technologies, Inc.	www.crtech.com
SINDA/G	Network Analysis, Inc.	www.sinda.com
SINET	EPCON International	www.epcon.com
SNAP	Advantica	
SPS	Stoner Associates, Inc.	www.stoner.com
TOPAZ	Engineering Sciences Centre	www.esc.sandia.gov
TRAC-P	USNRC	www.nrc.gov/RES/TRAC-P
WAVE	Ricardo Plc	www.ricardo.com

Table 2.1: *List of software to model transient compressible flow.*

Clearly a great amount of development work has been done on transient compressible flow in pipe networks for commercial software. A large part of this work has not been published, sometimes to maintain a competitive advantage.

2.6 Conclusion

As mentioned, the book by Winterbone and Pearson (2000) contains details on the modelling of boundary conditions, junctions and non-inertial elements for one-dimensional network analysis. They predominantly made use of the two-step Lax-Wendroff method with Davies TVD term in their work. Satisfactory results were obtained with this method. For this study, the cases considered will not contain transients with gradients as sharp as for shock waves. It was therefore decided to use the normal two-step Lax-Wendroff method without including flux limiters. This can always be added if oscillations in the vicinity of sharp gradients complicate the validation process.

In the previous paragraph, some of the advantages of using RELAP5 as a commercial benchmark were discussed. The US NRC gave permission for the code to be used for this study. Unfortunately, the code has not been used extensively to model helium systems. This should, however, not be a problem due to the fact that compressible flow using other gases has been validated.

CHAPTER THREE: THE TWO-STEP LAX-WENDROFF METHOD

3.1 Introduction

In the previous chapter, the two-step Lax-Wendroff method was selected as the method of choice for developing a benchmark for Flownet. In this chapter, the application of the method to one-dimensional pipe networks is discussed.

Firstly, a general scheme is derived using the partial differential equations describing conservation of mass, momentum and energy. Two forms of the momentum equation are used to derive two variants of this scheme. The first variant uses static pressure in the momentum conservation equation, while the second variant uses total pressure. Using the general scheme, the method is then extended to handle boundary conditions as well as to incorporate non-inertial elements, junctions and tanks. With these basic models, an elementary explicit pipe network simulation code was developed using C++. The results produced by this simulation code will be compared with results of the IPCM in Chapters 4 and 5.

3.2 Partial differential equations

There are three conservation laws that apply to all fluid flow, the conservation of mass (continuity), momentum and energy. These laws are the foundation upon which methods such as the MOC, Lax-Wendroff and the IPCM are based. By assuming one-dimensional flow, the application of these laws in a pipe network is greatly simplified. At each point in the pipe, the average values at that cross-section are taken as the properties of the fluid at that point. With this assumption, flow only occurs in the direction of the pipe. Therefore properties only vary in the direction of flow, and not perpendicular to the pipe.

Consider a fluid flowing through an infinitesimal length of pipe or duct with heat transfer. For this infinitesimal pipe element, these three conservation laws can then be described using partial differential equations. In Appendix A, these equations are derived by applying these laws for an infinitesimal control volume. The partial differential equation for each conservation law will now be presented.

3.2.1 Continuity

Equation (3.1) describes conservation of mass in a pipe or duct with a variable cross-sectional area.

$$\frac{\partial \rho}{\partial t}+\frac{\partial(\rho VA)}{A\partial x}=0 \tag{3.1}$$

The first term in this equation describes the rate at which the mass in an infinitesimal pipe section ($A\partial x$) changes with time. This is influenced by the amount of mass leaving this infinitesimal pipe section. This quantity is given by the second term in (3.1).

3.2.2 Momentum

In Equation (3.2), a variation of pipe cross-sectional area is again taken into account for a description of conservation of momentum.

$$\frac{\partial(\rho V)}{\partial t}+\frac{\partial(\rho V^2 A)}{A\partial x}+\frac{\partial p}{\partial x}+\rho g\cos\theta+\frac{f\rho V|V|}{2D}=0 \tag{3.2}$$

For an infinitesimal pipe section the first term gives the rate at which momentum increases with time. The second term represents the net efflux of momentum, and the third the net pressure force on the fluid in the pipe section. When the pipe runs at an angle to the horizontal, a gravitational force affects the flow. This is taken into account by the fourth term. Frictional forces on the walls of the pipe are given by the fifth term of (3.2).

3.2.3 Energy

Equation (3.3) describes the conservation of energy likewise for a pipe with variable cross-sectional area.

$$\frac{\partial}{\partial t}(\rho u_0)+\frac{\partial\{(h_0+gz)\rho VA\}}{A\partial x}-\dot{q}=0 \tag{3.3}$$

The first term gives the rate at which energy changes with time in an infinitesimal pipe section. This is influenced by the net flux of energy due to the fluid and the heat transfer $\dot{q}$. In the second term, this net flux of energy due to the fluid is described. To write Equation (3.3) in its current form, the heat transfer is taken as the heat transfer per unit volume of the pipe.

3.3 The standard two-step Lax-Wendroff method

Figure 3.1 shows the time space discretization scheme for the two-step Lax-Wendroff method. One can distinguish between three time levels: the current time level; an intermediate time level; and the next time level. Variables taken at the current time level are denoted with a superscript 0, and those taken at the intermediate level with an accent. Values without any superscript are at the new time level $t + \Delta t$.

3.3.1 Step one

For the first step of the Lax-Wendroff method, the time derivative of the Navier Stokes equations is discretized for half a time step. This is done for a staggered grid in relation to the current time step.

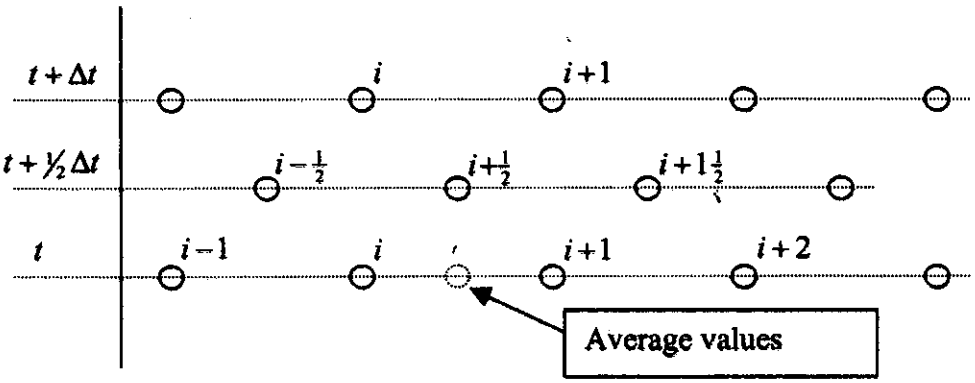


Figure 3.1: *Time space discretization of the Two-step Lax-Wendroff method.*

Consider the continuity equation (3.1). Forward differencing is used to discretize the time derivative and central differencing for the spatial derivative. For the first staggered half time step, conservation of mass is approximated by

$$\frac{\rho'_{i+\frac{1}{2}} - \frac{1}{2}\left(\rho_i^0 + \rho_{i+1}^0\right)}{\frac{1}{2}\Delta t} + \frac{(\rho VA)_{i+1}^0 - (\rho VA)_i^0}{A_{i+\frac{1}{2}}\Delta x} = 0 \qquad (3.4)$$

The average value of the density at the current time step is used to obtain a staggered value at the current time step. From this point onward, average values will be denoted with values at half an increment, for example $\rho_{i+\frac{1}{2}}^0 = \frac{1}{2}\left(\rho_i^0 + \rho_{i+1}^0\right)$. In Equation (3.4), the area in the second term's denominator is also taken to be the average value $A_{i+\frac{1}{2}} = \frac{1}{2}\left(A_i + A_{i+1}\right)$. The density at the intermediate time step can then be determined with

$$\rho'_{i+\frac{1}{2}} = \rho^0_{i+\frac{1}{2}} - \tfrac{1}{2}\Delta t \frac{(\rho VA)^0_{i+1} - (\rho VA)^0_i}{A_{i+\frac{1}{2}}\Delta x} \tag{3.5}$$

Next, a similar procedure is followed for the conservation of momentum. Again using forward differencing for the partial derivative in time and central differencing for the spatial derivatives gives

$$\frac{(\rho V)'_{i+\frac{1}{2}} - (\rho V)^0_{i+\frac{1}{2}}}{\tfrac{1}{2}\Delta t} + \frac{(\rho V^2 A)^0_{i+1} - (\rho V^2 A)^0_i}{A_{i+\frac{1}{2}}\Delta x} + \frac{p^0_{i+1} - p^0_i}{\Delta x} + (\rho g \cos\theta)^0_{i+\frac{1}{2}} + \left(\frac{f\rho V|V|}{2D}\right)^0_{i+\frac{1}{2}} = 0 \tag{3.6}$$

Equation (3.6) can be rewritten as

$$(\rho V)'_{i+\frac{1}{2}} = (\rho V)^0_{i+\frac{1}{2}} - \tfrac{1}{2}\Delta t\left[\frac{(\rho V^2 A)^0_{i+1} - (\rho V^2 A)^0_i}{A_{i+\frac{1}{2}}\Delta x} + \frac{p^0_{i+1} - p^0_i}{\Delta x} + (\rho g \cos\theta)^0_{i+\frac{1}{2}} + \left(\frac{f\rho V|V|}{2D}\right)^0_{i+\frac{1}{2}}\right] \tag{3.7}$$

Dividing the mass flow per unit area (ρV) by the density gives the velocity at the intermediate time level.

Discretizing the energy conservation equation in a similar way, it is found that

$$\frac{(\rho u_0)'_{i+\frac{1}{2}} - (\rho u_0)^0_{i+\frac{1}{2}}}{\tfrac{1}{2}\Delta t} + \frac{\{(h_0 + gz)\rho VA\}^0_{i+1} - \{(h_0 + gz)\rho VA\}^0_i}{A_{i+\frac{1}{2}}\Delta x} - (\dot{q})^0_{i+\frac{1}{2}} = 0 \tag{3.8}$$

Equation (3.8) can be rewritten as

$$(\rho u_0)'_{i+\frac{1}{2}} = (\rho u_0)^0_{i+\frac{1}{2}} - \tfrac{1}{2}\Delta t\left[\frac{\{(h_0 + gz)\rho VA\}^0_{i+1} - \{(h_0 + gz)\rho VA\}^0_i}{A_{i+\frac{1}{2}}\Delta x} - (\dot{q})^0_{i+\frac{1}{2}}\right] \tag{3.9}$$

From Equation (3.9), the total internal energy at the intermediate time level can be calculated.

With the density, velocity and total internal energy known at the intermediate time level, all other quantities can be calculated using the following equations. The internal energy is calculated using

$$u = u_0 - \tfrac{1}{2}V^2 \tag{3.10}$$

Temperature is calculated by

$$T = \frac{u}{c_v} \tag{3.11}$$

Using the ideal gas law, the static pressure can be determined.

$$p = \rho RT \tag{3.12}$$

Knowing the temperature, the enthalpy can be calculated using

$$h = c_p T \tag{3.13}$$

With these static quantities, the other stagnation (total) properties can be determined. The total enthalpy is calculated with

$$h_0 = h + \tfrac{1}{2}V^2 \tag{3.14}$$

Given the total enthalpy, one can calculate the total temperature using Equation (3.13) $h_0 = c_p T_0$. With the temperature known, the acoustic velocity and Mach number are calculated by

$$c = \sqrt{\gamma RT} \tag{3.15}$$

$$M = \frac{V}{c} \tag{3.16}$$

With the Mach number known, the total pressure can be calculated.

$$\frac{p_0}{p} = \left(1 + \frac{\gamma - 1}{2} M^2\right)^{\gamma/(\gamma-1)} \tag{3.17}$$

3.3.2 Step two

In the first step of the Lax-Wendroff method, variables were determined at the intermediate time level. In step two, variables will be determined for the next time level. For this step time, discretization takes place over a full time step between the current and next time level (central differencing). Instead of discretizing spatial derivatives at the current time level, this is done at the intermediate time level. For the continuity equation this results in

$$\frac{\rho_i - \rho_i^0}{\Delta t} + \frac{(\rho VA)'_{i+\frac{1}{2}} - (\rho VA)'_{i-\frac{1}{2}}}{A_i \Delta x} = 0 \tag{3.18}$$

The density at the next time level can then be calculated by rewriting Equation (3.18).

$$\boxed{\rho_i = \rho_i^0 - \Delta t \frac{(\rho VA)'_{i+\frac{1}{2}} - (\rho VA)'_{i-\frac{1}{2}}}{A_i \Delta x}} \tag{3.19}$$

Conservation of momentum for the next time level is written as

$$\frac{(\rho V)_i - (\rho V)_i^0}{\Delta t} + \frac{\left(\rho V^2 A\right)'_{i+\frac{1}{2}} - \left(\rho V^2 A\right)'_{i-\frac{1}{2}}}{A_i \Delta x} + \frac{p'_{i+\frac{1}{2}} - p'_{i-\frac{1}{2}}}{\Delta x} + (\rho g \cos\theta)'_i + \left(\frac{f \rho V |V|}{2D}\right)'_i = 0 \quad (3.20)$$

Here the influence of gravity and friction is evaluated at the intermediate time level. Using the density calculated in Equation (3.19) and rewriting Equation (3.20), the velocity at the next time level can be calculated from

$$(\rho V)_i = (\rho V)_i^0 - \Delta t \left[\frac{\left(\rho V^2 A\right)'_{i+\frac{1}{2}} - \left(\rho V^2 A\right)'_{i-\frac{1}{2}}}{A_i \Delta x} + \frac{p'_{i+\frac{1}{2}} - p'_{i-\frac{1}{2}}}{\Delta x} + (\rho g \cos\theta)'_i + \left(\frac{f \rho V |V|}{2D}\right)'_i \right] \quad (3.21)$$

Discretizing conservation of energy for the next time step is done in the same way as for continuity and conservation of momentum.

$$\frac{(\rho u_0)_i - (\rho u_0)_i^0}{\Delta t} + \frac{\left\{(h_0 + gz)\rho VA\right\}'_{i+\frac{1}{2}} - \left\{(h_0 + gz)\rho VA\right\}'_{i-\frac{1}{2}}}{A_i \Delta x} - (\dot{q})'_i = 0 \quad (3.22)$$

The heat transfer per unit volume is also evaluated at the intermediate time level. Using the density calculated in Equation (3.19) and rewriting Equation (3.22), the total energy at the next time level can be calculated by

$$(\rho u_0)_i = (\rho u_0)_i^0 - \Delta t \left[\frac{\left\{(h_0 + gz)\rho VA\right\}'_{i+\frac{1}{2}} - \left\{(h_0 + gz)\rho VA\right\}'_{i-\frac{1}{2}}}{A_i \Delta x} - (\dot{q})'_i \right] \quad (3.23)$$

With the density, velocity and total internal energy known at the next time level, all other quantities can be calculated using Equations (3.10) to (3.17). It has been proven that the two-step Lax-Wendroff method applied in this fashion is second-order accurate. This is due to the application of central differencing in space and time for the second step.

3.4 Method based on total pressures

Solving flow through junctions can prove to be problematic. This will be further discussed in paragraph 3.7. In Flownet this has been overcome by solving for total pressure at junctions. In order to accomplish this, the momentum equation was rewritten using total pressures. This also results in different averaged values used when calculating the intermediate time step. To determine the impact of such a

change, the same set of equations in Flownet was applied using the Lax-Wendroff method. Only small differences were found, as will be seen in Chapter 4.

By rewriting the momentum equation in a non-conservative form, we get that

$$\rho\frac{\partial V}{\partial t}+V\frac{\partial \rho}{\partial t}+V\frac{\partial(\rho VA)}{A\partial x}+\rho VA\frac{\partial V}{A\partial x}+\frac{\partial p}{\partial x}+\rho g\cos\theta+\frac{f\rho V|V|}{2D}=0 \qquad (3.24)$$

Using Equation (3.1) the second and third term of Equation (3.24) reduces to 0 giving

$$\rho\frac{\partial V}{\partial t}+\rho V\frac{\partial V}{\partial x}+\frac{\partial p}{\partial x}+\rho g\cos\theta+\frac{f\rho V|V|}{2D}=0 \qquad (3.25)$$

It can be shown that

$$\rho V\frac{\partial V}{\partial x}+\frac{\partial p}{\partial x}=\frac{p}{p_0}\frac{\partial p_0}{\partial x}+\frac{\rho V^2}{2T_0}\frac{\partial T_0}{\partial x} \qquad (3.26)$$

The proof of this theorem is given in Appendix A.5. Substitution into Equation (3.25) gives

$$\rho\frac{\partial V}{\partial t}+\frac{p}{p_0}\frac{\partial p_0}{\partial x}+\frac{\rho V^2}{2T_0}\frac{\partial T_0}{\partial x}+\rho g\cos\theta+\frac{f\rho V|V|}{2D}=0 \qquad (3.27)$$

3.4.1 Step one

In the first step, values are calculated at the intermediate time level. Only the revised momentum equation is discussed in this paragraph. For continuity and the conservation of energy, the method remains the same. Space and time discretization is performed in the same way as for the method based on static pressures.

$$\rho^0_{i+\frac{1}{2}}\frac{V'_{i+\frac{1}{2}}-V^0_{i+\frac{1}{2}}}{\frac{1}{2}\Delta t}+\left(\frac{p}{p_0}\right)^0_{i+\frac{1}{2}}\frac{p^0_{0i+1}-p^0_{0i}}{\Delta x}+\left(\frac{\rho V^2}{2T_0}\right)^0_{i+\frac{1}{2}}\frac{T^0_{0i+1}-T^0_{0i}}{\Delta x}+(\rho g\cos\theta)^0_{i+\frac{1}{2}}+\left(\frac{f\rho V|V|}{2D}\right)^0_{i+\frac{1}{2}}=0 \qquad (3.28)$$

To calculate the velocity at the intermediate time level, Equation (3.28) is written as

$$V'_i=V^0_{i+\frac{1}{2}}-\frac{\frac{1}{2}\Delta t}{\rho^0_{i+\frac{1}{2}}}\left[\left(\frac{p}{p_0}\right)^0_{i+\frac{1}{2}}\frac{p^0_{0i+1}-p^0_{0i}}{\Delta x}+\left(\frac{\rho V^2}{2T_0}\right)^0_{i+\frac{1}{2}}\frac{T^0_{0i+1}-T^0_{0i}}{\Delta x}+(\rho g\cos\theta)^0_{i+\frac{1}{2}}+\left(\frac{f\rho V|V|}{2D}\right)^0_{i+\frac{1}{2}}\right] \qquad (3.29)$$

3.4.2 Step two

Here again, the methodology is the same as for the method based on static pressures.

$$\rho_i' \frac{V_i - V_i^0}{\Delta t} + \left(\frac{p}{p_0}\right)_i' \frac{p_{0i+\frac{1}{2}}' - p_{0i-\frac{1}{2}}'}{\Delta x} + \left(\frac{\rho V^2}{2T_0}\right)_i' \frac{T_{0i+\frac{1}{2}}' - T_{0i-\frac{1}{2}}'}{\Delta x} + \left(\rho g \cos\theta\right)_i' + \left(\frac{f\rho V|V|}{2D}\right)_i' = 0 \quad (3.30)$$

By rewriting Equation (3.30), the velocity for the next time level can be calculated.

$$V_i = V_i^0 - \frac{\Delta t}{\rho_i'}\left[\left(\frac{p}{p_0}\right)_i' \frac{p_{0i+\frac{1}{2}}' - p_{0i-\frac{1}{2}}'}{\Delta x} + \left(\frac{\rho V^2}{2T_0}\right)_i' \frac{T_{0i+\frac{1}{2}}' - T_{0i-\frac{1}{2}}'}{\Delta x} + \left(\rho g \cos\theta\right)_i' + \left(\frac{f\rho V|V|}{2D}\right)_i'\right] \quad (3.31)$$

3.5 Implementation of boundary conditions

When solving transient flow, the solution is primarily influenced by the initial and boundary conditions. The accurate modelling of boundary conditions is therefore of great importance. In this paragraph, the implementation of the following boundaries for pipes will be discussed:

- Fixed mass flow boundaries.
- Total pressure boundaries.

3.5.1 Fixed mass flow boundaries

For fixed mass flow boundaries, mass flow per unit area (ρV) is known at the boundary. The momentum equation (3.21) is therefore redundant at the boundary. Figure 3.2 shows nodes for each time step at the boundary and adjacent to the boundary. Clearly the normal scheme for calculating ρ_i and $(\rho u_0)_i$ at the next time step does not apply. Density at the next time step can still be calculated by using a different discretization for conservation of mass.

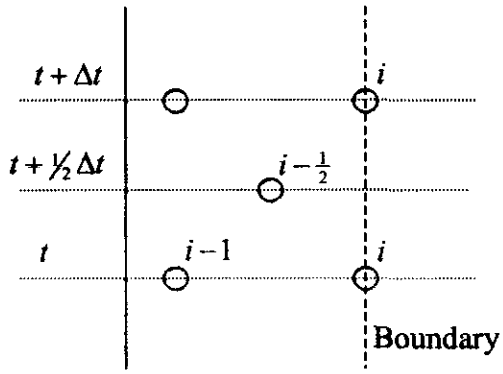


Figure 3.2: *Time space discretization at boundary node.*

For the first Lax-Wendroff step, $\rho'_{i-\frac{1}{2}}$ and $(\rho V)'_{i-\frac{1}{2}}$ is calculated using the normal scheme. For the second Lax-Wendroff step, spatial derivatives are evaluated over the last half increment at the intermediate time step. Equation (3.1) is then discretized as

$$\frac{\rho_i - \rho_i^0}{\Delta t} + \frac{(\rho VA)'_i - (\rho VA)'_{i-\frac{1}{2}}}{A_i \Delta x/2} = 0 \tag{3.32}$$

For the intermediate time step, $(\rho V)'_i$ is set equal to the specified boundary condition value $(\rho V)_i$. Rewriting Equation (3.32) using $(\rho V)'_i = (\rho V)_i$ gives the density at the next time step as

$$\rho_i = \rho_i^0 - 2\Delta t \frac{(\rho VA)_i - (\rho VA)'_{i-\frac{1}{2}}}{A_i \Delta x} \tag{3.33}$$

With density known, the velocity can be calculated for the specified boundary condition value $(\rho V)_i$.

For gas entering a boundary, the total temperature of the gas is specified. Temperature can then be calculated with $T = T_0 - V^2/2c_p$. Other quantities at the boundary can be calculated using Equations (3.10) to (3.17). When gas leaves the boundary, $(T_0)_i$ can be estimated using a quasi-steady formulation of the energy equation. With the transient term removed, Equation (3.3) can be discretized and rewritten with $(T_0)_i$ at the boundary given by

$$(T_0)_i = (T_0)_{i-1} + \frac{\dot{q}'_i \Delta x}{c_p (\rho V)_i} \tag{3.34}$$

In this study, the fixed mass flow boundary will only be used to model the sudden closure of a valve (zero mass flow boundary).

3.5.2 Total pressure boundaries

One can solve the flow for total pressure boundaries by firstly guessing a mass flow value (ρV) at the boundary. For this guess value, all quantities at the boundary can be determined using the method described in the previous paragraph (fixed mass

flow boundary). The guessed value for ρV is then adjusted using a Newton Raphson method until the known total pressure at the boundary is reached.

To increase the stability and speed of the Newton Raphson method, the total pressure at the next time step was written as an explicit function of ρV.

$$(p_0)_i = f(\rho V)_i = \frac{\rho_i R}{(T_0)_i}\left\{1 - \frac{(\rho V)_i^2}{2c_p \rho_i^2 (T_0)_i}\right\}^{1/(1-k)} \tag{3.35}$$

This function is derived in Appendix C. Here ρ_i and $(T_0)_i$ are also functions of $(\rho V)_i$ as defined in Equations (3.33) and (3.34). An analytical derivative $\frac{\partial p_{0,i}}{\partial (\rho V)_i}$ of Equation (3.35) was also determined in Appendix C. This was done to eliminate the use of numerical approximation for derivatives in the Newton Raphson method.

3.6 Non-inertial elements

The classical Lax-Wendroff method applies for elements that take into account a derivative for mass flux (see Equation (3.1)). In case of non-inertial elements such as orifices or valves, special treatment is necessary to deal with these kinds of elements. Flow through such elements is only dependent on the current boundary conditions. Consequently, boundaries or flow conditions at previous time steps have no effect on the current solution.

In pipe network solvers pumps, turbines, compressors and other components are often modelled as non-inertial elements. It is therefore important to validate the way in which non-inertial elements are treated in a simulation code. Validating different element models are however beyond the scope of this study. Only an orifice element was implemented using Lax-Wendroff to determine the validity of the way in which such elements are treated in Flownet.

The orifice model that was implemented using Lax-Wendroff will now be discussed. The basic theory for turbine and compressor models is also presented as an example of other non-inertial elements.

3.6.1 Orifices

For a simple orifice model, the total pressure drop is dependent on the inlet density and velocity.

$$\Delta p_0 = \tfrac{1}{2} k \rho V^2 \tag{3.36}$$

With no heat transfer or work acting on the fluid, the total temperature across an orifice remains constant.

3.6.2 Turbines and compressors

Operating characteristics for turbo machines are usually expressed by plotting turbine efficiency η and total pressure ratio p_{0in}/p_{0out} against non-dimensional mass flow $m\sqrt{T_{0in}}/p_{0in}$ (Cohen et al, 1999:319).

For turbines, efficiency is defined as

$$\eta_t = \frac{T_{0,in} - T_{0,out}}{T_{0,in} - \left(T_{0,out}\right)_s} \tag{3.37}$$

and for compressors as

$$\eta_c = \frac{\left(T_{0,out}\right)_s - T_{0,in}}{T_{0,out} - T_{0,in}} \tag{3.38}$$

where $\left(T_{0out}\right)_s$ is the outlet temperature for an isentropic process. From the p_{0in}/p_{0out} vs. $m\sqrt{T_{0in}}/p_{0in}$ plot the outlet total pressure is known. The isentropic outlet total temperature can be determined with the following relation.

$$\frac{T_{0,in}}{\left(T_{0,out}\right)_s} = \left(\frac{p_{0,in}}{p_{0,out}}\right)^{(\gamma-1)/\gamma} \tag{3.39}$$

For the non-inertial elements discussed the mass flow and outlet total temperature can be calculated given the inlet and outlet total pressure as well as the inlet total temperature. Junctions are used to integrate these elements into the Lax-Wendroff method.

3.7 Junctions and tanks

In the context of this study, a junction is defined as the connection point between an arbitrary number of pipes and non-inertial elements. Figure 3.3 shows such an arbitrary connection of elements to a junction.

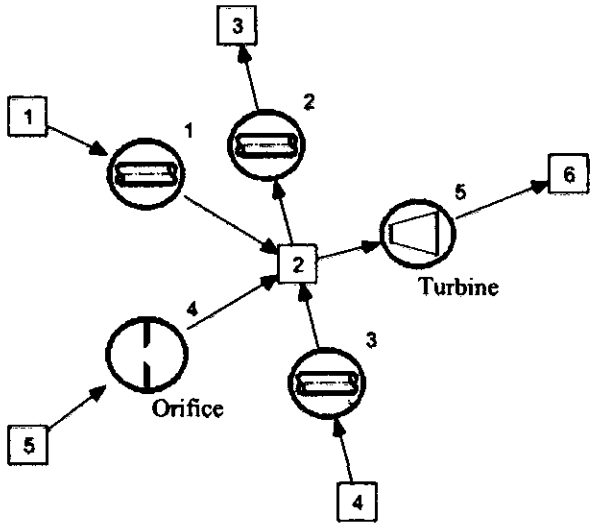


Figure 3.3: *Junction with discretized and non-inertial elements in Flownet.*

Junctions with a volume are used to model tanks. For such junctions, the velocity in the volume is assumed to be zero.

The continuity and energy conservation equations for junctions are given by

$$\left(\rho_i - \rho_i^0\right)\cdot \forbidden - \Delta t \sum_{e=1}^{n} \left(m_i\right)_e = 0 \tag{3.40}$$

$$\left\{\left(\rho u_0\right)_i - \left(\rho u_0\right)_i^0\right\}\cdot \forbidden - \Delta t \left\{\sum_{e=1}^{n} \left(mc_p T_0\right)_{i,e} + Q\right\} = 0 \tag{3.41}$$

If a junction has a volume, $\forbidden$, the first term in Equations (3.40) and (3.41) represents the change in mass and internal energy respectively. With a zero junction volume, these terms fall away. The second term in Equations (3.40) and (3.41) represents the net influx of mass and energy respectively for all elements (e) connected to the junction. For a zero volume junction, these net flux values should be zero.

Assume all values have been solved for the current time step. The solution of the junction total pressure $\left(p_0\right)_i$ and temperature $\left(T_0\right)_i$ for the next time step will now be discussed.

Assume as an initial guess value that the next time step junction total temperature is equal to the current time step value. Also assume a fixed total pressure at the opposite end of non-inertial elements (Nodes 5 and 6 in Figure 3.3). For a guessed junction total pressure, the mass flow at each pipe boundary and non-inertial element can be determined. For pipe elements this is done using the same procedure for fixed pressure boundaries as discussed in paragraph 3.5.2. If the junction volume is not zero, the preliminary density for the next time step is calculated using the ideal gas law (with zero velocity $\rho = p_0/RT_0$). Inserting the density and element mass flows into Equation (3.40) will in general result in a mass conservation error. This error can be driven to zero by varying the total pressure guess value by means of the Secant method (Kreyszig, 1993:933). Remember that for a zero volume junction the first term of Equation (3.40) falls away. If the total pressure at the opposite side of non-inertial elements is not fixed, the total pressure at both junctions will have to be solved simultaneously to achieve mass conservation for both junctions. This can be done using the multi-variable Secant method.

The preliminary solution calculated in this way satisfies mass conservation (Equation (3.40)) but not energy conservation (Equation (3.41)). Using Equation (3.41), the junction total temperature for the next time step is updated. If the junction has a volume, the total temperature is given by $(T_0)_i = (\rho u_0)_i / \rho_i c_v$ (Junction volume velocity is zero). In this case, the total temperature of fluid streams leaving the junction is set equal to the junction total temperature at the current time step. If the junction volume is zero, the next time step junction total temperature is given by

$$(T_0)_i = \left\{ \sum_{e=1}^{n} (mc_p T_0)_{i,influx,e} + Q \right\} \Big/ \sum_{e=1}^{n} (mc_p)_{i,influx,e} \qquad (3.42)$$

This is the average total temperature of fluid entering the junction with heat transfer to the junction added.

After updating the next time step junction total temperature, the mass flow calculated for various elements in the previous mass conservation iteration needs to be updated. Generally the variation in mass flow for this update is not large. By keeping the updated total temperatures constant, the Secant method is again used to find junction total pressure values that satisfy mass conservation. By alternating between solving total pressures for mass conservation and updating the energy equation, a

solution is reached that satisfies both continuity and energy conservation at each junction.

The approach that was followed above was to update junction temperatures after solving the pressure equation to a high level of convergence. Another approach would be to update junction temperatures after solving the pressure equation only partially. A third approach would be to solve the temperature equation after each iteration of the pressure equation. This may lead to instabilities.

To examine the validity of this junction model, consider a pipe with steady flow initially. A transient is then induced with by closing a valve at the downstream end of the pipe. The pipe can also be simulated as two pipes of half the original size connected by a junction. By comparing this result with that of a single pipe, the effect of a junction model on a fast transient can be isolated. Figure 3.4 shows such a comparison for a 10 m long 0.065 mm diameter pipe. The pipe was subdivided into 20 increments, i.e. 21 nodes. Total pressure was plotted at the middle of the pipe for the single pipe. For the two half pipes connected with a junction, the total pressure of the junction was plotted. It is clear that inclusion of the junction model caused a decrease in the frequency of the pressure wave. Besides this variance in frequency, the results compare very well.

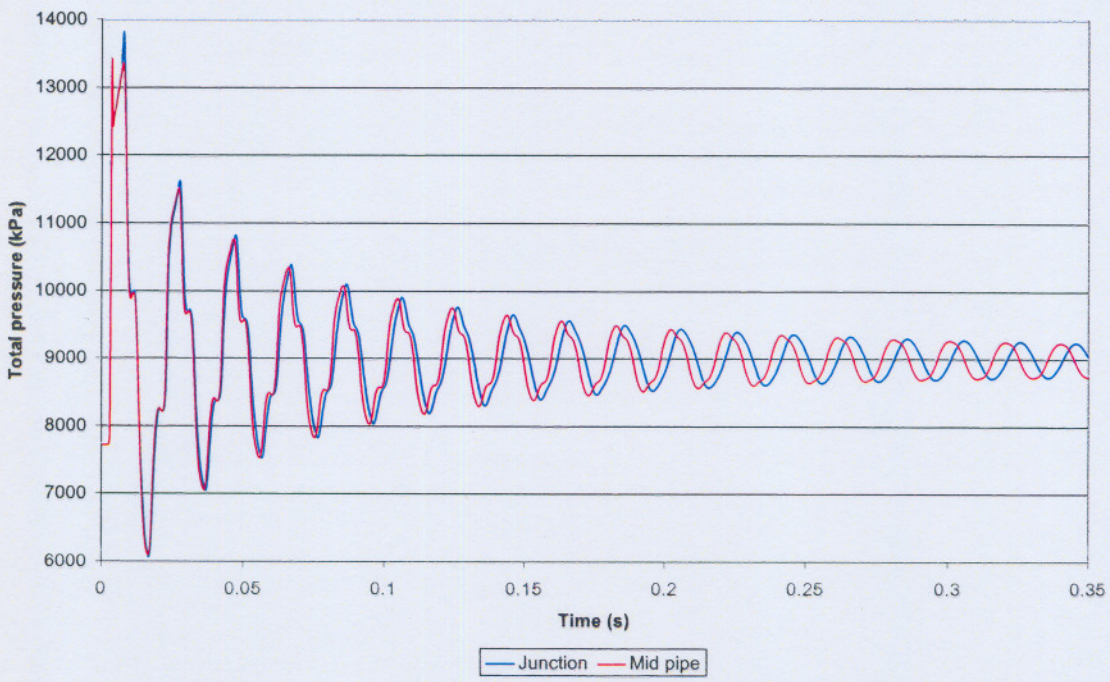


Figure 3.4: *Effect of junction model on pipe transient – 20 increments.*

This analysis was repeated with a finer grid of 80 subdivisions. Results are shown in Figure 3.5.

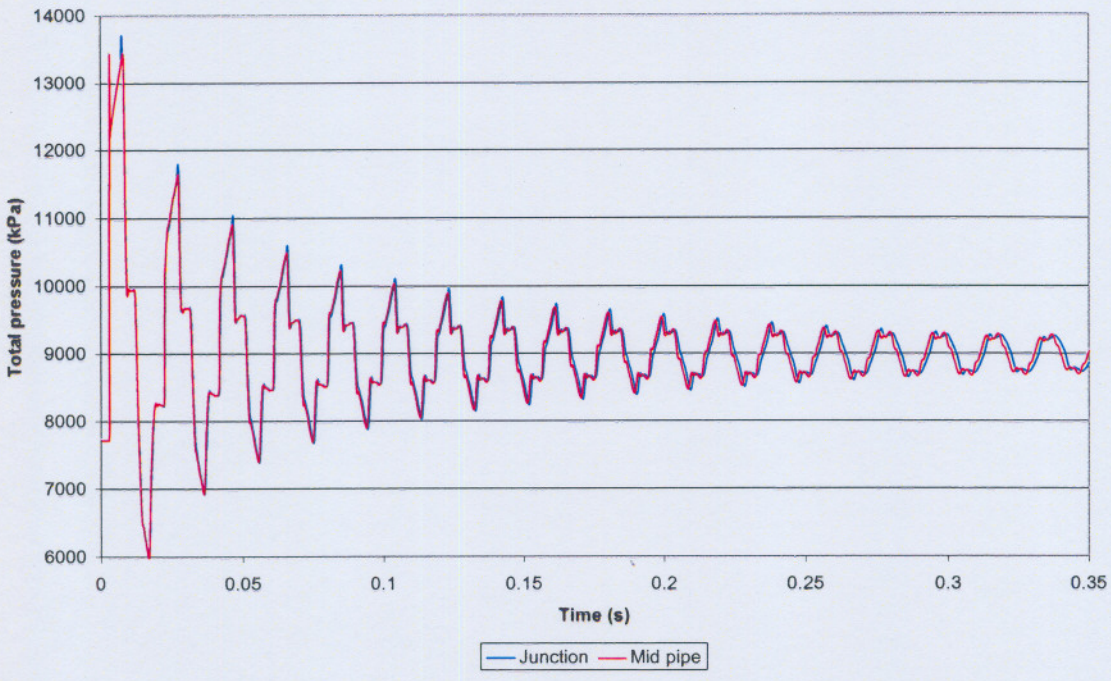


Figure 3.5: *Effect of junction model on pipe transient – 80 increments.*

Virtually no trace remained of the variance in frequency. A frequency difference for the single pipe was found to exist between the coarse and the fine grid. For the coarse grid, the frequency was found to be lower. One can therefore deduce that total pressure boundaries probably cause this delay in frequency. One junction in this case introduces two extra total pressure boundaries into the flow.

3.8 Conclusion

In this chapter, the basic building blocks required to implement an explicit pipe network simulation code were developed. Conservation of mass, energy and momentum was applied in this process. Using the Lax-Wendroff method, these models were implemented as part of a one-dimension network simulation code using C++. Flownet and RELAP5 use a different implementation of these building blocks. Using the simulation code that was developed, comparative analyses can now be performed for these building blocks, as well as for their integration into arbitrary structured networks.

CHAPTER FOUR: COMPARATIVE STUDY FOR DIFFERENT PIPE FLOW SCENARIOS

4.1 Introduction

In this chapter, the Lax-Wendroff method and RELAP5 are used to validate various component models in Flownet through comparison. Where possible, analytical results are also added. Models that were developed for use in the Lax-Wendroff method were discussed in Chapter 3. Two variants of the momentum conservation equation were implemented using the Lax-Wendroff method. For most of the cases presented in this chapter, these two implementations gave almost identical results. Often, only results for the method based on static pressures are therefore given.

4.2 Structure of the validation process

For thorough validation, it is important to focus on specific aspects of a network before considering the results of more complex problems. In this manner the cause of an anomaly can more easily be identified. Aspects that will be considered are pipe elements, boundary conditions, loss factors, heat transfer, non-inertial elements (orifices), tanks and junctions.

Flow in this context can be classified into three categories: steady-state; slow transients; and fast transients. Steady-state flow arises when all boundary conditions and the flow in every element remain constant with time. Slow transients occur when boundary conditions or element characteristics change slowly with time. If this change were to suddenly stop, there would be very little or no continuation of change in any element. In the case of a fast transient, this change of boundary conditions or element characteristics is more rapid. Large flow variations follow even after the change has stopped.

A summary of the validation process is given in Table 4.1. Paragraph numbers are shown for each flow scenario. In Table 4.1, Not Relevant (NR) indicates where a flow scenario would not give additional information concerning the validity of the particular component model.

Component	Steady-state	Slow Transient	Fast Transient
Pipes	4.3	NR	4.6
Boundary conditions	4.3	4.5	4.6
Loss Factors	4.3	NR	NR
Orifices	4.4	NR	4.7
Tanks	NR	4.5	NR
Nodes	5.2	NR	5.3

Table 4.1: *Components tested as part of validation.*

4.3 Steady-state flow in a pipe element

4.3.1 General

The mass flow through a pipe is influenced by the inlet total pressure and temperature, outlet total pressure, pipe geometry (friction), heat transfer and the type of fluid used. Gravity also has an effect in the case of inclined pipes. In this study, all pipes are assumed to be horizontal, which nullifies this effect. Helium will be used as working fluid with the following properties:

$$\begin{aligned} R &= 2080 \quad J/kg.K \\ c_p &= 5200 \quad J/kg.K \\ \mu &= 0.00002 \quad kg/m.s \end{aligned} \tag{3.43}$$

In the momentum conservation equation, the effect of geometry is accounted for by fL/D, where f is the friction factor, L is the length and D is the diameter of the pipe. Friction factor is a function of the Reynolds number and relative pipe roughness (e/D), and can be obtained using Moody's chart or correlations as described in Shames (1992:365). In terms of pipe geometry, the L/D ratio is therefore important. To envelope a large number of possible geometries, L/D ratios of 10, 100 and 1 000 will be evaluated in this part of the study.

The Mach number varies along the length of a pipe for compressible flow. For adiabatic flow, this Mach number variation in Flownet is validated for the three different L/D ratios. Subsequently, mass flow results are compared for a large combination of parameters that affect the flow through pipes. Forward and reverse

flow, positive and negative heat transfer, isothermal flow and additional pressure losses are some of the parameters taken into account. The object of the latter is to envelope a large number of pipe flow scenarios. These results are grouped into the three L/D ratios considered, 10, 100 and 1 000.

4.3.2 Mach number variation in a pipe for different L/D ratios

The diameter selected for each case was 1, 0.1 and 0.01 m respectively, with a constant length of 10 m. For each pipe the roughness was taken as $e = 30\ \mu m$, total outlet pressure as 300 kPa, and inlet total temperature as 15 °C. Without heat transfer, the outlet total temperature is equal to the inlet total temperature (15 °C). In each case the inlet total pressure was taken to be such that an outlet Mach number of 0.9 should be reached. Table 4.2 gives a summary of the input data used for Flownet, RELAP5 and Lax-Wendroff.

L/D	$D(m)$	$(p_o)_{in}(kPa)$	$(T_o)_{in}(°C)$	$(p_o)_{out}$	$L(m)$	$e(\mu m)$
10	1	316.5	15	300	10	30
100	0.1	444.6				
1 000	0.01	1 215.3				

Table 4.2: *Steady-state input data for Mach number vs. pipe position plot.*

The inlet total pressure for each case was calculated using an analytical method. This method is based on the following analytical equation (Shames, 1992:524).

$$\left(\frac{1}{M^2}-1\right)+\frac{\gamma+1}{2}\ln\left\{\frac{(\gamma+1)M^2}{2+(\gamma-1)M^2}\right\}=\frac{f\gamma L_{ch}}{D} \tag{3.44}$$

Equation (3.44) describes the variation of Mach number (M) in a pipe with a given diameter (D) and friction factor (f). L_{ch} gives the distance between the current position and the theoretical point at which the flow will choke. Therefore if $L_{ch}=0$ then $M=1$.

For the current problem, the outlet Mach number is specified as 0.9. Using Equation (3.44), the theoretical length to choking at the outlet $(L_{ch})_{outlet}$ can be

calculated. At any other position, L_{ch} is then equal to the distance to the outlet added to $(L_{ch})_{outlet}$. With L_{ch} known, the Mach number at that specific position in the pipe can then be calculated using (3.44). Knowing the outlet total temperature and pressure as well as the Mach number enables one to calculate the mass flow per unit area, G, using Saad (1985:97).

$$G = \sqrt{\frac{\gamma}{R}} \frac{P_0}{\sqrt{T_0}} \frac{M}{\left\{1+\left[(\gamma-1)/2\right]M^2\right\}^{(\gamma+1)/[2(\gamma-1)]}} \tag{3.45}$$

With the inlet total temperature and Mach number known, the inlet static pressure can then be calculated using Shames (1992:525)

$$p = \frac{G}{M}\left\{\frac{RT_0}{\gamma\left[1+M^2(\gamma-1)/2\right]}\right\}^{1/2} \tag{3.46}$$

From this, all other properties, including the total pressure, can be calculated at the inlet as well as at any other position in the pipe.

This concludes the overview of the analytical method used. As mentioned, the inlet total pressure obtained with this method was then used as input to the other three methods. Figure 4.1 shows the results compiled using Flownet, RELAP5, Lax-Wendroff and the analytical method for different L/D ratios.

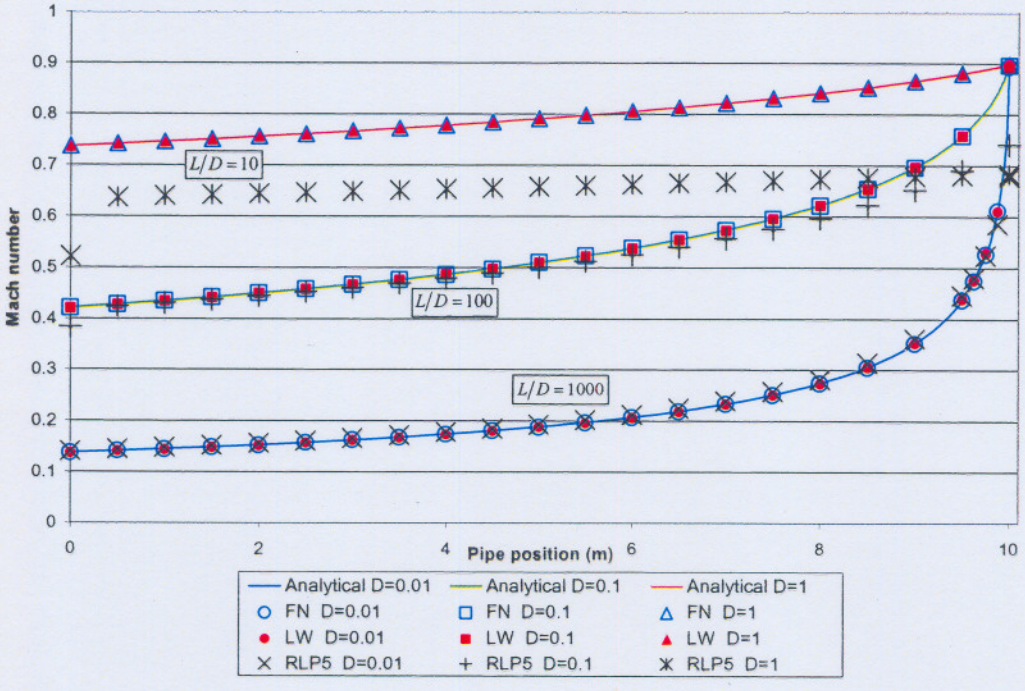


Figure 4.1: *Mach number vs. pipe position for different L/D values.*

Each of the pipes modelled was subdivided into 80 increments to ensure a grid-independent solution. A sub-incrementation of 40 was found to be sufficient for the Lax-Wendroff method based on total pressures in paragraph 4.8 (exit Mach number 0.9). This was, however, for a pipe with $L/D = 100$. Due to larger Mach number gradients that occur for $L/D = 1\,000$, a higher sub-incrementation of 80 was chosen.

In Figure 4.1, Flownet and Lax-Wendroff corresponded well with the analytical solution for all three L/D ratios. RELAP5, however, deviated from the other solutions at high Mach numbers. It is possible that the compressible flow models in RELAP5 were not intended to model flow at high Mach numbers. From the results, one can conclude that Flownet accurately models the variation of flow conditions in a pipe for compressible flow.

In the following paragraphs, adiabatic, non-adiabatic and isothermal flow conditions are also considered. Attention will now be given to the pipe mass flow for a large number of different pipe flow scenarios as opposed to the detail variation of flow within a pipe. For each paragraph, a particular L/D value was used.

4.3.2.1 Different pipe flow scenarios – $L/D = 10$

Simulations were performed with the same pipe geometry as in the previous paragraph. An analytical solution was obtained using the method discussed in Appendix D. Isothermal flow, positive and negative heat transfer, and adiabatic flow conditions were considered. For isothermal flow, the static temperature remains constant throughout the pipe.

In Figure 4.2 and Figure 4.3, total pressure differential Δp_0 across the pipe is plotted against the outlet mass flow and Mach number respectively. In these figures, adiabatic flow results are indicated by 'Adi', isothermal by 'Iso', and flow with heat transfer is indicated by 'Q'. For reverse flow (negative Δp_0), an additional pipe loss coefficient ($k = 1$) was distributed along the pipe. This results in lower mass flows and lower outlet Mach numbers for the same Δp_0 as for the positive flow direction.

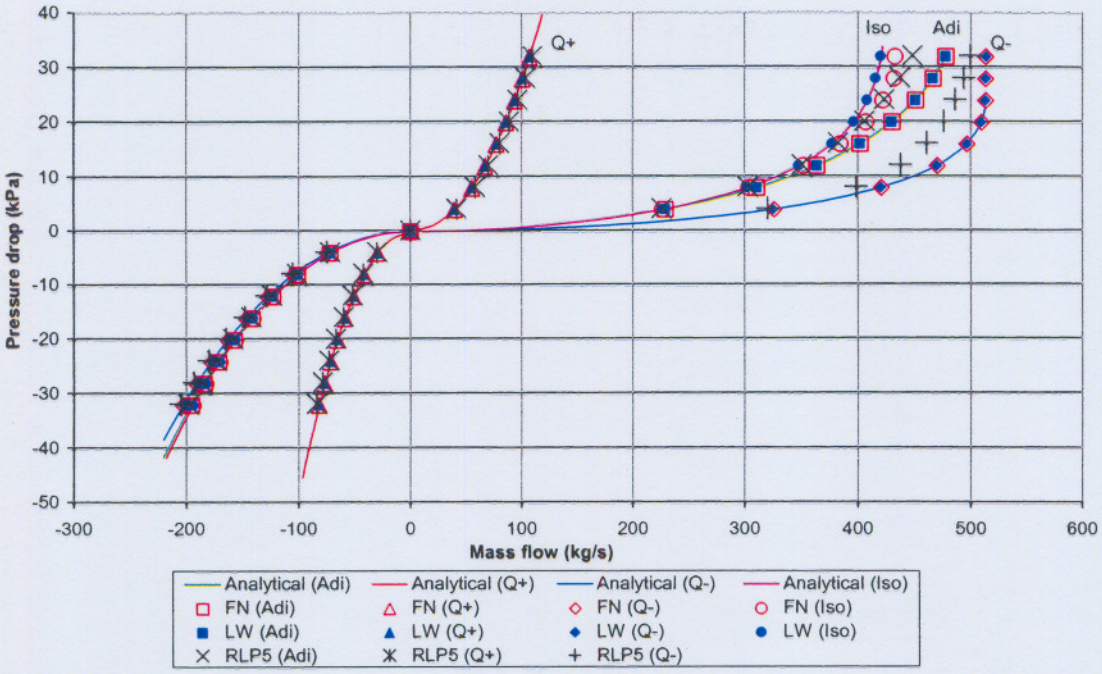


Figure 4.2: *Total pressure drop vs. mass flow for* $L/D = 10$.

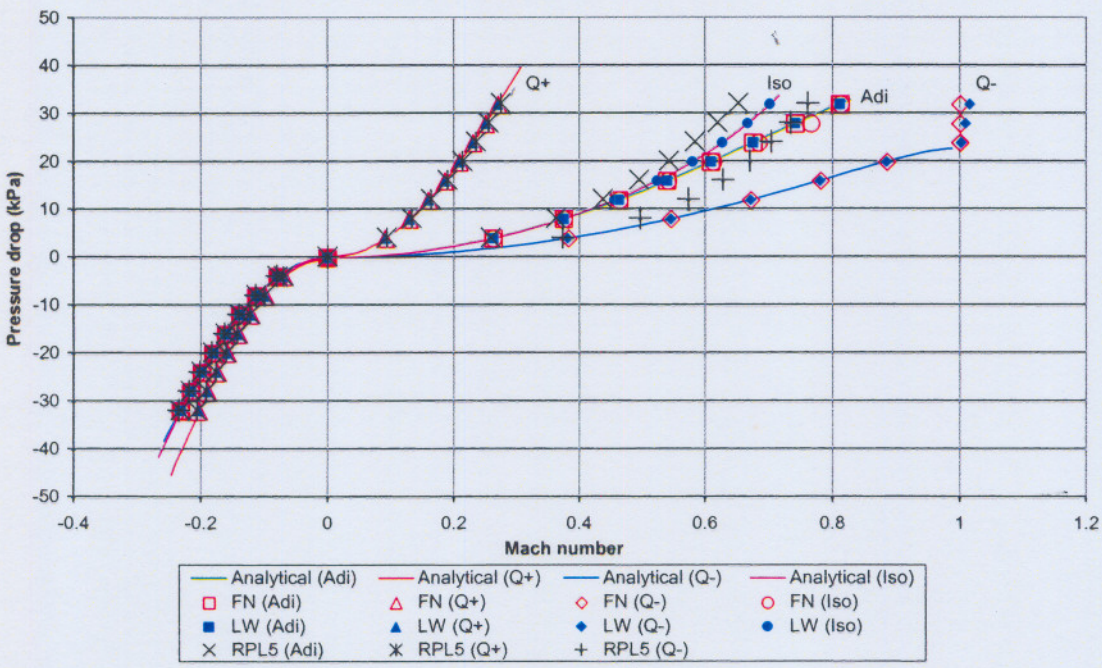


Figure 4.3: *Total pressure drop vs. exit Mach number for* $L/D = 10$.

Heat transfer is applied for each (Δp_0) case so that a given total outlet temperature is reached. Table 4.3 shows the input parameters for flow with heat transfer, adiabatic and isothermal flow.

Heat Transfer	$(p_0)_{in}(kPa)$	$(p_0)_{out}(kPa)$	$(T_0)_{in}(°C)$	$(T_0)_{out}(°C)$
Positive	700	668 to 700	15	1 015
Negative				0
Adiabatic				15
Isothermal			$T_{st}=15$ °C	

Table 4.3: *Steady-state input data for* $L/D=10$.

Figure 4.2 and Figure 4.3 indicate a good correlation between Flownet, Lax-Wendroff and the analytical solution. Again, the deviation of RELAP5 at high Mach numbers is apparent. An anomaly between Flownet and the analytical solutions was found for isothermal flow at high Mach numbers. The isothermal flow model in Flownet has no influence on the solution of other flow cases. Further, isothermal flow is not used to model the PBMR. For the purpose of this study, this anomaly was therefore considered to be of lesser importance. No choking model has been implemented for Lax-Wendroff. Consequentially Lax-Wendroff gave exit Mach numbers greater than unity.

Table 4.4 gives the solution time in seconds for each code.

Heat Transfer	Number of Nodes	Solution Time (s)			
		Flownet	RELAP5	LW Static	LW Total
Adiabatic	81	18.51	507.781	518.578	525.812
Isothermal			n/a	414.671	423.515
Positive HT			839.188	587.171	431.281
Negative HT			732.859	485.171	476.734

Table 4.4: *Steady-state solution time for* $L/D=10$.

One should consider the following before drawing conclusions from these results. Flownet and Lax-Wendroff use the total outlet temperature as input. Heat transfer is then solved iteratively for each Δp_0. RELAP5 does not have this capability, and can only take the heat transfer as input. Heat transfer calculated with Lax-Wendroff was used as input for RELAP5. This implies far less calculations for RELAP5 to obtain the same answer. Another factor influencing these results is the different convergence

criteria used by each code. Nevertheless, these results give a good indication of the relative speed of the different codes.

Flownet reached a steady-state solution in far less time than Lax-Wendroff and RELAP5. All the test cases run on Flownet took about 18.5 s. This is made possible with the implicit solver implemented in Flownet.

4.3.2.2 Different pipe flow scenarios – $L/D = 100$

Here the simulation procedure is exactly the same as in the previous paragraph. Different input values are used to attain sensible outlet Mach numbers, and are shown in Table 4.5. Results are shown in Figure 4.4 to Figure 4.6.

Heat Transfer	$(p_0)_{in}\,(kPa)$	$(p_0)_{out}\,(kPa)$	$(T_0)_{in}\,(°C)$	$(T_0)_{out}\,(°C)$
Positive	700	500 to 700	15	1 015
Negative				-85
Adiabatic				15
Isothermal			$T_{st} = 15$ °C	

Table 4.5: *Steady-state input data for* $L/D = 100$.

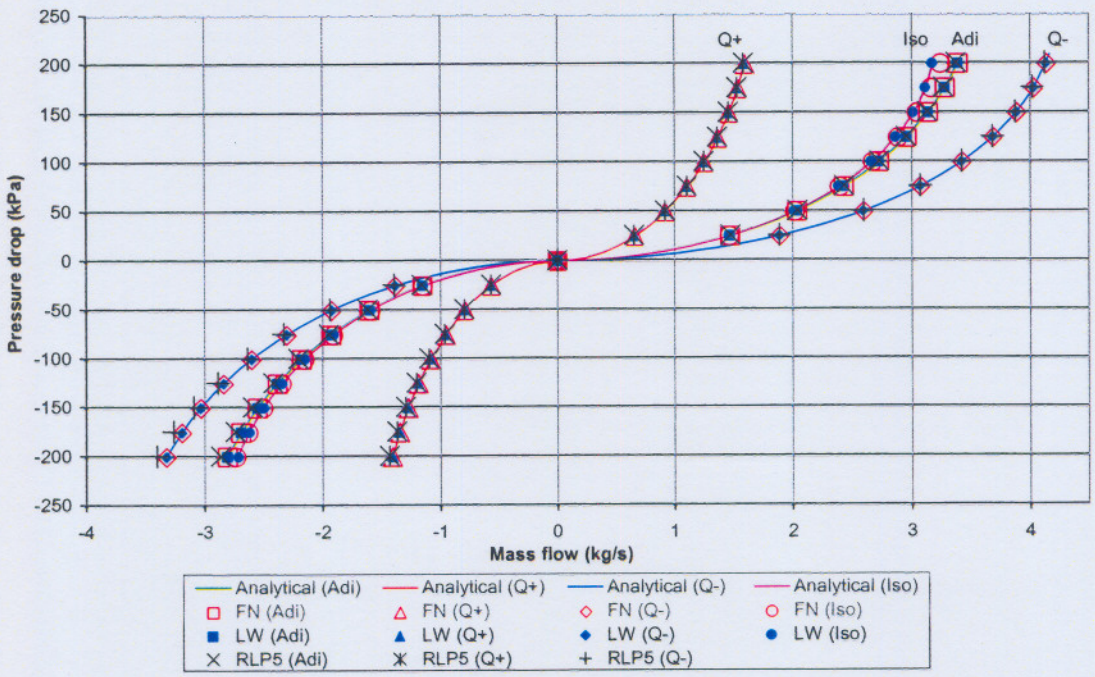


Figure 4.4: *Total pressure drop vs. mass flow for* $L/D = 100$.

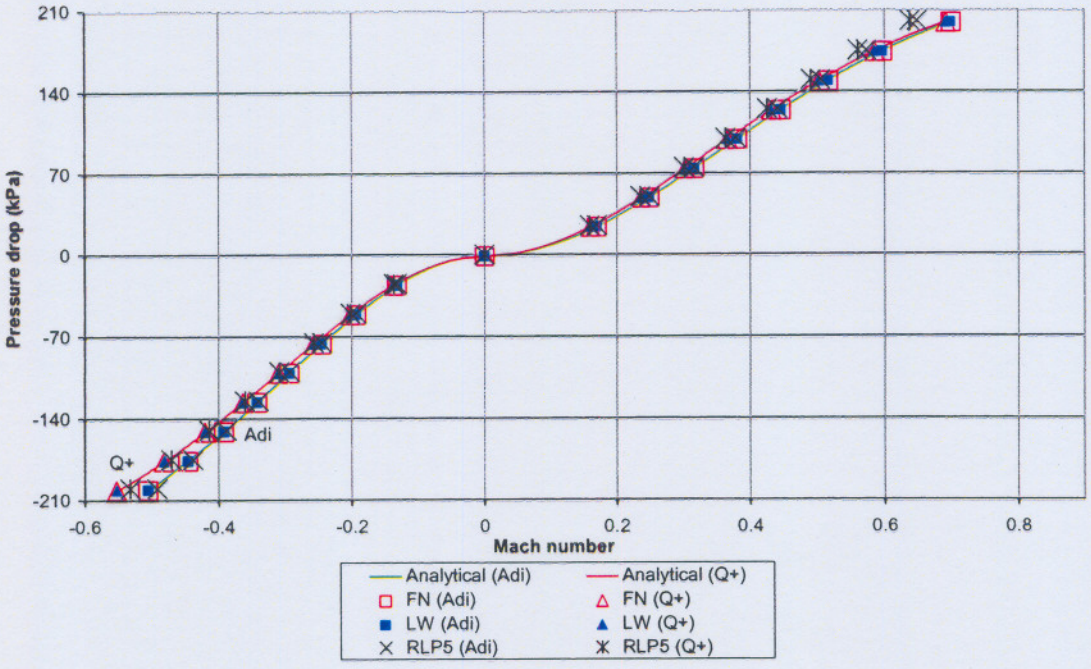


Figure 4.5: *Total pressure drop vs. exit Mach number for* $L/D = 100$ *- Plot 1.*

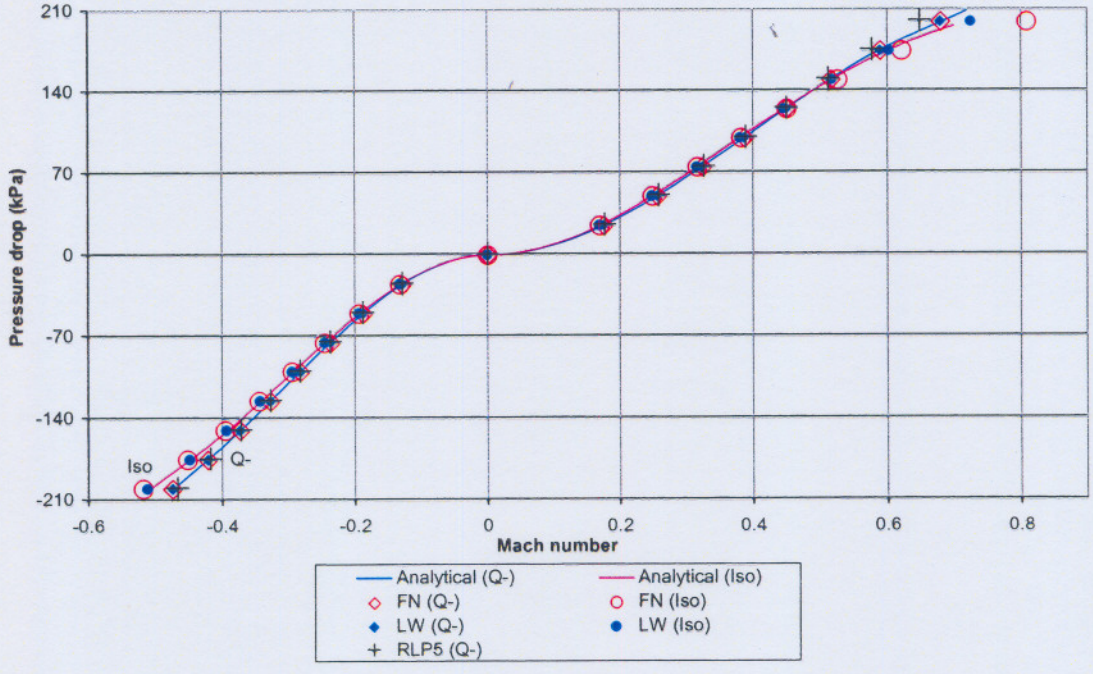


Figure 4.6: *Total pressure drop vs. exit Mach number for* $L/D = 100$ *- Plot 2.*

Here again, total pressure differential Δp_0 across the pipe is plotted against the outlet mass flow and Mach number respectively. For the Mach number plots, the deviation of RELAP5 at high Mach numbers can be seen. In this case, the same

anomaly for isothermal flow was found using Flownet. For the Mach number plots, a smaller difference was found between the results for non-adiabatic and adiabatic flow than in the $L/D=10$ case. With a longer pipe as is the case, frictional effects will have a greater effect on the flow relative to the effect of heat transfer.

Table 4.6 gives the solution time for each code. The same remarks as for the $L/D=10$ case apply here.

Heat Transfer	Number of Nodes	Solution Time (s)			
		Flownet	RELAP5	LW Static	LW Total
Adiabatic	81	7.03	520.406	140.89	120.687
Isothermal			n/a	104.75	89.968
Positive HT			1 401.23	481.531	229.968
Negative HT			630.906	239.109	215.375

Table 4.6: *Steady-state solution time for* $L/D=100$.

4.3.3 Different pipe flow scenarios – $L/D = 1\,000$

Here the simulation procedure is exactly the same as in the previous two paragraphs. Different input values are used to attain sensible outlet Mach numbers and is shown in Table 4.7.

Heat Transfer	$(p_0)_{in}\,(kPa)$	$(p_0)_{out}\,(kPa)$	$(T_0)_{in}\,(°C)$	$(T_0)_{out}\,(°C)$
Positive	900	260 to 900	15	415
Negative				-85
Adiabatic				15
Isothermal			$T_{st}=15$ °C	

Table 4.7: *Steady-state input data for* $L/D=1\,000$.

Results are shown in Figure 4.7 to Figure 4.9 with total pressure differential Δp_0 across the pipe plotted against the outlet mass flow and Mach number respectively. For the Mach number plots, the deviation of RELAP5 at high Mach numbers can be seen.

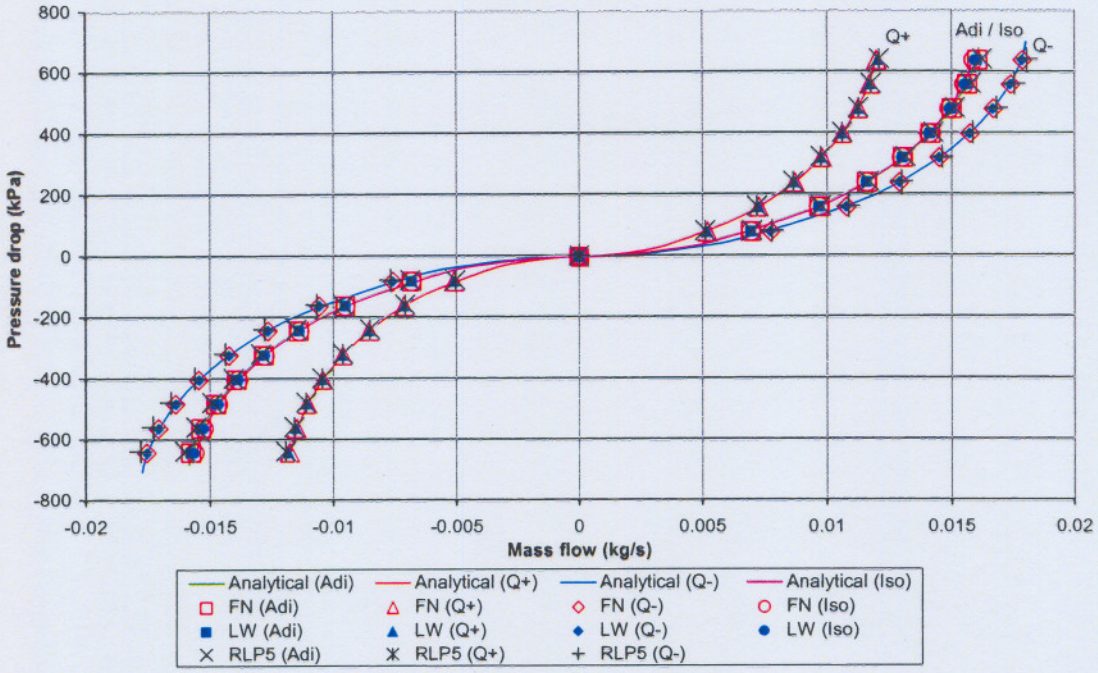


Figure 4.7: *Total pressure drop vs. mass flow for* $L/D = 1\,000$.

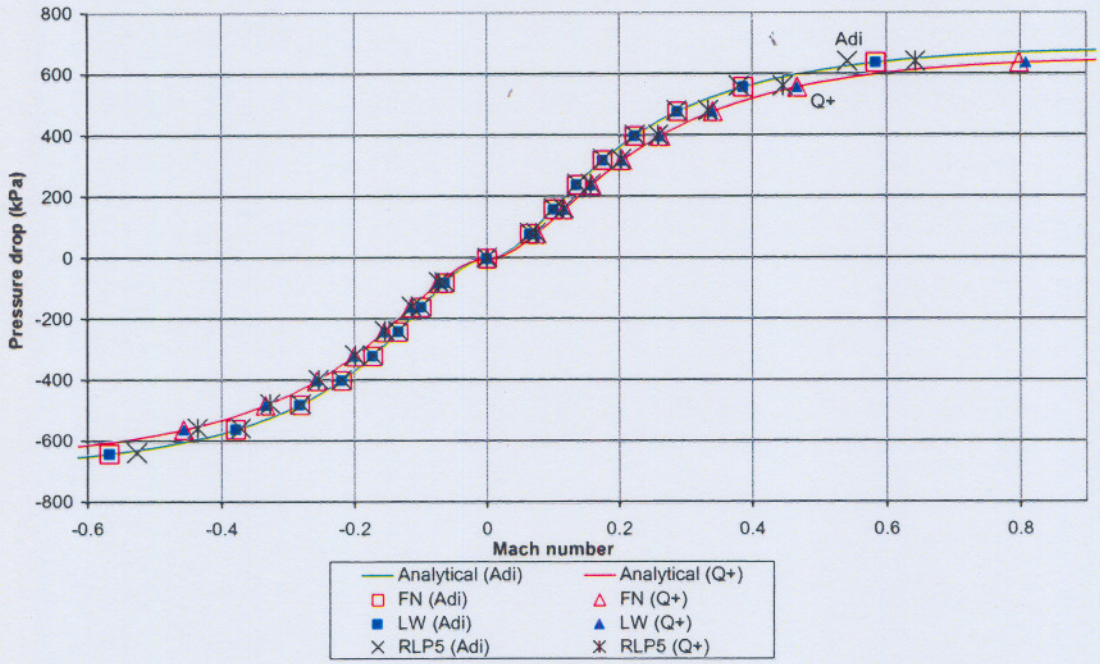


Figure 4.8: *Total pressure drop vs. exit Mach number for* $L/D = 1\,000$ *- Plot 1.*

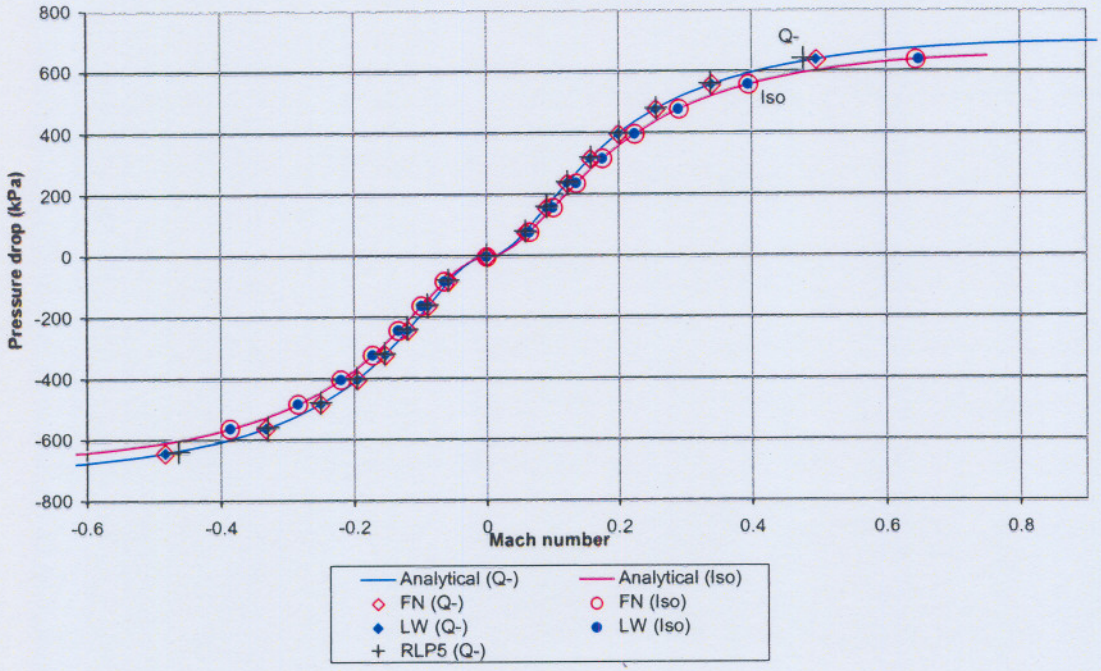


Figure 4.9: *Total pressure drop vs. exit Mach number for* $L/D = 1\,000$ *- Plot 2.*

Table 4.8 gives the solution time for each code. The same remarks as for the $L/D = 10$ case apply here.

Heat Transfer	Number of Nodes	Solution Time (s)			
		Flownet	RELAP5	LW Static	LW Total
Adiabatic	81	4.34	352.656	80.093	71.937
Isothermal			n/a	21.5	19
Positive HT			778.313	175.859	152.875
Negative HT			335.938	158.296	144.39

Table 4.8: *Steady-state solution time for* $L/D = 1\,000$.

4.4 Steady-state flow through an orifice

An orifice model was described for the Lax-Wendroff method in paragraph 3.6. Equivalent models exist in Flownet and RELAP5. In this paragraph, results obtained using the orifice model in each of these codes are compared with an analytical solution.

The same pipe geometry is used as in the previous paragraph with $L/D = 100$. An orifice is inserted in the middle of the pipe with 40 sub-increments in the left and right 5 m sections as depicted in Figure 4.10. An inlet total pressure of 444.6 kPa, inlet total temperature of 15 °C and outlet total pressure of 300 kPa was selected.

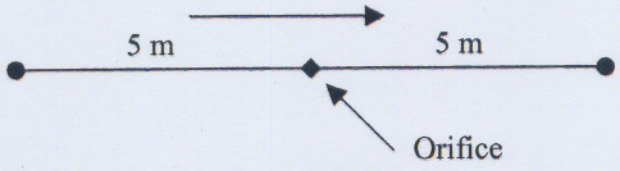


Figure 4.10: *Pipe geometry for orifice validation.*

By varying the loss factor (k-value), a range of steady state conditions can be analysed. The range of loss factors selected with their resultant mass flow rates is given in Table 4.1. For each loss factor, the fraction of the mass flow with regard to the zero loss factor (open pipe) result is also given.

No.	Loss Factor (k)	Fraction of Open Pipe Mass Flow	
		Percentage	Value (kg/s)
1	0.013	99.8%	2.188
2	0.077	98.8%	2.166
3	0.177	97.3%	2.133
4	0.717	90.0%	1.973
5	1.677	80.0%	1.754
6	3.039	70.0%	1.535
7	5.101	60.0%	1.315
8	8.485	50.0%	1.096
9	14.68	40.0%	0.877
10	28.04	30.0%	0.658
11	66.22	20.0%	0.438
12	272.5	10.0%	0.219
13	1 717	4.0%	0.088
14	2 7525	1.0%	0.022

Table 4.9: *Loss factors for validation of orifice model.*

These k-values were determined analytically in the following manner. Inlet and outlet total pressure and temperature have been specified. For a given mass flow rate (fraction of open pipe mass flow), the flow in any part of the pipe section is determined using the analytical method based on (3.44). All variables upstream and downstream of the orifice can therefore be determined. Using Equation (3.36), an associated k value can then be calculated for the given mass flow rate. It was found that the k values increased almost exponentially as the mass flow fraction decreased. These k values were used with the given boundary conditions as input for the three codes. The results obtained for these simulations will now be discussed.

In Figure 4.11, an orifice inlet and outlet Mach number is plotted for various loss factors on a logarithmic scale. The two lines indicate the analytical solution just before (in) and after (out) the orifice. Results are shown for Flownet, Lax-Wendroff and RELAP5.

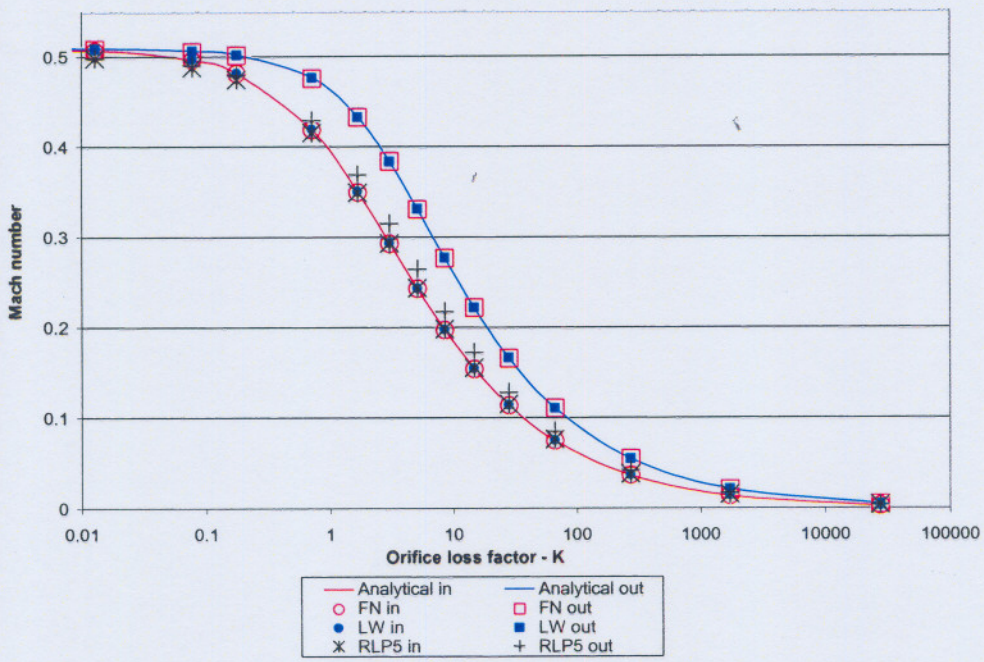


Figure 4.11: *Mach number at orifice inlet and outlet vs. loss factor.*

RELAP5 clearly gives a very inaccurate value for the outlet Mach number. The loss factors in RELAP5 were specified at a junction between the two pipe sections. A clear description of the implementation of these loss factors could not be found. Another perspective on this anomaly is given in Figure 4.12, where the total temperature at the orifice inlet and outlet is given for RELAP5.

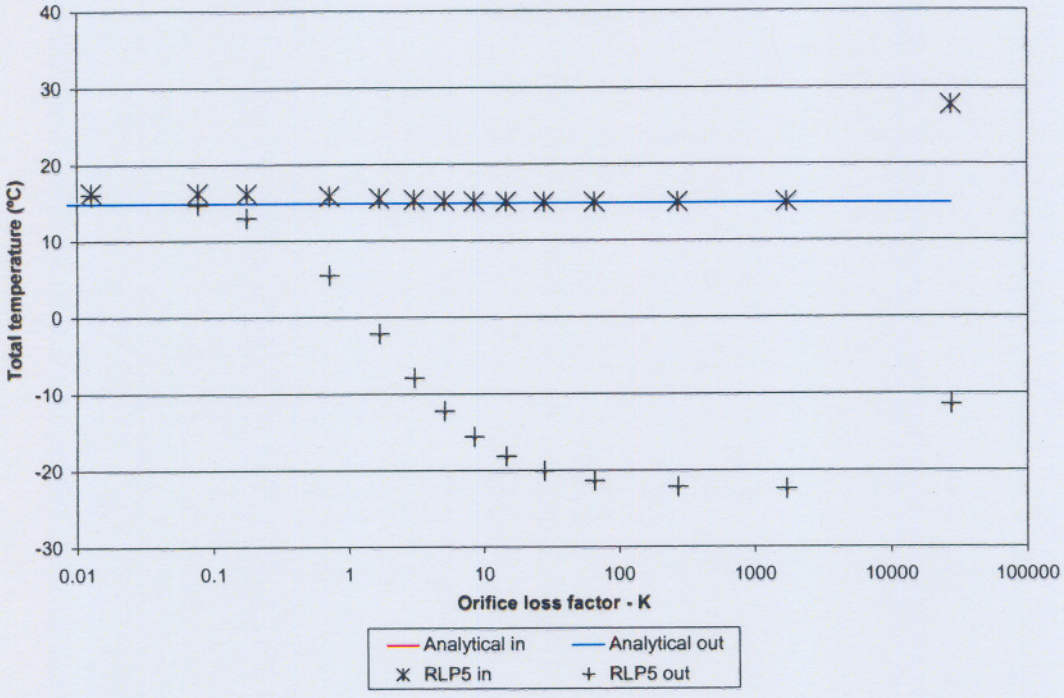


Figure 4.12: *RELAP5 total temperature at orifice inlet and outlet.*

For steady flow, the total temperature should remain constant at 15 °C. RELAP5 gives a lower outlet total temperature, which indicates a loss of energy across the orifice.

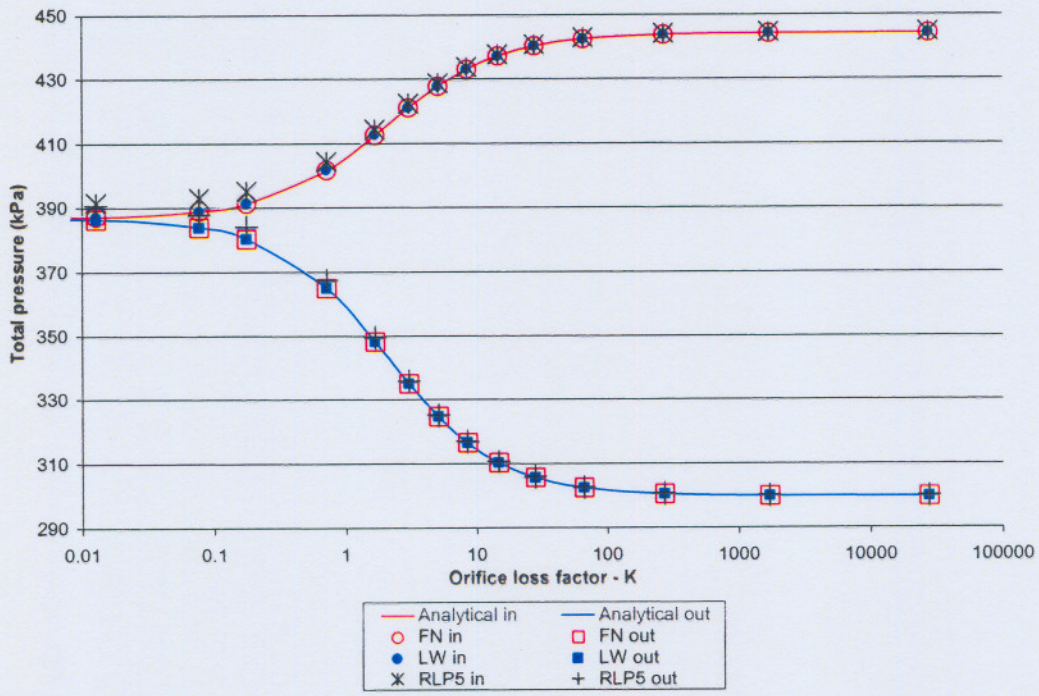


Figure 4.13: *Total pressure at orifice inlet and outlet vs. loss factor.*

Figure 4.13 shows the orifice inlet and outlet total pressures plotted logarithmically against k. RELAP5 gives higher total pressures for low loss factors. At these conditions, a Mach number close to 0.9 is reached at the system outlet. For high Mach numbers, RELAP5 reaches a different steady-state solution, as was seen in the previous paragraph. Results obtained using Flownet and Lax-Wendroff compared very well with the analytical solution in Figure 4.11 and Figure 4.13.

This concludes the evaluation of steady flow through elements. Slow transients between tanks will be considered next.

4.5 Slow transients between tanks

The following is a scenario where slow transients occur between two tanks at different initial pressures.

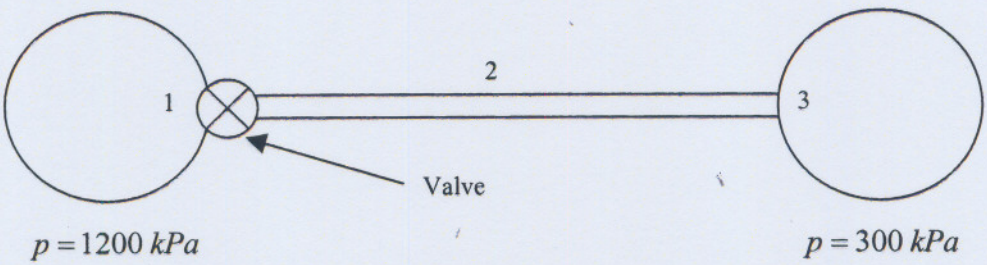


Figure 4.14: *Slow transient between two tanks.*

Initially, the valve in Figure 4.14 is closed and zero flow conditions are maintained throughout the system. After the valve is opened, helium flows from point 1 (1 200 kPa) to 3 (300 kPa) until the pressure equalizes. A 10 m pipe with a 0.01 m diameter is used ($e/D = 0.00003$), and each tank has a volume of 0.4 m^3. For all codes, the pipe is subdivided into 40 sub-increments to ensure a grid independent solution. Before the valve opens, the temperature throughout the system is set to 15 °C.

For this validation total pressure, total temperature and Mach number are plotted for 20 s in Figure 4.15, Figure 4.16 and Figure 4.17 respectively. Values are plotted for each tank (1 and 2) and in the middle of the pipe (3). Mach number values at positions 1 and 2 are evaluated at the pipe ends (velocity in tanks is zero).

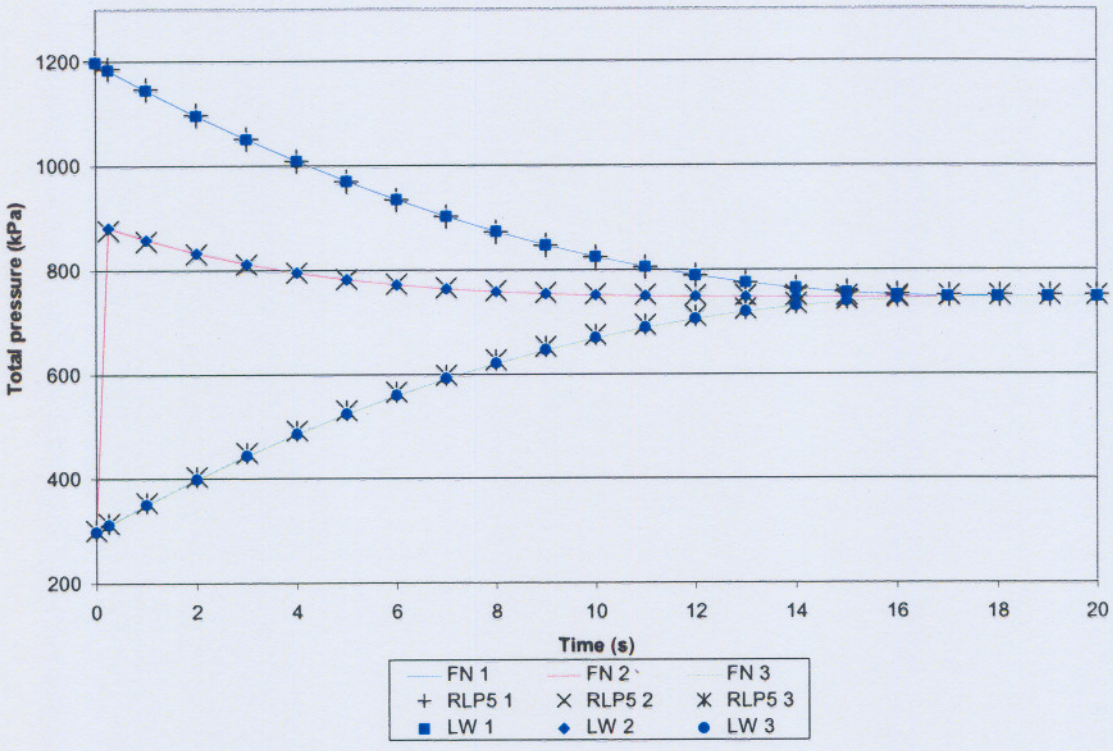


Figure 4.15: *Total pressure variation during slow transient.*

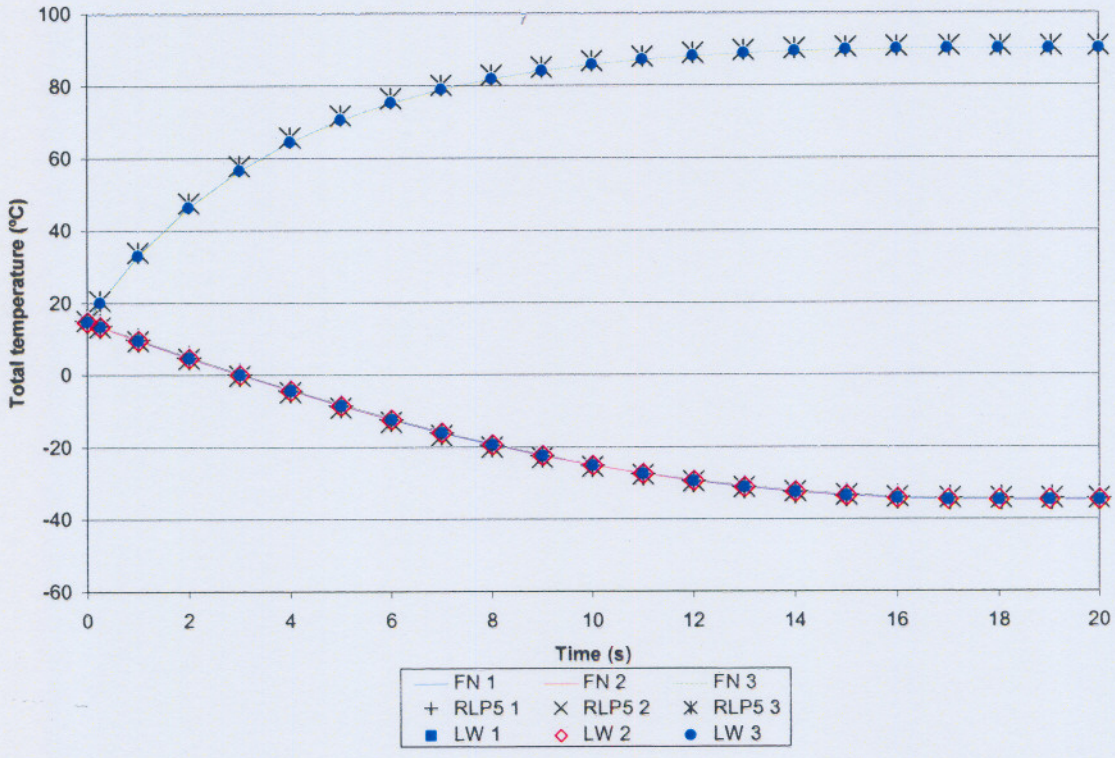


Figure 4.16: *Total temperature variation during slow transient.*

In Figure 4.15, the pressure in the middle of the pipe is seen to be higher than the average value. As the transient progresses and the fluid velocity decreases, this phenomenon diminishes. This is due to the pressure distribution in the pipe at high Mach numbers. For high Mach numbers, the largest pressure drop due to friction is found at the end of the pipe. Due to the pressure change in each tank, the total temperature in Tank 1 drops and increases in Tank 3. This explains the resulting temperatures seen in Figure 4.16. The only serious anomaly was found where RELAP5 deviates at high Mach numbers in Figure 4.17, position 3.

Solution times for each code are given in Table 4.10. It is interesting to note that the solution times for Flownet and Lax-Wendroff are comparable when time step sizes differ by a factor of 50.

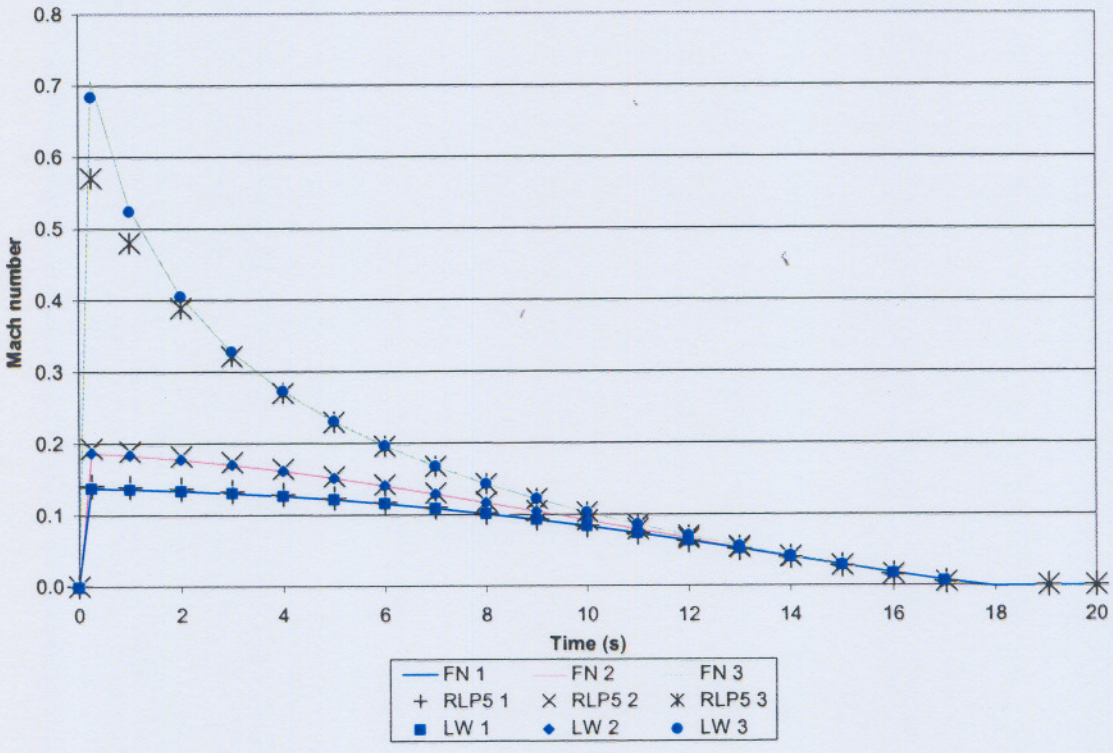


Figure 4.17: *Mach number variation during slow transient.*

Code	Time Step (s)	Solution Time (s)
Flownet	0.01	89.7
Lax Static	0.00015	48.9
Lax Total	0.00015	49.5
RELAP5	Not constant	65.5

Table 4.10: *Solution time for slow transient between tanks.*

Up to this point, steady-flow and slow transients were considered. For the remainder of this chapter, attention will be given to fast transients.

4.6 Fast transients in a pipe

Fast transients usually occur after a rapid change in boundary condition or element characteristic. This sudden change can cause pressure waves moving through the pipe network. Momentum and frictional effects determine the amplitude and attenuation of these waves. A high system pressure will result in higher densities and larger momentum effects. This includes higher wave amplitudes and higher pressure gradients. Such a situation will thoroughly test each code's implementation of the transient momentum conservation equation.

For validation purposes, a pipe with $L/D = 100$ was chosen. The initial condition for the transient simulation was a steady-state solution with boundary conditions as given in Table 4.11.

L/D	$D(m)$	$L(m)$	$e(\mu m)$	$(p_o)_{in}(kPa)$	$(T_o)_{in}(°C)$	$(p_o)_{out}$
100	0.1	10	30	5 100	15	4 000

Table 4.11: *Steady-state input data for transient flow in pipes.*

After steady-state conditions are reached, a valve is closed instantaneously at the outlet of the pipe. Due to sudden deceleration of flow, the pressure increases at the valve end. This pressure increase proceeds to the inlet as a pressure wave. This simulation was done for adiabatic and isothermal flow as well as flow with positive and negative heat transfer.

For each of the transients a Crank-Nicolson parameter of 0.6 was used in Flownet (refer to paragraph 1.3 for a definition). A value of 0.5 would give the maximum accuracy (second-order accurate in time) for this method. Such a parameter value often results in dispersion problems with Flownet (Van Ravenswaay 1998:119). With a value of 0.6, some 'smoothing' of the transient will occur due to the lower order of the resulting method. For each case, the total pressure and temperature was plotted at the closed end and at the middle of the pipe ($0.5\,L$).

Figure 4.18 and Figure 4.19 show results for adiabatic flow at the valve and at $x = 0.5\,L$.

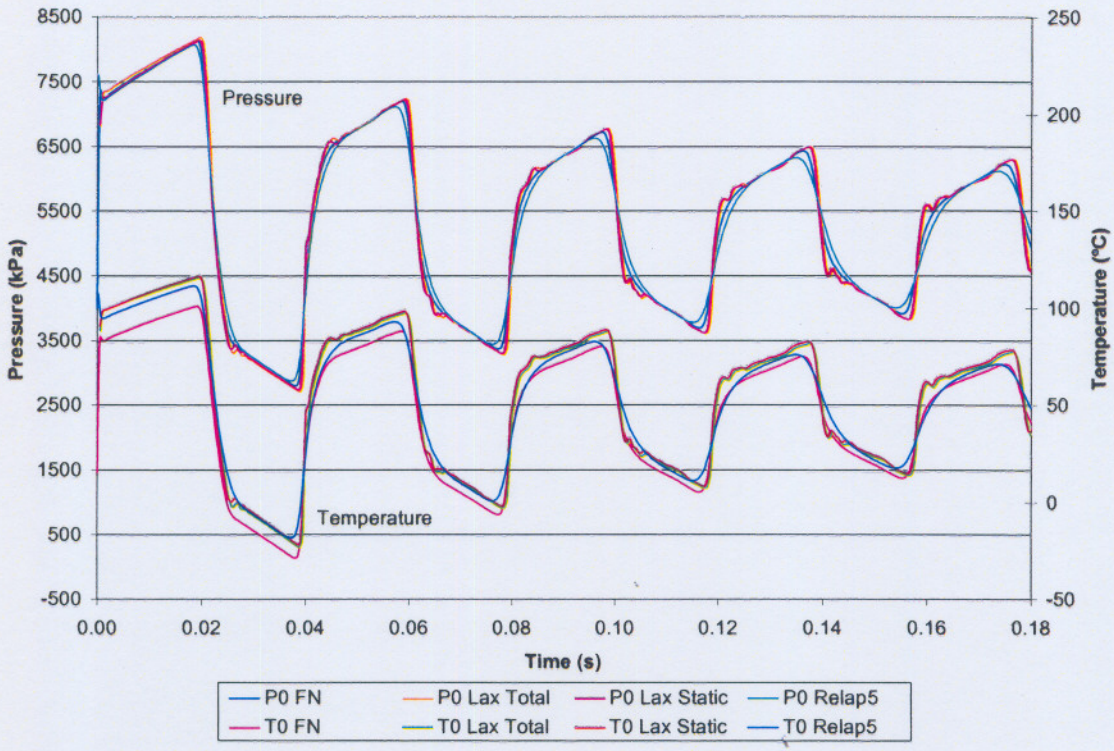


Figure 4.18: *Fast transient for adiabatic flow in a pipe, result at* $x = L$.

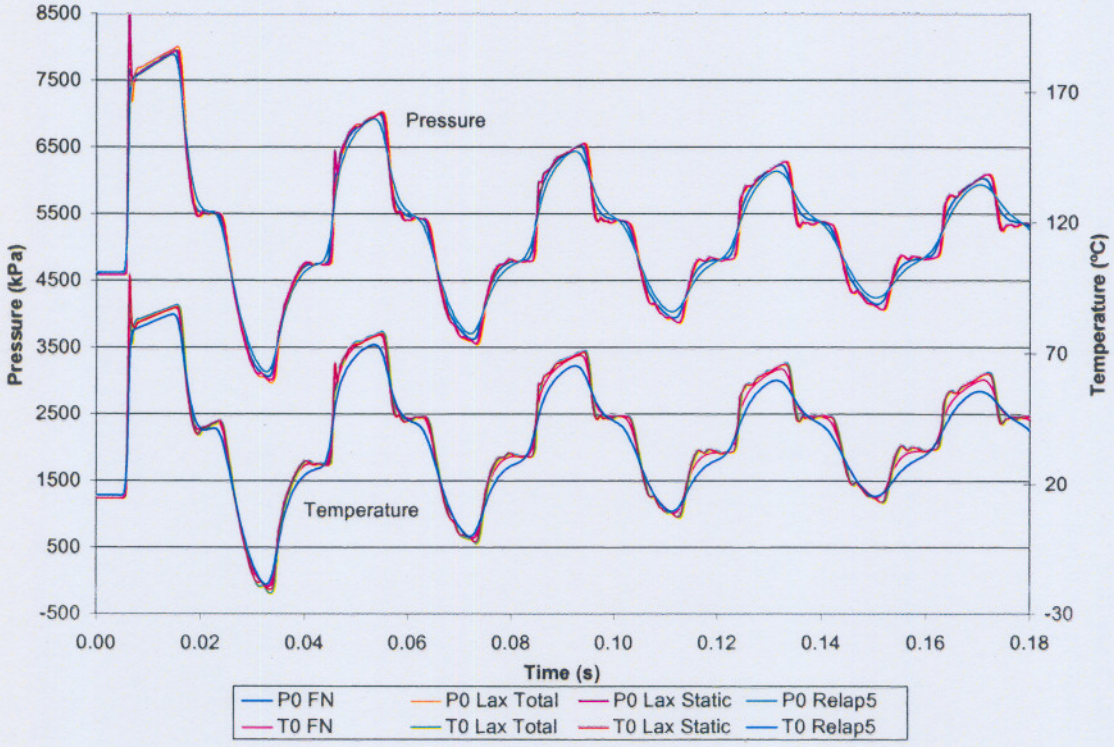


Figure 4.19: *Fast transient for adiabatic flow in a pipe, results at* $x = 0.5\,L$.

Results obtained with RELAP5, Flownet and Lax-Wendroff correspond very well. As time progresses, the results for RELAP5 and Flownet appear to be 'smoother' than those of Lax-Wendroff. The same effect is noticed in Figure 4.22 and Figure 4.23 for negative heat transfer.

For positive heat transfer, heat was transferred to the fluid at a rate of 10 MW. Results for positive heat transfer can be seen in Figure 4.20 and Figure 4.21.

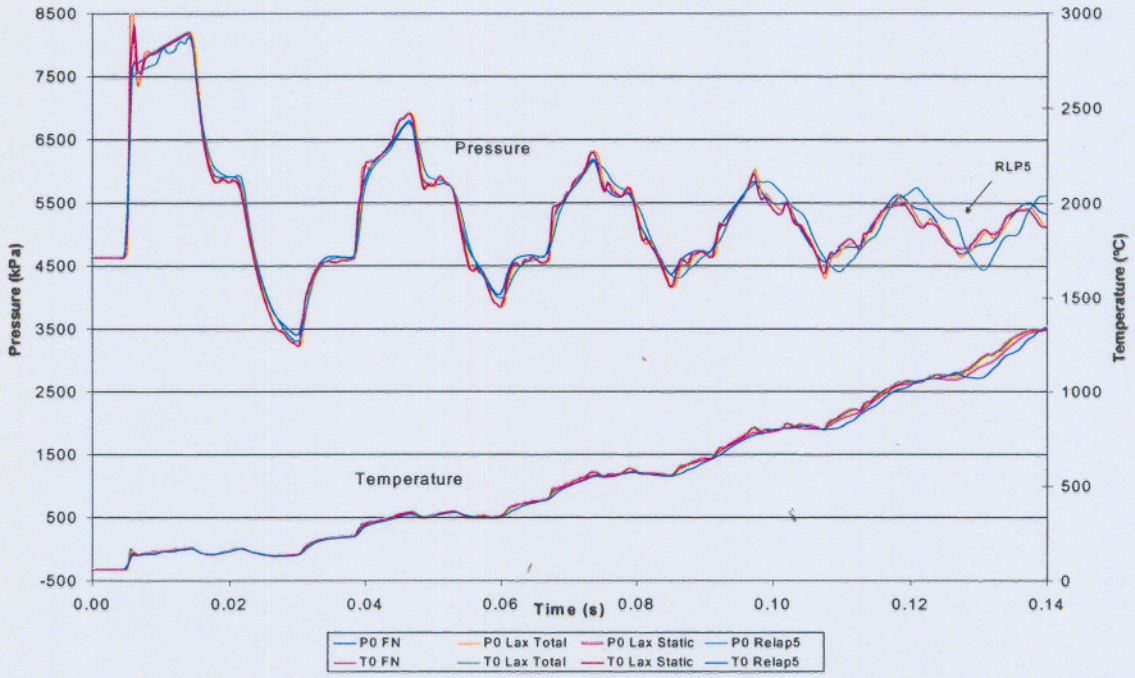


Figure 4.20: *Pipe fast transient with positive heat transfer, results at* $x = 0.5\,L$.

The frequency and amplitude calculated by RELAP5 differs increasingly as the transient progress. One must keep in mind that a slight deviation between codes will probably 'grow' as the solution progresses. This seems to be the case here. In Figure 4.21, a difference in total temperature was found between Flownet and the other two codes. This difference was found to occur only in the vicinity of the boundary node. A possible explanation could be the difference in boundary modelling between the codes.

By comparing Figure 4.18 and Figure 4.21, a difference in wave frequency is noticed between the adiabatic flow and positive heat transfer cases. For the positive heat transfer case, temperatures are higher. This results in a higher acoustic velocity in this pipe. Pressure waves will therefore propagate up and down the pipe at a higher speed.

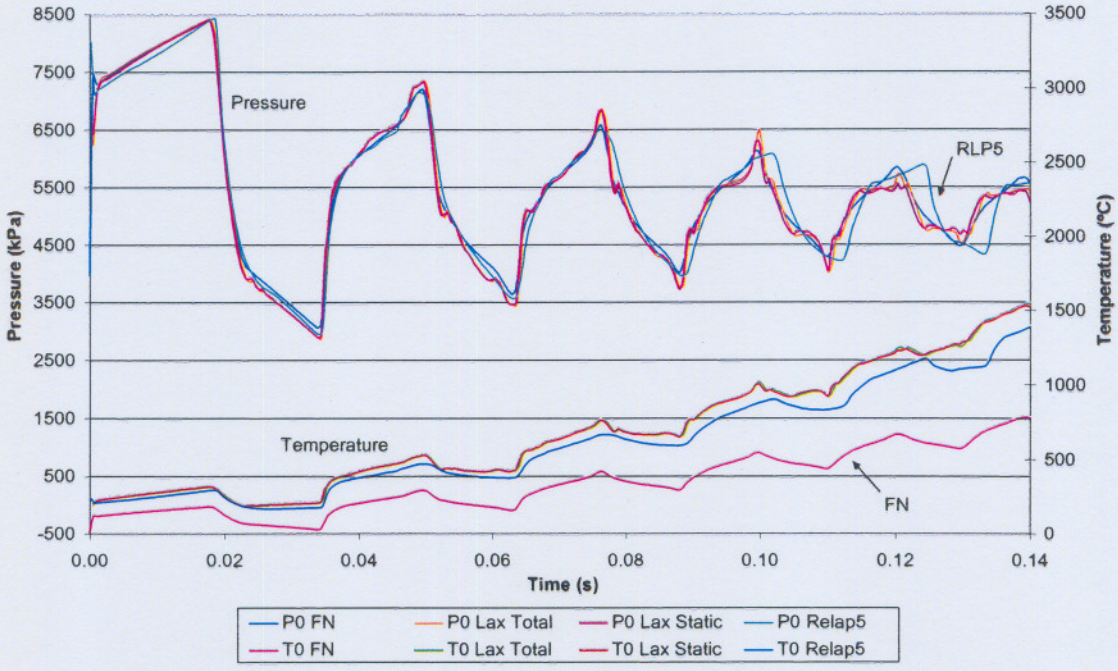


Figure 4.21: *Pipe fast transient with positive heat transfer, result at* $x = L$.

Heat was transferred from the fluid at a rate of 4 MW for the negative heat transfer case. Results are given in Figure 4.22 and Figure 4.23.

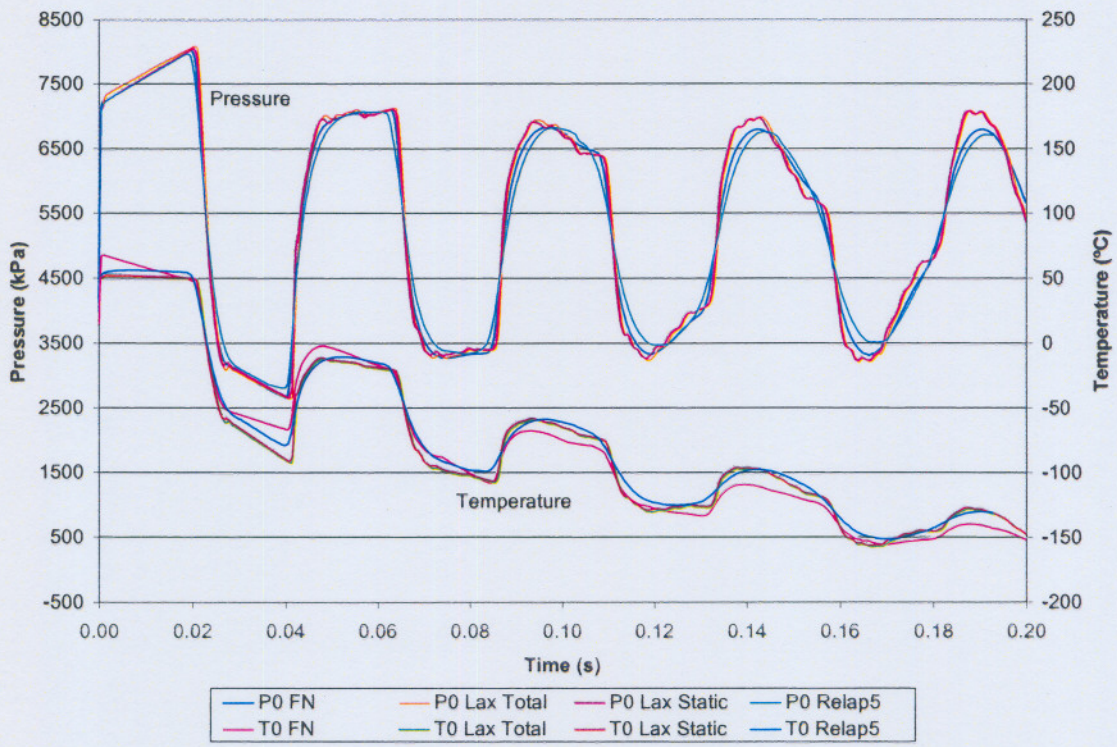


Figure 4.22: *Pipe fast transient with negative heat transfer, result at* $x = L$.

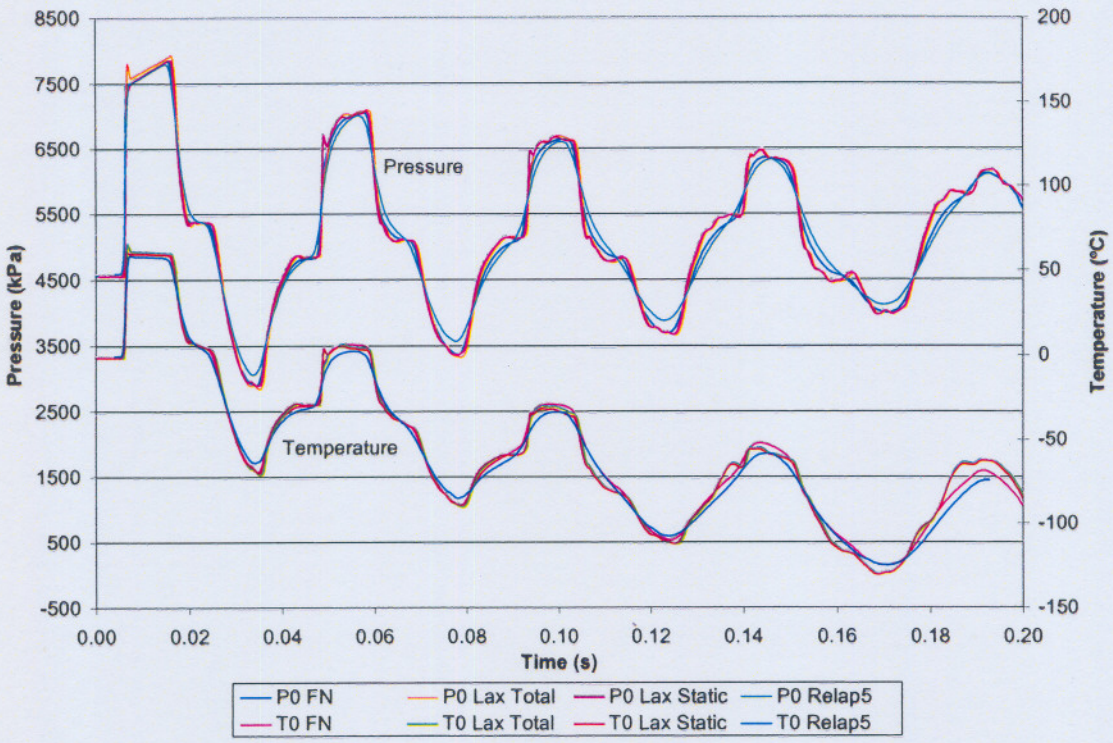


Figure 4.23: *Pipe fast transient with negative heat transfer, results at* $x = 0.5\,L$.

In this case, lower temperatures in the pipe lead to a lower acoustic velocity. This is the reason for a slightly lower wave frequency.

For isothermal flow, results are shown in Figure 4.24 and Figure 4.25. RELAP5 cannot model isothermal flow, and was not included in this case. For isothermal flow the static temperature was specified as 15 °C. With no velocity at the closed pipe end, the total temperature is equal to the static temperature. This is seen in Figure 4.24 with the total temperature remaining at 15 °C. In Figure 4.25, the variation in total temperature due to the fluid velocity can be seen. In Flownet this variation is not calculated, and is therefore plotted at a constant value of 15 °C. Total pressure and temperature calculated using Flownet and Lax-Wendroff compared well for the isothermal transient case.

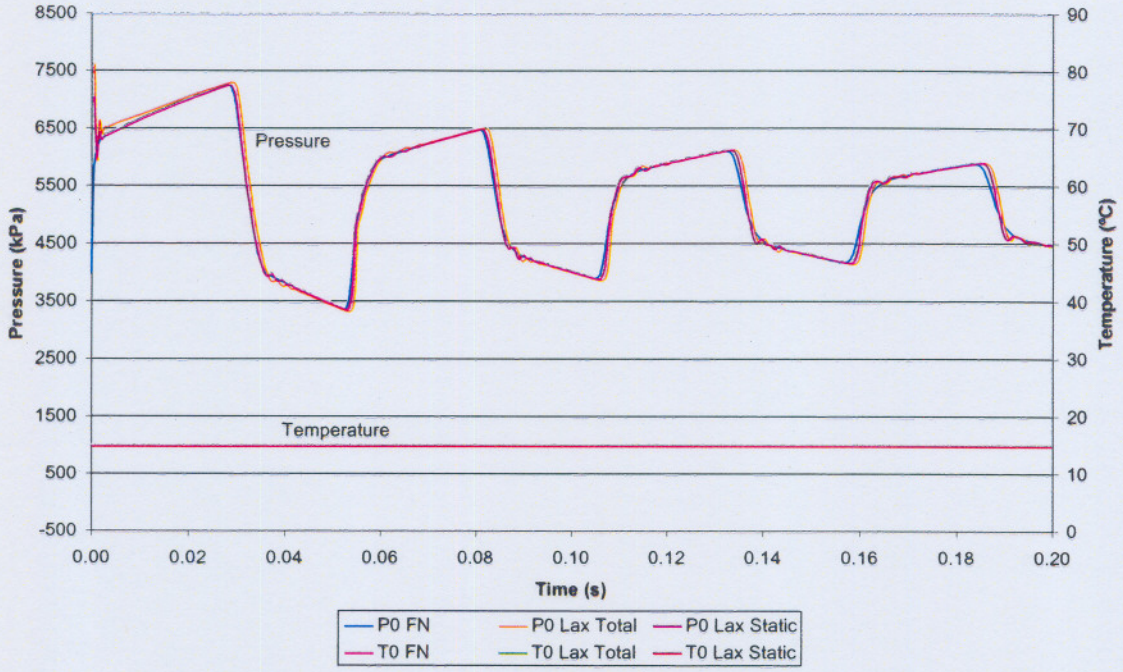


Figure 4.24: *Fast transient for isothermal flow in a pipe, result at* $x = L$.

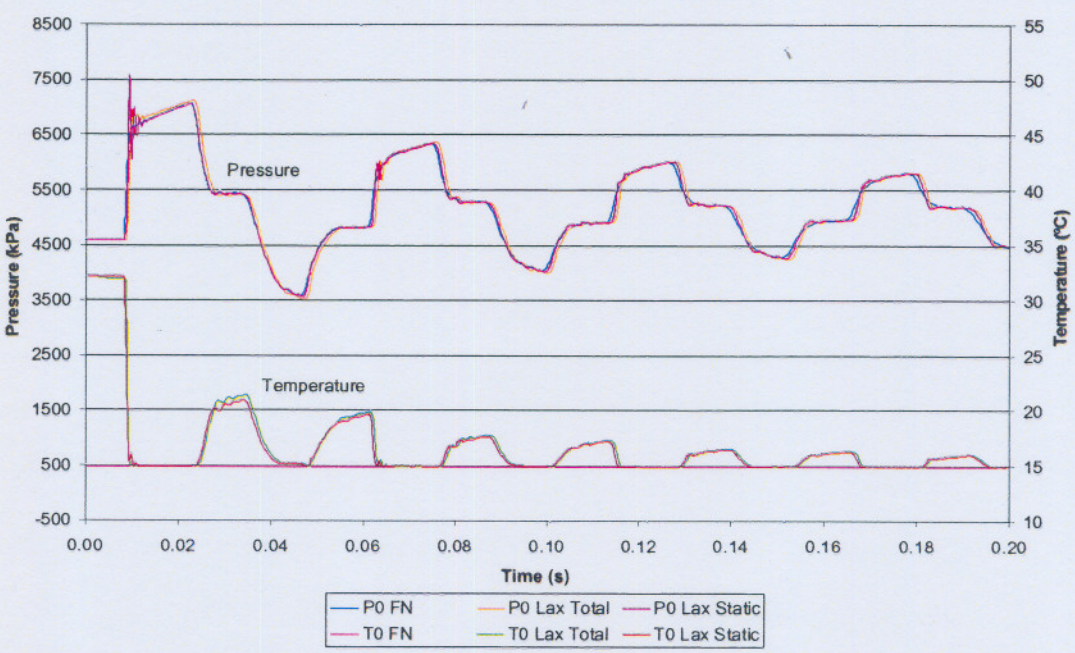


Figure 4.25: *Fast transient for isothermal flow in a pipe, results at* $x = 0.5\,L$.

In all of the above cases, transient flow was simulated for 0.2 s after the transient was started. The actual time each code took to reach steady-state conditions and to solve the transient is shown in Table 4.12.

Code	Adiabatic		+ Heat Tr.		− Heat Tr.		Isothermal	
	SS	Trans	SS	Trans	SS	Trans	SS	Trans
Flownet	1.25	363	1.36	867	1.34	289	1.00	64
Lax Static	1.90	2.24	2.67	4.47	1.38	1.67	1.90	2.16
Lax Total	1.90	2.34	2.28	4.44	1.31	1.72	1.34	2.72
RELAP5	43.8	43.8	86.5	86.5	34.2	34.2		
Time step (s)	6.5e-005		3.2e-005		8.5e-005		6.5e-005	

Table 4.12: *Solution time for transients in pipes.*

In each case, the same time step was used for every code. The time step was calculated using a Courant number of approximately 0.7. RELAP5 has the capability to adjust its time step as the transient progresses. However, the time step sizes it calculated independently gave inaccurate smoothed results. The time steps in the table were therefore enforced and gave more accurate results. To reach steady-state conditions, RELAP5 was run for 0.2 s with an open valve. The same time step was used for the steady-state and transient parts of the analysis.

From Table 4.12, the advantage of using an explicit method when shorter time steps are required, is apparent.

4.7 Fast transients through an orifice

In paragraph 4.4, a loss factor of 10 gave a larger pressure drop across the orifice than across each pipe. For the transient analysis of an orifice, the same pipe geometry will be used with this loss factor of 10. The average system pressure will, however, be increased. This is done to increase momentum effects and decrease wave attenuation.

Steady flow for each code was reached with an inlet pressure of 8 MPa, an outlet pressure of 4 MPa and an inlet temperature of 15 °C. A valve is then instantly closed at the downstream end of the pipe. The total pressure and temperature is plotted against time at the closed pipe end, orifice outlet and at the orifice inlet. These results are plotted in Figure 4.26, Figure 4.27 and Figure 4.28 respectively.

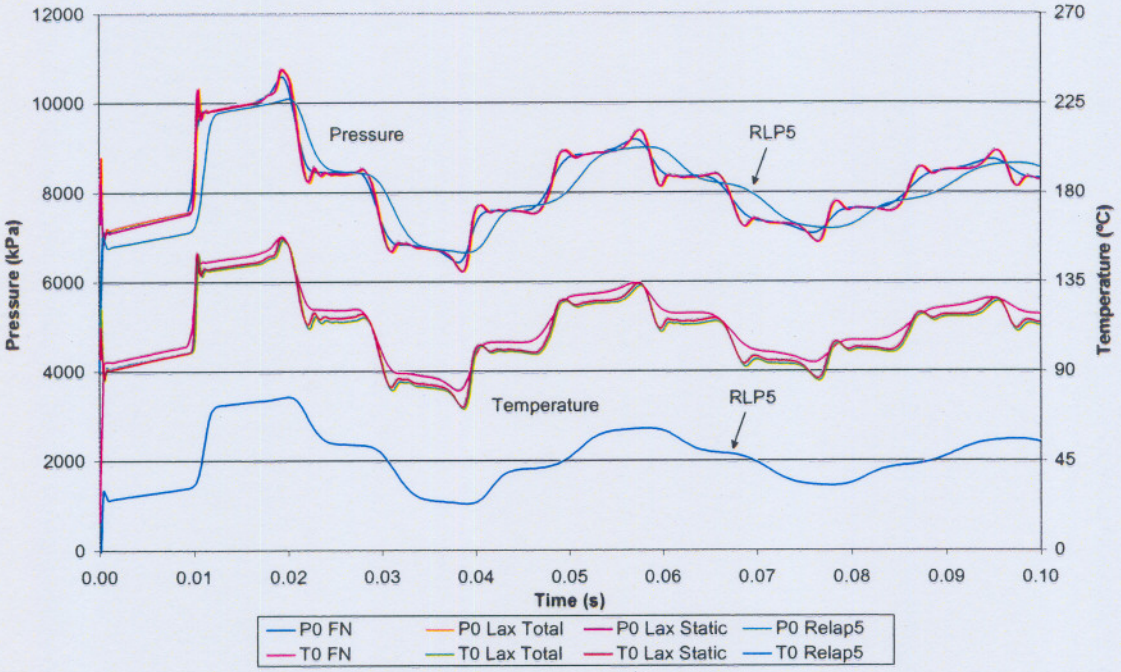


Figure 4.26: *Transient flow through an orifice, result at* $x = L$.

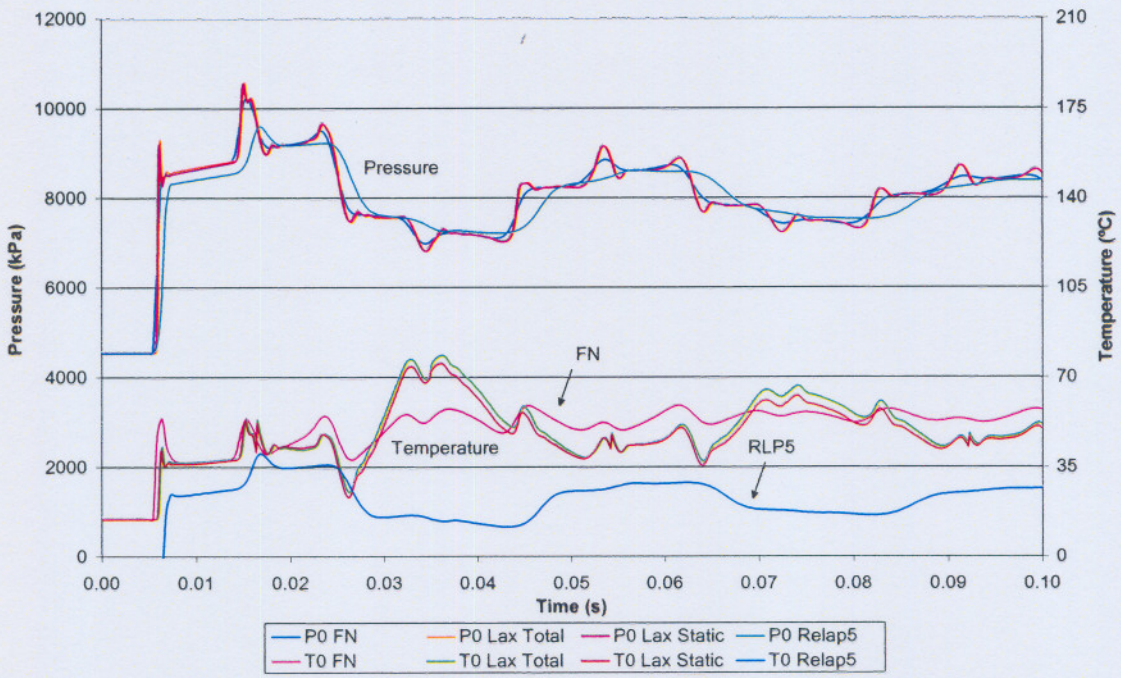


Figure 4.27: *Transient flow through an orifice, result at orifice outlet.*

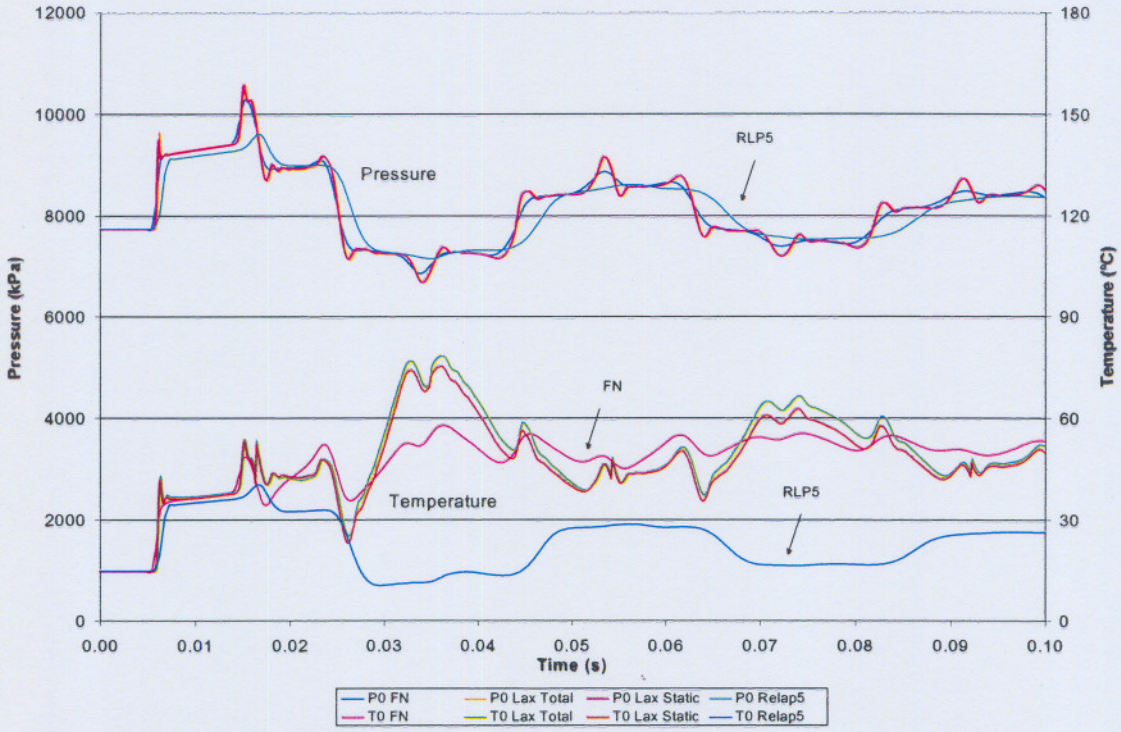


Figure 4.28: *Transient flow through an orifice, result at orifice inlet.*

In paragraph 4.4, it was seen that RELAP5 gave a lower orifice outlet total temperature for steady flow. This affects the transient results obtained in this paragraph. RELAP5 gives lower than actual total temperatures at the orifice outlet and the closed pipe end (Figure 4.27 and Figure 4.26). Initially, the total temperature at the orifice inlet (Figure 4.28) compares well for all three codes. As soon as the flow reverses, the lower total temperature helium in RELAP5 passes through the orifice and causes the anomaly seen in Figure 4.28. Notice how the pressure wave simulated in RELAP5 has a lower frequency due to the overall lower temperatures in the pipe.

A larger than normal difference was found between the total temperatures calculated by Lax-Wendroff and Flownet just before and after the orifice. A possible cause is the difference in boundary conditions modelling between the two codes.

For each code, a time step of $\Delta t = 7\times10^{-5}$ was used for transient flow after valve closure. This implies an equivalent Courant number of 0.7 at 170 °C. Steady-state and transient solution times for each code are given in Table 4.13. Here the advantage in terms of computational time of an explicit method when simulating fast transients is also apparent.

Code	Duration (s)	
	Steady-state	Transient
Flownet	1.74	168.9
Lax Static	40.7	9.7
Lax Total	61.6	9.5
RELAP5	60.0	20.0
Time step (s)	7×10^{-5} s	

Table 4.13: *Solution time for transient flow through an orifice.*

4.8 Effect of discretization

For any finite difference or finite volume scheme, it is important to obtain a grid independent solution. In this paragraph, the effect of grid coarseness is studied for each code. This is done for steady-state and transient flow.

4.8.1 Steady-state flow

For steady flow, grid sensitivity was determined at different pipe exit Mach numbers. For each case, the minimum number of elements/nodes needed to stay within a 1% error margin of the specified outlet Mach number was determined (nodes=elements+1). For this analysis, the same pipe geometry as in paragraph 4.3 was used with $L/D=100$. A constant total outlet pressure of 300 kPa was used with an inlet total temperature of 15 °C. The inlet total pressure was varied to obtain different outlet Mach numbers. The required inlet total pressure to obtain a given outlet Mach number was calculated analytically using the same method as in paragraph 4.3. Outlet Mach numbers with corresponding inlet total pressures are given in Table 4.14.

M_{out}	0.1	0.2	0.3	0.4	0.5	0.6	0.7	0.8	0.9	0.95
$(p_0)_{in}$ (kPa)	368.9	509.1	665.8	814.8	944.8	1050.8	1130.7	1184.9	1215.3	1222.4

Table 4.14: *Boundary conditions used in steady-state grid analysis.*

Results are given in Table 4.15 and shown graphically in Figure 4.29.

Mach Number	Number of Nodes			
	Flownet	RELAP5	Lax Total	Lax Static
0.1	2	3	3	3
0.2	2	4	3	3
0.3	2	6	3	3
0.4	2	6	3	3
0.5	2	6	4	3
0.6	2	-	6	5
0.7	2	-	8	6
0.8	3	-	12	11
0.9	5	-	39	22
0.95	7	-	115	62

Table 4.15: *Nodes required to stay within 1% of analytical solution.*

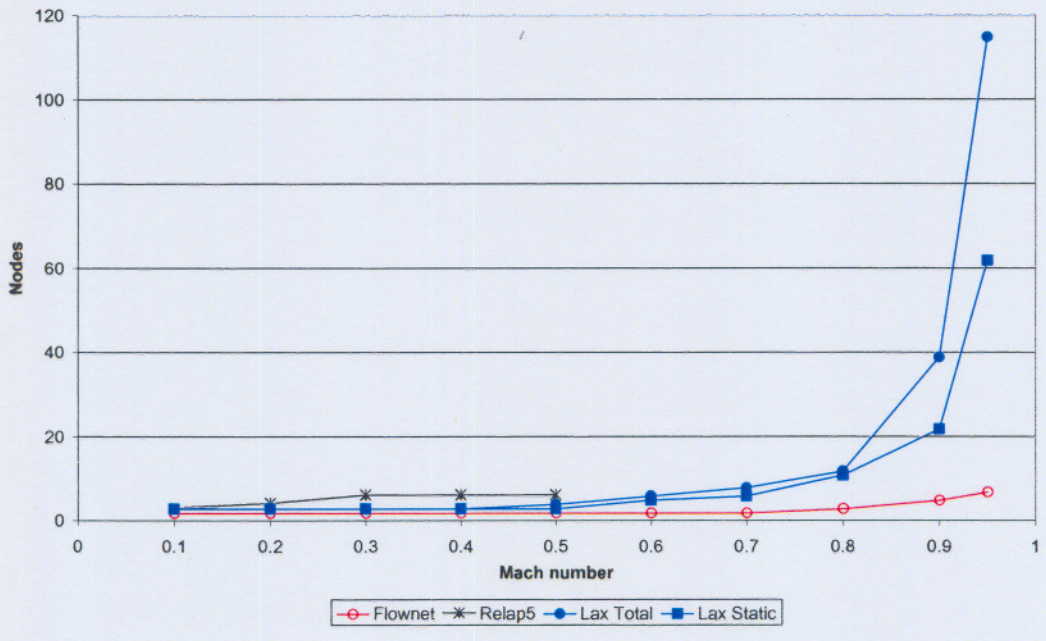


Figure 4.29: *Required discretization at different Mach numbers.*

At Mach numbers of 0.6 and higher, RELAP5 was not able to give results that are within the specified range of accuracy. Flownet clearly requires substantially fewer elements to obtain the same or a better result as RELAP5 and Lax-Wendroff.

4.8.2 Transient flow

As no analytical solution exists for transient flow, each code was evaluated on its own merit. For each code, a grid independent solution was obtained by subdividing a pipe into 80 sections. Solving networks with this amount of subdivision would be very time-consuming. One would prefer to obtain an acceptable solution with the minimum amount of subdivisions. This is referred to as the ***grid-sensible*** solution.

A transient solution was defined as a grid-sensible solution if the first maximum amplitude deviates by < 5% and the fifth maximum by < 50% from the grid independent solution. This deviation is defined as

$$Err = \left(p_{0,ind} - p_{0,s}\right) / \left(p_{0,ind} - p_{0,inlet}\right) \tag{3.47}$$

where $p_{0,ind}$ is the total pressure of the independent solution, $p_{0,s}$ the grid-sensible solution, and $p_{0,inlet}$ the inlet or final total pressure. Figure 4.30 illustrates this concept for a grid-sensible solution using Flownet.

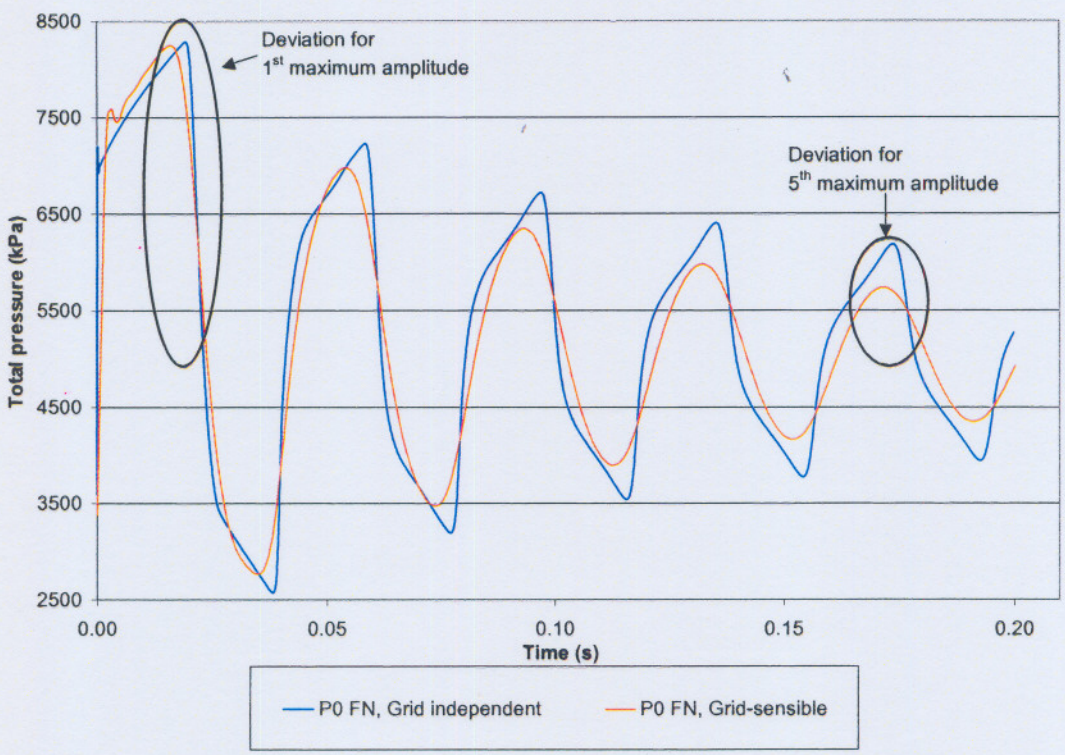


Figure 4.30: *Deviation between grid independent and grid-sensible solutions.*

For this particular example, the fifth total pressure deviation (40%) was the limiting value. For a coarser grid, this deviation exceeded 50%.

The scenario simulated is similar to the simulations done in paragraph 4.6. A pipe with the same geometry ($L/D = 100$) was used. Steady flow is simulated, after which a valve is closed at the outlet. Various steady-state initial conditions were used to simulate flow for outlet Mach numbers ranging from 0.1 to 0.95. The inlet total pressure for these simulations was kept at 5 000 kPa. This ensured that the final pressure ($p_{0,inlet}$) before the valve is the same for all the simulations. Required outlet total pressure values for a given Mach numbers were calculated analytically using the same method as in paragraph 4.3. Outlet Mach numbers with associated outlet total pressure values are given in Table 4.16.

M_{out}	0.1	0.2	0.3	0.4	0.5	0.6	0.7	0.8	0.9	0.95
$(p_0)_{in}$ (kPa)	4 938.0	4 766.9	4 521.7	4 247.4	3 984.3	3 759.9	3 587.1	3 468.2	3 400.4	3 384.2

Table 4.16: *Boundary conditions used in transient grid analysis.*

Results showing the number of nodes required to obtain a grid-sensible solution are presented in Figure 4.31.

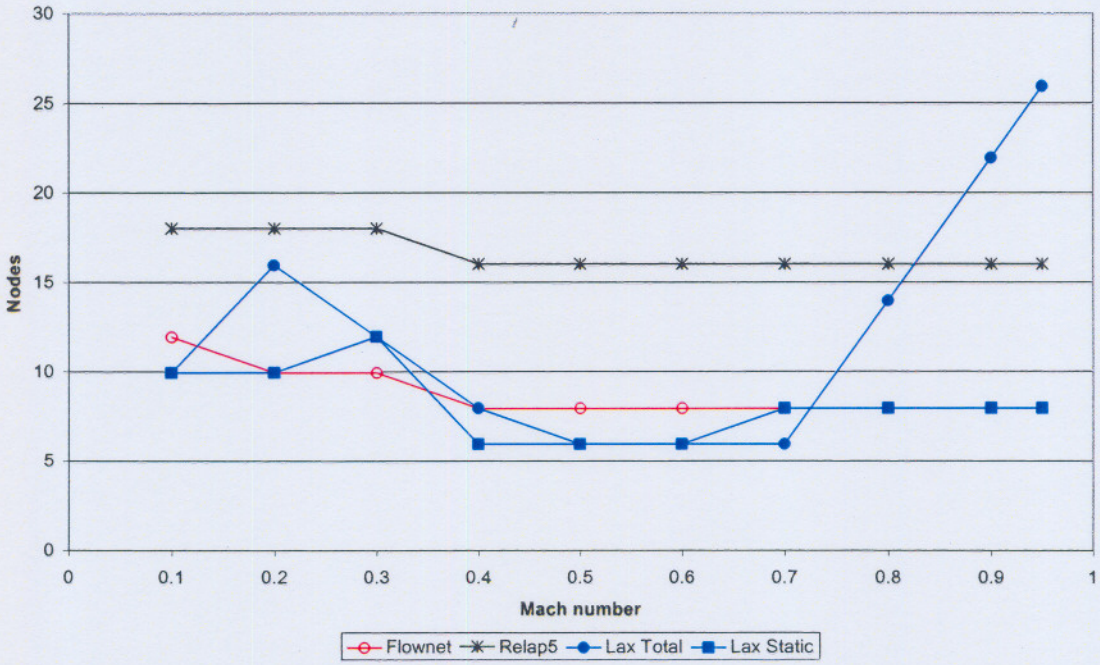


Figure 4.31: *A grid-sensible solution at different Mach numbers.*

Flownet and the Lax-Wendroff method based on static pressures required fewer subdivisions to obtain a grid sensible solution. For the steady state and transient

results, the Lax-Wendroff method based on total pressure under performed in comparison to the static version. This is due to the different way in which average values for the first time step are calculated in the momentum equation.

4.9 Conclusion

In this chapter, various aspects of Flownet were validated for steady-state and transient flow. This was accomplished by using analytical solutions where possible, as well as benchmarking Flownet against RELAP5 and the explicit Lax-Wendroff method. Some of the aspects that were validated include:

- boundary conditions;
- compressible flow in pipes with and without heat transfer as well as isothermal flow;
- flow through non-inertial elements; and
- tanks.

Some differences were found between RELAP5 and analytical solutions at high Mach numbers. A problem with energy conservation in RELAP5 when solving flow through an orifice was also discussed. Where these anomalies did not impact on the solution, a good comparison was found between Flownet, Lax-Wendroff and RELAP5. Where these anomalies did have an impact, Flownet and Lax-Wendroff still compared well.

Some differences were noted, but these had very little or no impact on the validity of using Flownet to model the PBMR. These differences were found for isothermal flow at high Mach numbers and total temperature values for fast transients at pipe boundaries. The latter was a localized effect only found when little or no flow crossed the boundary, together with fast pressure transients at the boundary.

In the last paragraph of this chapter, attention was given to grid size sensitivity. For steady-state flow, Flownet gave superior results with less grid points (elements) than the other codes. In the transient case, the grid refinement necessary to obtain a satisfactory solution was similar to the Lax-Wendroff method, based on static pressures.

With the basic building blocks of Flownet validated, attention will now be given to the validation of junctions and arbitrary structured networks.

CHAPTER FIVE: COMPARATIVE STUDY FOR ARBITRARY STRUCTURED NETWORKS

5.1 Introduction

One further aspect that requires validation before considering arbitrary structured networks, is flow through junctions. In this chapter, the results of benchmarking flow through junctions are given for steady-state and transient flow. Subsequently, all validated aspects or models are then used in an arbitrary structured network. Steady and transient results are then compared for this network. In Chapter 4, no significant difference was found between the Lax-Wendroff implementations based on static and total pressures. In this chapter, only results obtained using the implementation based on static pressures are therefore given.

5.2 Slow transient through a junction

One can easily show that conservation of mass, energy and momentum is satisfied by comparison with analytical results. A simple way to test this over a range of conditions is to consider a quasi-steady blow down between three tanks. Figure 5.1 shows the network used in Flownet.

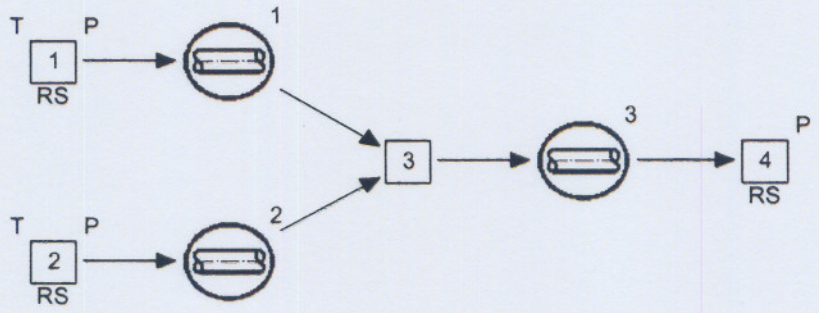


Figure 5.1: *Flownet network for quasi-steady blow down.*

The input data for the network is given in Table 5.1. Each pipe was subdivided into 10 increments. Initially the pressures and temperatures at tanks 1, 2 and 3 are fixed to obtain a steady-state solution. For this initial solution the results are compared in Table 5.2. Releasing the fixed pressure condition on the tanks results in a quasi-steady blow down.

Geometrical		Pressures (kPa)		Temperatures (°C)	
Length$_{1,2,3}$	100 m	P_{01}	9 000	T_{01}	15
Diameter$_{1,2,3}$	0.065 m	P_{02}	9 000	T_{02}	900
Volume$_{1,2,4}$	50 m^3	P_{04}	2 500	**Sub-incrementation**	
Roughness	30 μm			**Pipe$_{1,2,3}$**	10

Table 5.1: *Input to quasi-steady blow down network.*

Code	P_{03} (kPa)	T_{03} (°C)	m1 (kg/s)	m2 (kg/s)	m3 (kg/s)
Analytical	8 251.88	307.04	3.034	1.495	4.529
Flownet	8 251.47	307.04	3.035	1.495	4.530
Lax-Wendroff	8 252.70	307.04	3.033	1.494	4.527
RELAP5	8 121.83	316.03	3.186	1.594	4.780

Table 5.2: *Steady-state initial results for quasi-steady blow down.*

During this blow down, the tank pressure and temperature results in Flownet were used as boundary conditions to calculate steady-state analytical solutions at regular time intervals. This was done using a similar approach to that described in paragraph 4.3. The junction total pressure is varied and the flow in the pipes solved iteratively until mass and energy conservation is satisfied at the junction. Engineering Equation Solver (EES) was used to find this analytical solution (F-Chart Software, 2003).

At each node, the total pressure and temperature were compared, as can be seen in Figure 5.2 and Figure 5.3 respectively. A comparison of the mass flow in each pipe is given in Figure 5.4.

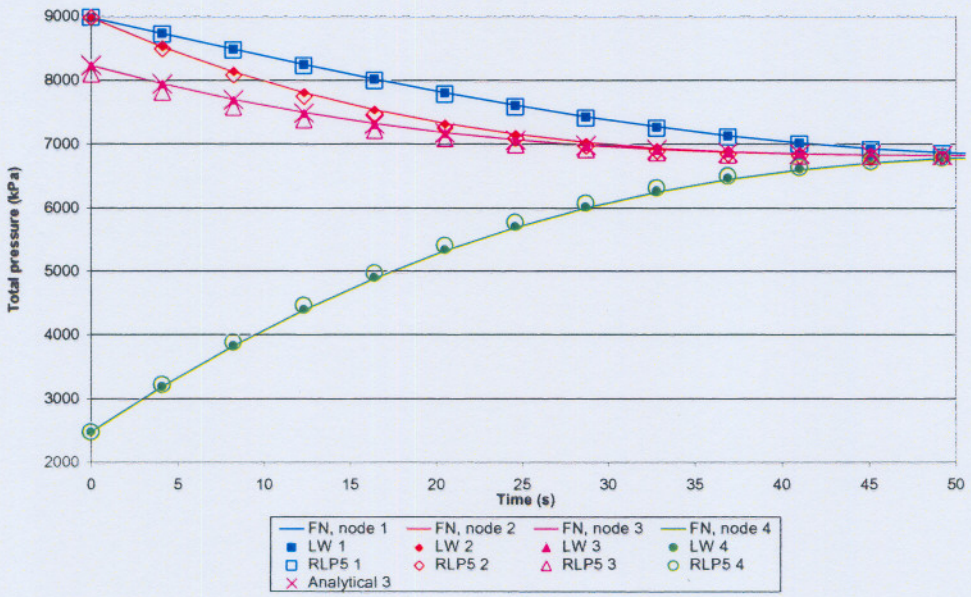


Figure 5.2: *P_0 vs. time for quasi-steady blow down.*

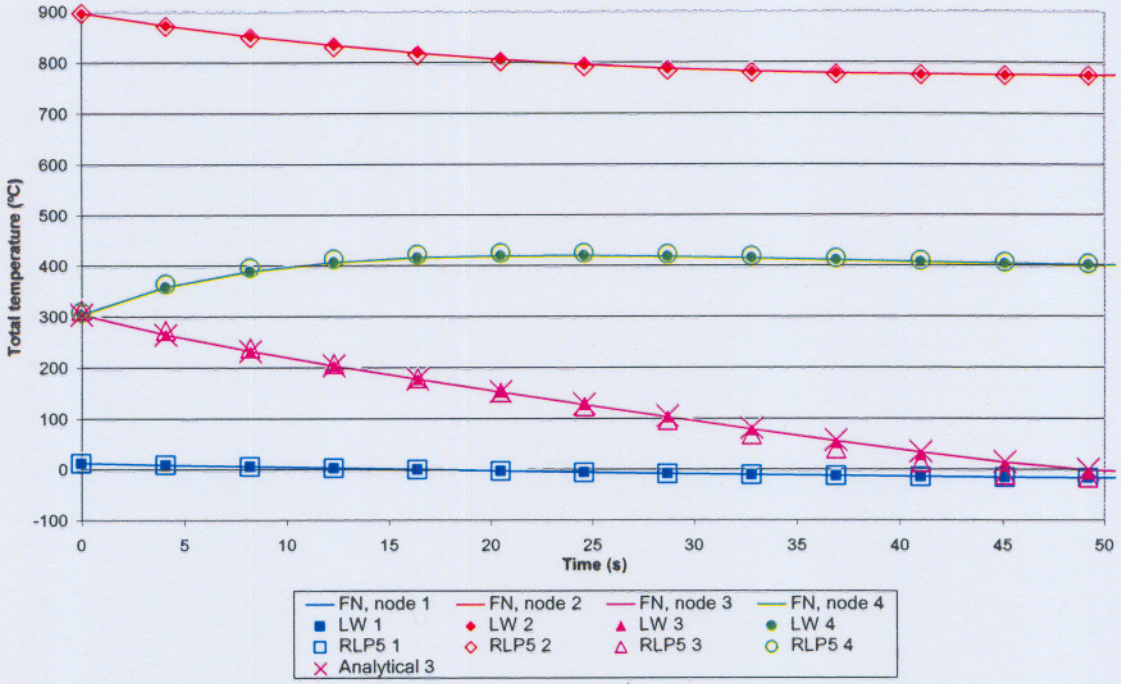


Figure 5.3: *T_0 vs. time for quasi-steady blow down.*

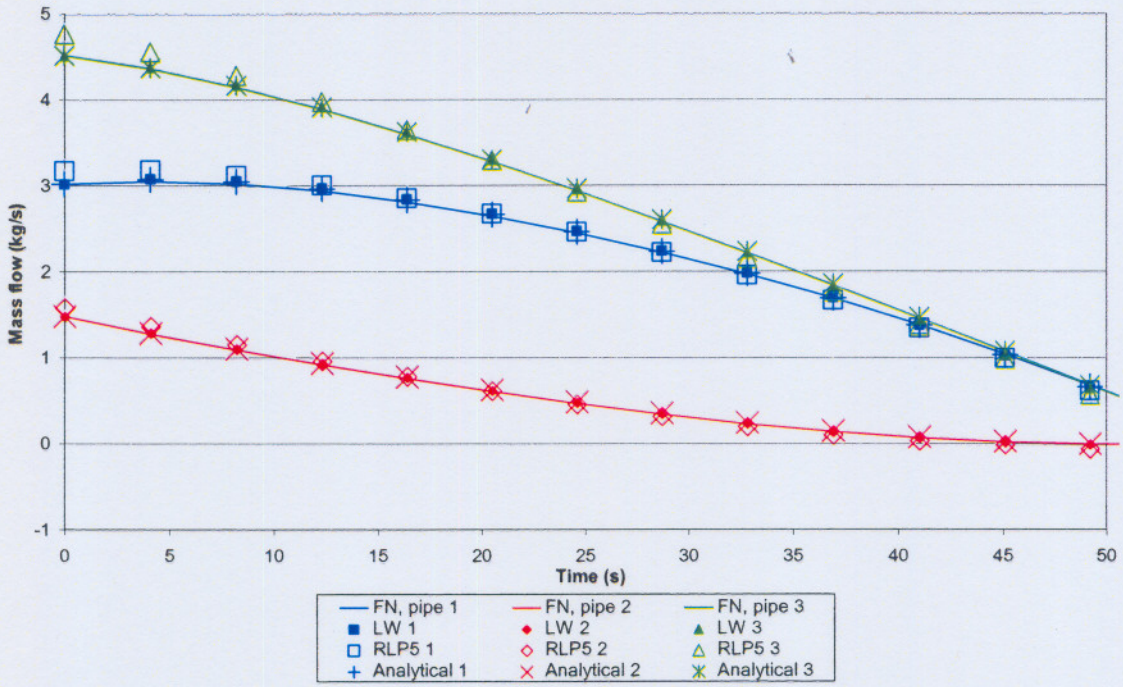


Figure 5.4: *Mass flow vs. time for quasi-steady blow down.*

In general, the results from RELAP5, Flownet, Lax-Wendroff and the analytical solution compare well. The slight deviation of RELAP5 can again be ascribed to the anomaly at high Mach numbers. It is interesting to note the initial

increase and later decrease in the temperature of Tank 4 (Figure 5.3). This occurs due to the large percentage of cold gas entering the tank at the end of the transient (refer to mass flow in pipe 1 Figure 5.4).

5.3 Fast transient through a junction

For transient flow through junctions, a similar configuration to that in the previous paragraph was used. Figure 5.5 shows the Flownet network used. The input to this network is given in Table 5.3. Forty subdivisions were used in each of the pipes. After reaching steady-state conditions, a valve is instantaneously closed at the downstream of Pipe 3. A summary of the steady-state initial solution is given in Table 5.4.

The transient total pressure and total temperature response at Node 3 and 4 is given in Figure 5.6 and Figure 5.7 respectively. In Figure 5.8, the mass flow at the downstream of Pipe 2 and the upstream of Pipe 3 is compared. Transient results obtained with RELAP5 seemed unrealistic, and will therefore not be presented here.

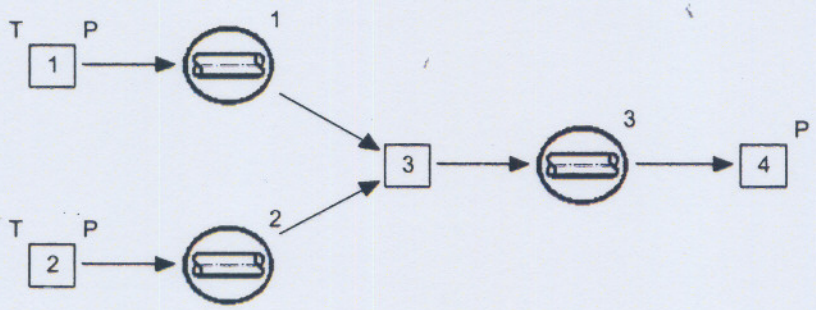


Figure 5.5: *Flownet network for transient flow through a junction.*

Geometrical		Pressures (kPa)		Temperatures (°C)	
Length$_{1,2,3}$	5 *m*	P_{01}	9 000	T_{01}	15
Diameter$_{1,2,3}$	0.065 *m*	P_{02}	9 000	T_{02}	15
Roughness	30 μm	P_{04}	7 000		

Table 5.3: *Input to transient junction network.*

Code	P_{03} (kPa)	T_{03} (°C)	m1 (kg/s)	m2 (kg/s)	m3 (kg/s)
Analytical	8 698.04	15.00	8.6089	8.6089	17.2177
Flownet	8 698.04	15.00	8.6089	8.6089	17.2177
Lax-Wendroff	8 698.04	15.00	8.6089	8.6089	17.2178
RELAP5	8 704.89	15.09	8.5558	8.5558	17.1120

Table 5.4: *Steady-state initial results for transient junction network.*

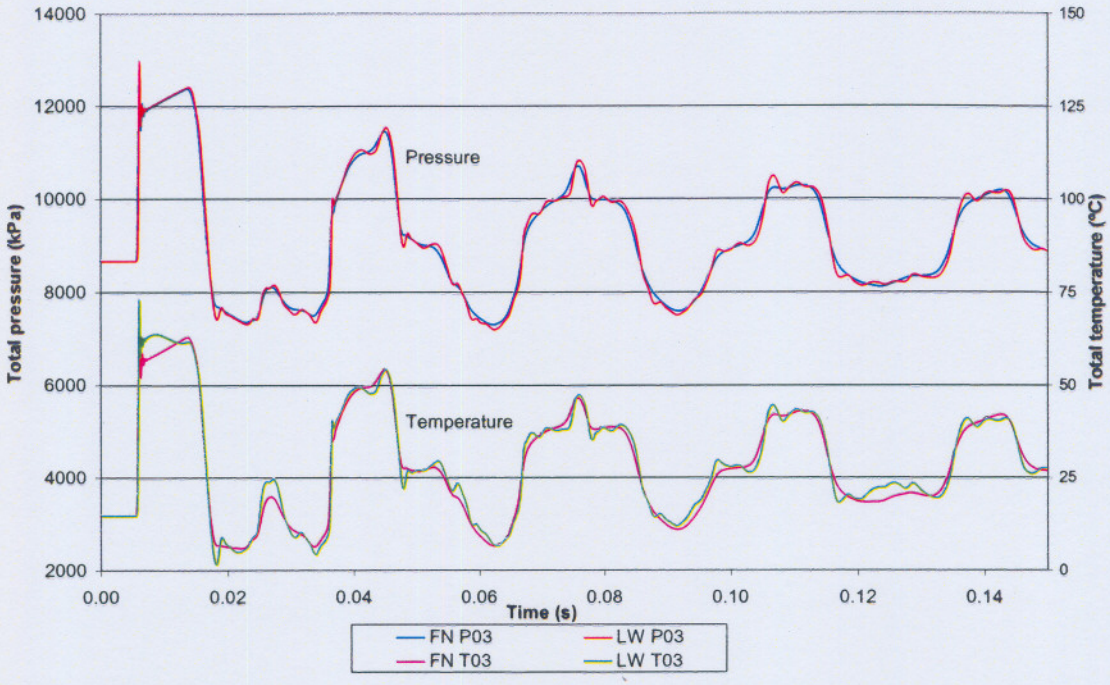


Figure 5.6: *P_0 and T_0 vs. time for transient junction network – Node 3.*

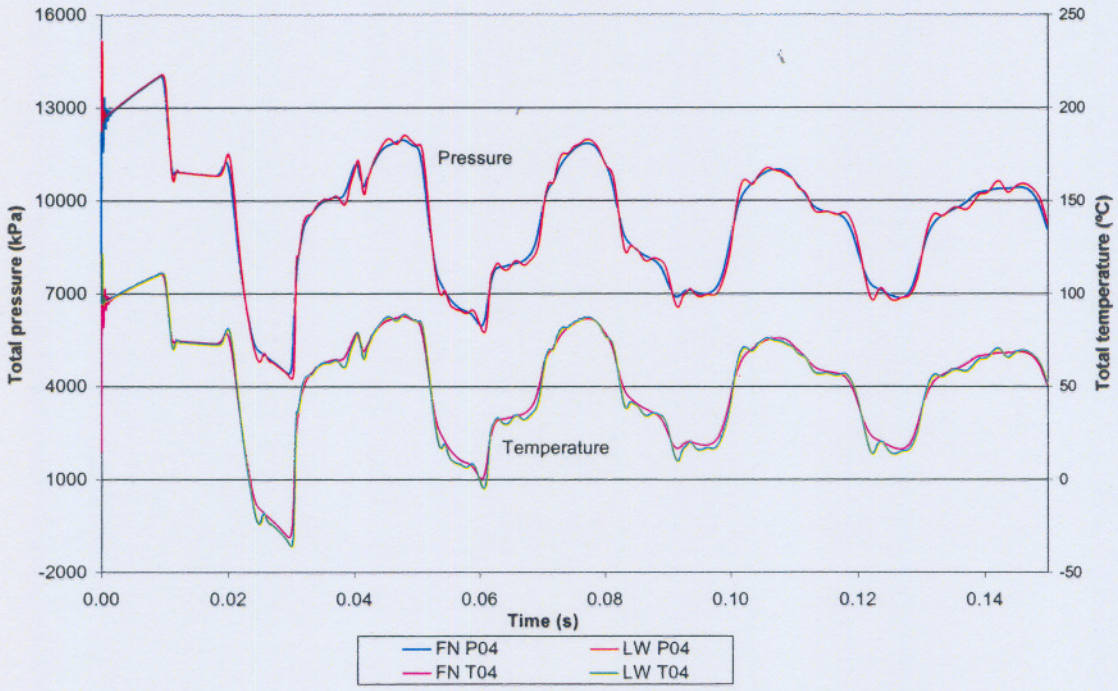


Figure 5.7: *P_0 and T_0 vs. time for transient junction network – Node 4.*

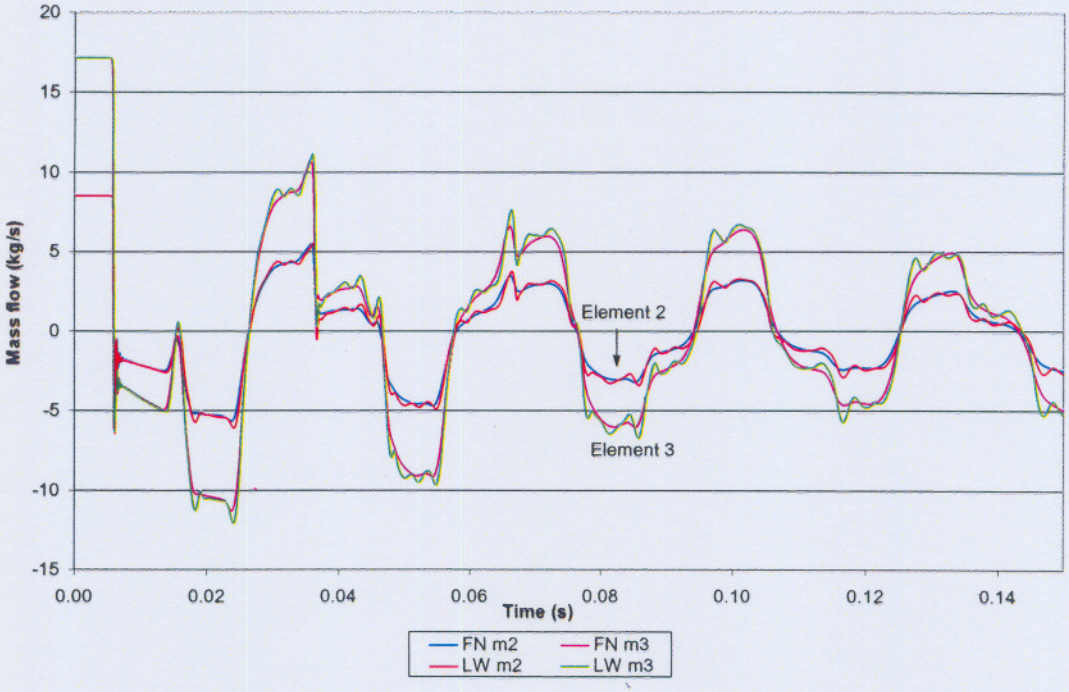


Figure 5.8: *Mass flow vs. time for transient junction network.*

With the network being symmetrical, the mass flow at the downstream of pipe 2 will be the same as in pipe 1. Consequently, the upstream mass flow of pipe 3 should be approximately twice as much as the downstream value in pipe 2, as can be seen in Figure 5.8. Results obtained using Flownet and Lax-Wendroff compared very well. With steady and transient flow through junctions benchmarked, more complex networks will now be evaluated.

5.4 Steady-state flow in a complex network

In setting up an arbitrary structured network to validate Flownet, the following should be considered:

- As many as possible of the aspects validated thus far should be included.
- It should be a closed loop, i.e. the net flux of mass and energy across the networks' boundary should be zero.
- After initiating a transient, the simulation should run to a new steady-state. At this new steady-state, a comparison should serve as a test for transient energy and mass conservation.

In Figure 5.9, the network that was chosen is shown as it was drawn in Flownet. Mass is circulated through this network by Element 10. This element serves no other purpose than to remove mass from Node 11 and add it to Node 15. For a closed network such as this, the pressure needs to be specified somewhere in the network. Specifying the pressure fixes the total mass in the in the system. Node 16 was chosen for this purpose, as it does not form part of the main flow path. If mass is conserved for steady flow, the flow in Element 8 will be zero. Volumes (tanks) were specified at Nodes 13, 14 and 16. Various combining and dividing junctions (11, 12, 13, 14, 15) are used to connect pipes with different lengths. An orifice also connects to Node 13, which includes the effect of a non-inertial element.

10 MW of heat is removed from Pipe 2 and 10 MW is added to Pipe 3. By specifying the temperature at Node 15, the energy level (temperatures) of the network is determined. If energy is conserved, the helium entering Pipe 10 will have the same total temperature as the specified value of Node 15. A very short Pipe 11 was added to initiate a transient that will be discussed in the next paragraph. This pipe is short enough to have no influence on the steady-state results of this network. To ensure the same temperature is used at the beginning of the transient simulation, the temperature in Node 16 was fixed for each code.

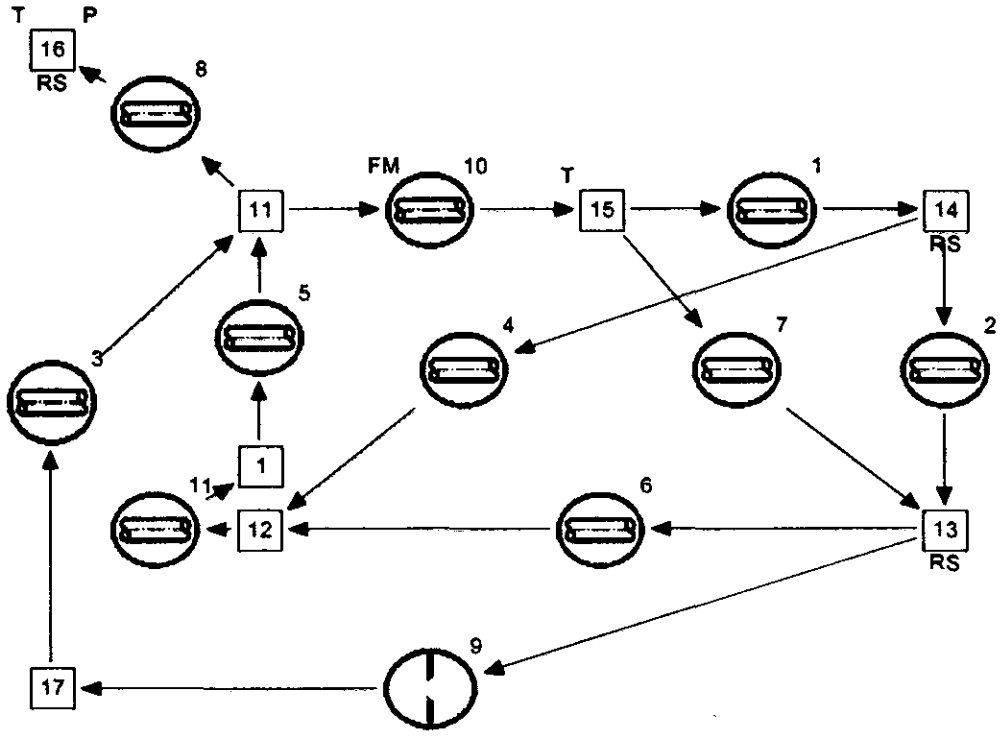


Figure 5.9: *Flownet arbitrary structured network.*

All pipes were sub-incremented into 0.25 m sections. The inputs that were used to construct this network are summarized in Table 5.5.

Geometrical		Pressures (kPa)	
$Length_{1,2,3}$	5 *m*	**$P0_{16}$**	7000
$Length_{4,5}$	15 *m*		
$Length_{6,7,8}$	10 *m*	**Temperatures (°C)**	
$Diameter_{all}$	0.065 *m*	**$T0_{15}$**	500
Roughness	30 μm	**$T0_{16}$**	500
$k\text{-}loss_9$	1	**Mass flow (kg/s)**	
$Volume_{3,4,6}$	10 m^3	**M_{10}**	10
Heat transfer pipe 2		-10 000 (kW)	
Heat transfer pipe 3		10 000 (kW)	

Table 5.5: *Input to arbitrary structured network.*

Using this network, steady-state solutions were calculated using Flownet, RELAP5 and the Lax-Wendroff method. These results are summarized in Table 5.6.

	Flownet	Lax-Wendroff	RELAP5
m1 (kg/s)	5.742	5.743	5.709
m2	3.822	3.823	3.735
m3	5.579	5.580	5.695
m4	1.920	1.919	1.974
m5	4.421	4.421	4.305
m6	2.501	2.502	2.331
m7	4.258	4.258	4.291
m8	0.000	0.000	0.000
m9	5.579	5.579	5.695
P011 (kPa)	7 000.00	7 000.00	7 044.45
P012	7 639.06	7 638.91	7 655.94
P013	7 745.54	7 745.44	7 770.34
P014	7 775.25	7 774.96	7 805.49
P015	8 184.54	8 184.34	8 176.72
P016	7 000.00	7 000.00	7 000.00
P017	7 539.12	7 538.97	7 571.58
T011 (°C)	500.00	500.00	509.26
T012	365.36	365.33	371.53
T013	261.99	262.02	261.68
T014	500.00	500.00	500.60
T015	500.00	500.00	501.23
T016	500.00	500.00	500.00
T017	261.99	262.02	273.84

Table 5.6: *Steady-state initial results for arbitrary structured network.*

A very good correlation was found between Flownet and Lax-Wendroff. Conservation of mass was maintained in all three codes. One can easily check this by

calculating the amount of helium that flows in and out of Pipe 10. Due to its inaccuracy at high Mach numbers and the discussed energy conservation problem, the RELAP5 results differ slightly. Conservation of energy was maintained in Flownet and Lax-Wendroff. This can be seen from the temperature at which the gas returns to Pipe 10 $\left(T_{0,11} = T_{0,15}\right)$.

5.5 Transient flow in a complex network

To investigate transient flow in an arbitrary structured network, the same network as in the previous paragraph was used. Steady-state conditions reached were used as the initial conditions for this transient.

The transient is initiated by setting the mass flow in Element 11 to zero. This is equivalent to suddenly closing a valve at the upstream of Pipe 5. At the same time, the pressure specification on Node 16 as well as the temperature specification at Nodes 15 and 16 were released. This implies that the pressure and temperature at these nodes are solved using mass and energy conservation. Throughout the transient, the mass flow through Pipe 10 is kept at 10 kg/s. For each code a time step of 0.0002 s was used. Simulations were run for 30 s after the start of the transient. Total pressure and total temperature at each node are plotted against time in Figure 5.10 to Figure 5.17. Time is given on a logarithmic scale.

From these results, two distinct parts to the transient response can be identified. The first is due the progression of pressure waves after the rapid valve closure. The second is the pressure, mass flow and temperature changes to reach a new steady-state. This second effect takes significantly longer due to the additional inertia of mass in the tanks.

Due to the energy conservation problem in RELAP5, energy errors will accumulate as the transient progress. To prevent this, the total temperature at Node 15 in RELAP5 was set to values based on the Flownet results (Figure 5.15). In Figure 5.10, a large difference in total temperature was found between RELAP5 and the other codes. Taking into account that RELAP5 started with different initial conditions and that energy conservation is not satisfied, total pressure still compared well with the other codes.

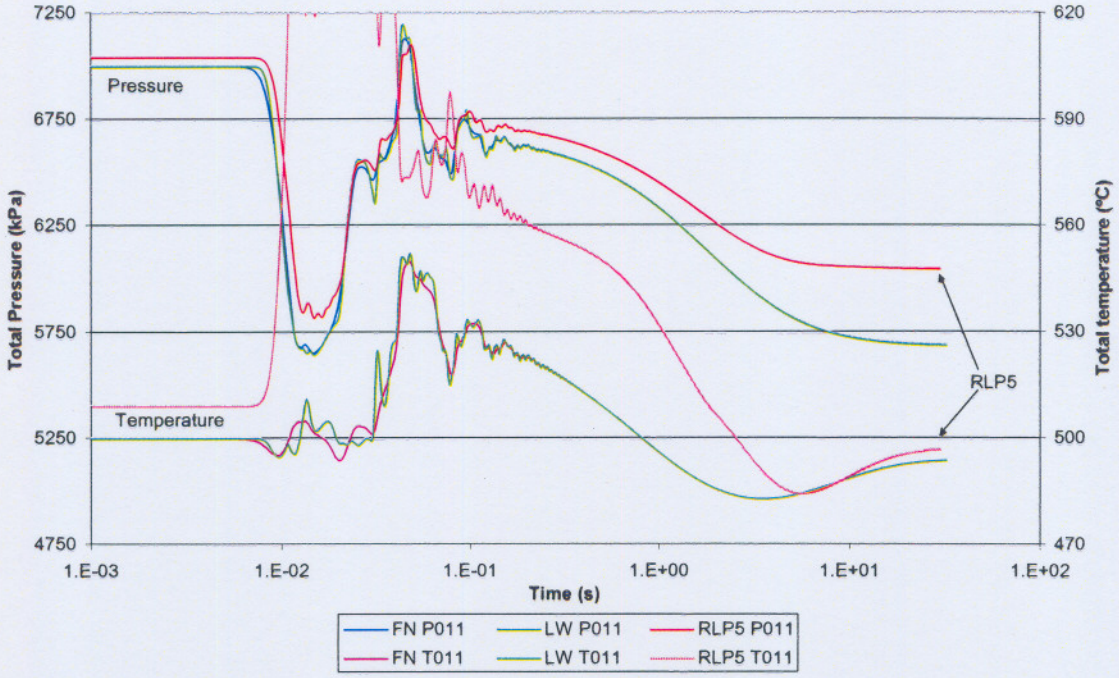


Figure 5.10: *Total pressure and total temperature at Node 11.*

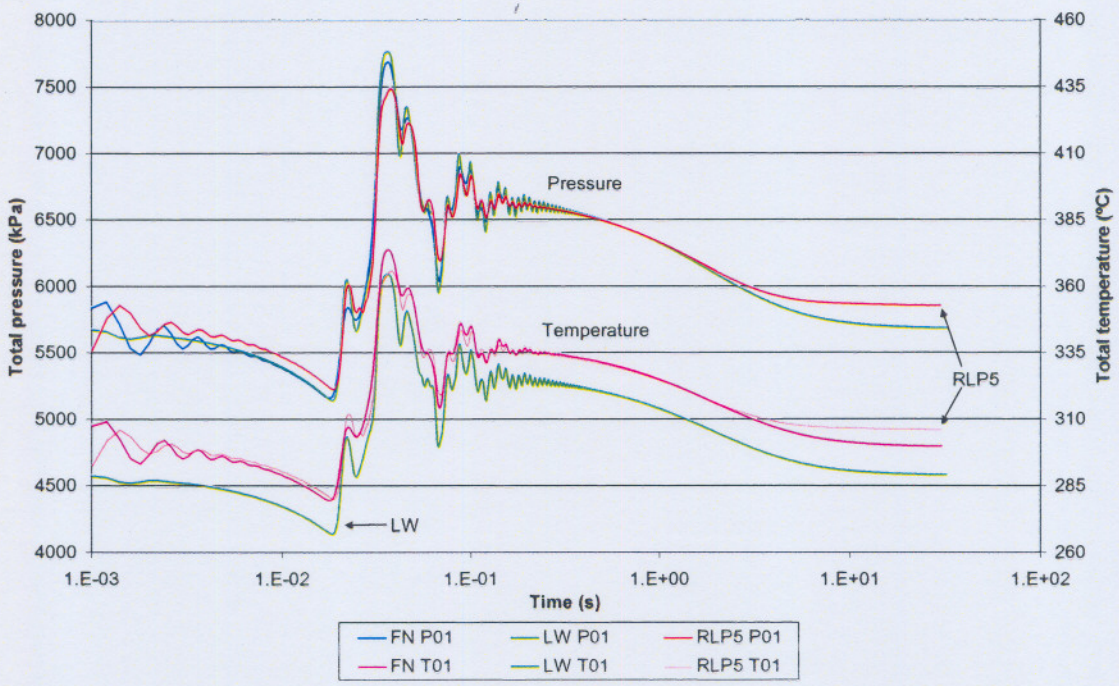


Figure 5.11: *Total pressure and total temperature at Node 1.*

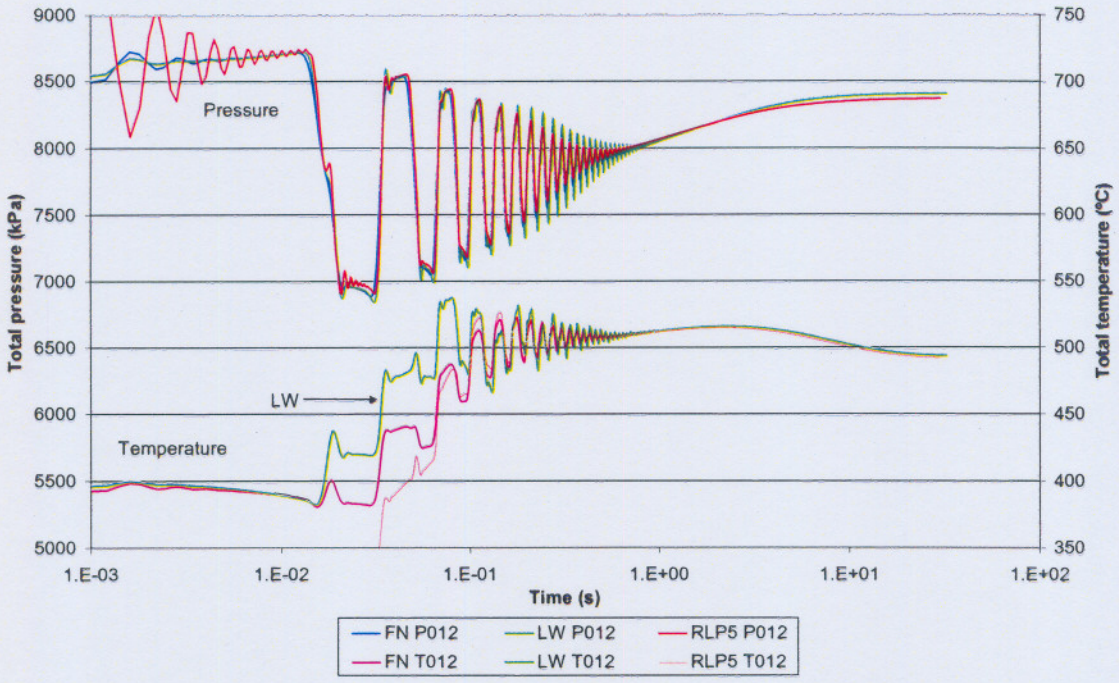


Figure 5.12: *Total pressure and total temperature at Node 12.*

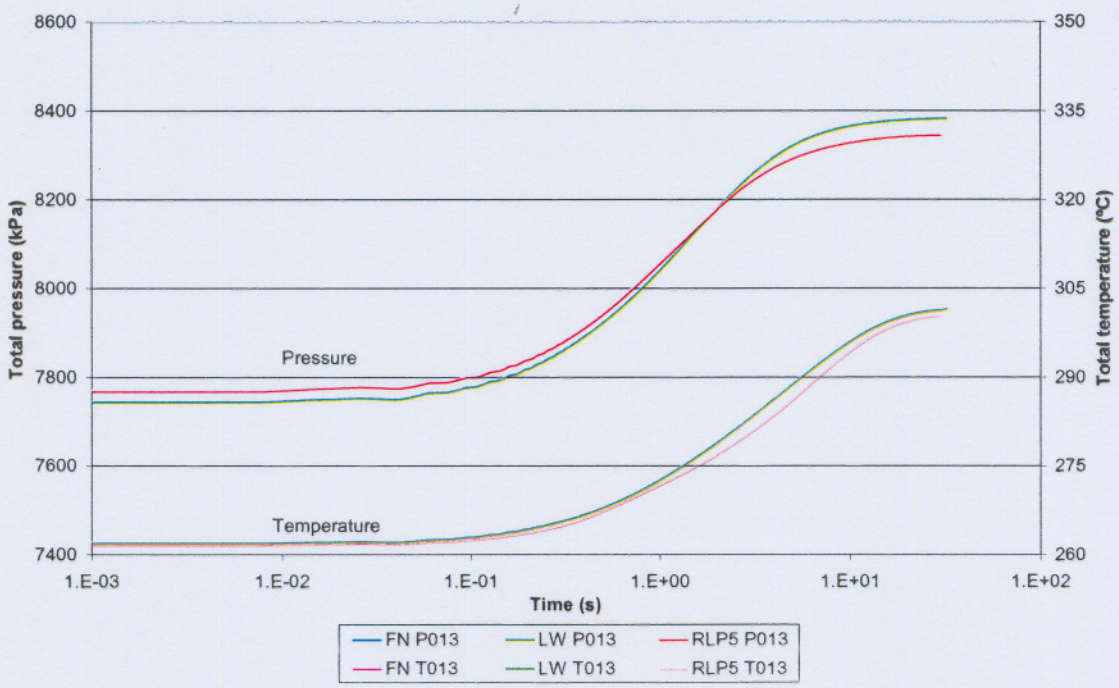


Figure 5.13: *Total pressure and total temperature at Node 13.*

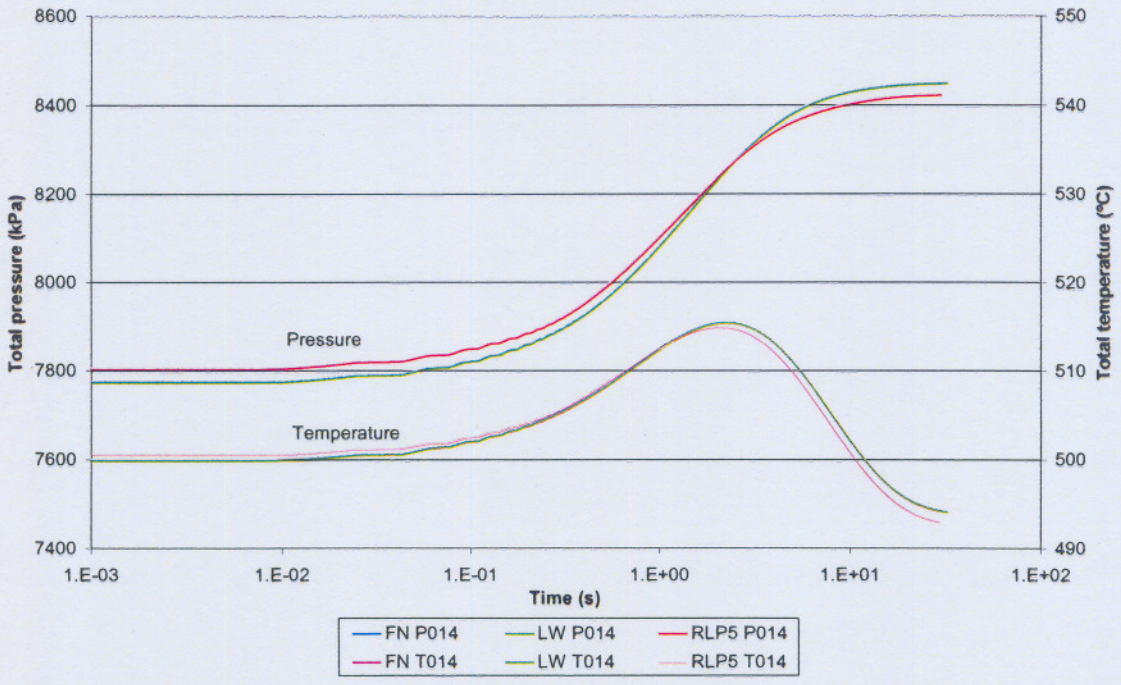


Figure 5.14: *Total pressure and total temperature at Node 14.*

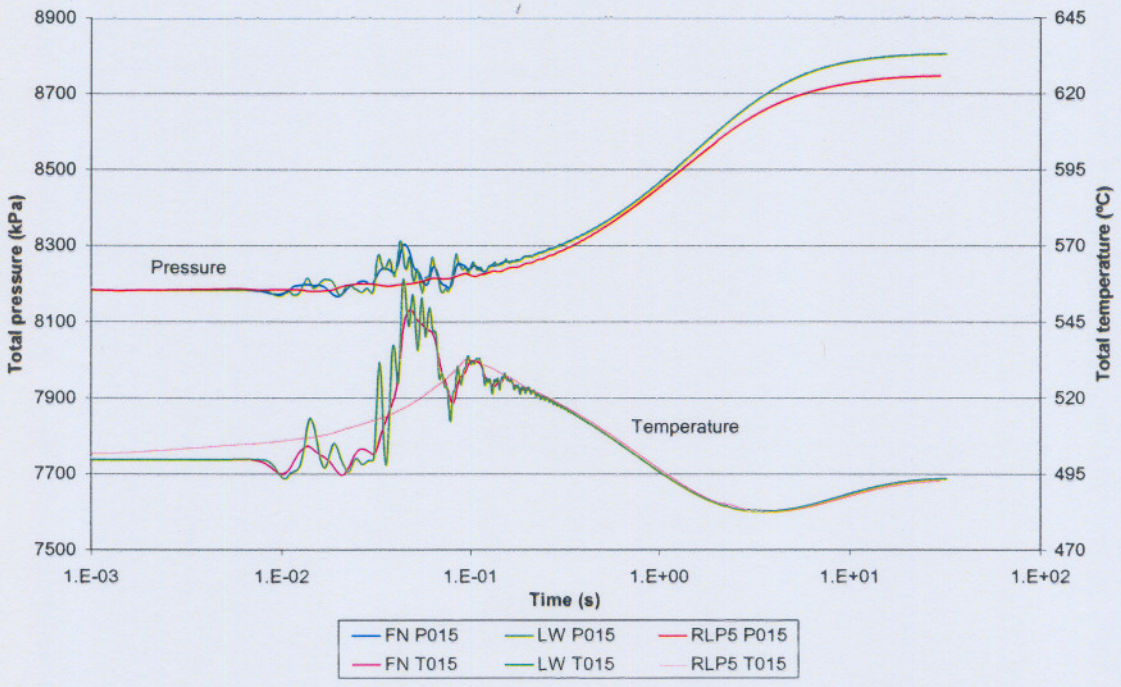


Figure 5.15: *Total pressure and total temperature at Node 15.*

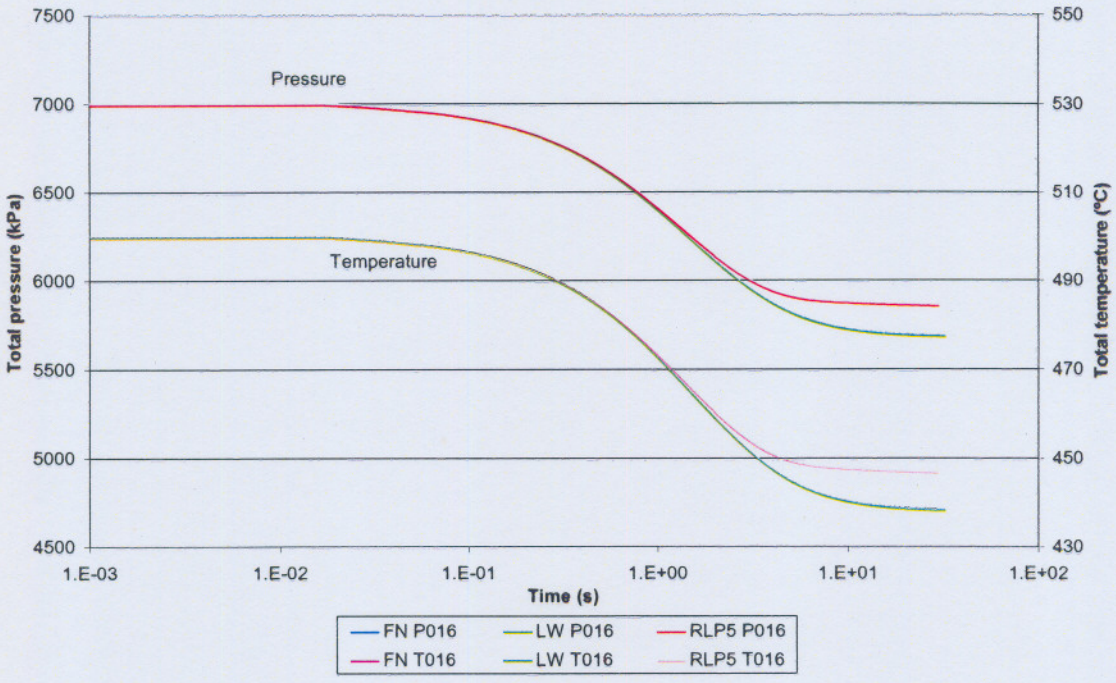


Figure 5.16: *Total pressure and total temperature at Node 16.*

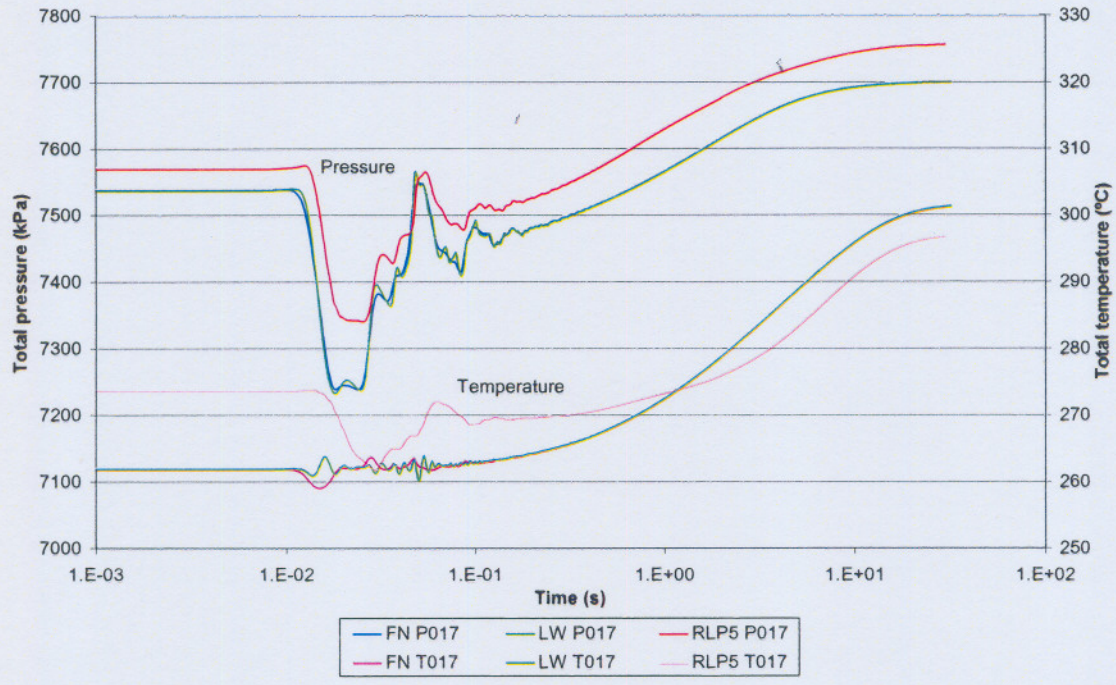


Figure 5.17: *Total pressure and total temperature at Node 17.*

Total pressure and total temperature results from Flownet and Lax-Wendroff compared very well. The difference in total temperature at boundaries with a combination of little or no flow and fast pressure transients can again be seen in

Figure 5.11 and Figure 5.12. In Figure 5.12, this difference diminishes due to the mass still flowing through the junction after the initial fast transient. In Figure 5.18 and Figure 5.19, mass flow through Pipe 8 and the orifice is given. For all three codes, the transient response of the mass flow compares very well.

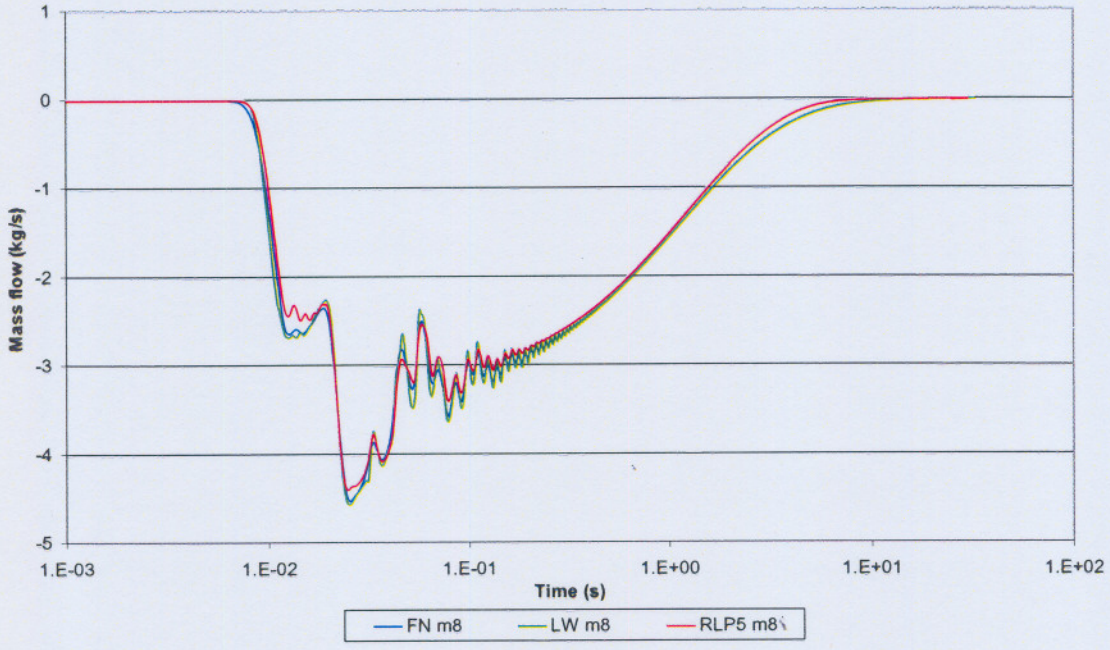


Figure 5.18: *Mass flow through Pipe 8.*

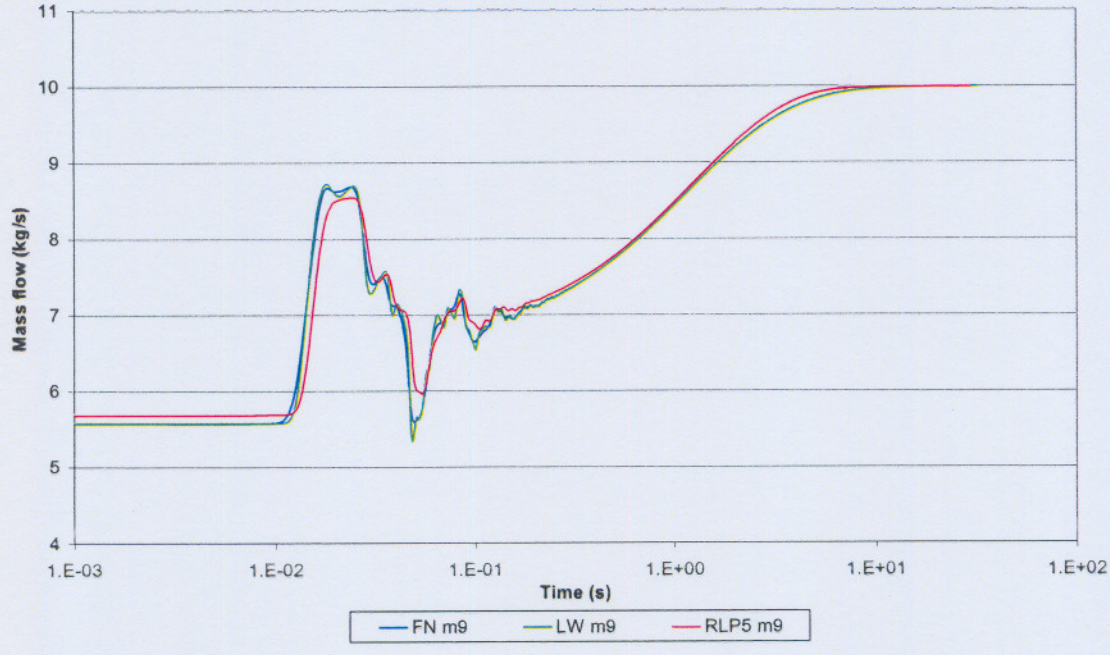


Figure 5.19: *Mass flow through orifice.*

5.6 Conclusion

Flownet produced acceptable results for steady and transient flow in junctions. Using junctions, an arbitrary structured network with all the components and models tested thus was constructed. This was used to validate the integration of these models and components.

Steady-state results from Flownet and Lax-Wendroff for this network compared very well. For the transient results, a very good comparison was found between Flownet and Lax-Wendroff. For quite a few of the transient variables that were considered, RELAP5 also compared well with Flownet. In the transient flow case, a total temperature difference between Flownet and Lax-Wendroff was found at boundaries with little or no flow in the presence of fast pressure transients. In all probability this anomaly was due to the differences in boundary condition modelling between the two codes (refer to Chapter 4.9).

CHAPTER SIX: CONCLUSION AND RECOMMENDATIONS

6.1 Introduction

Several concluding comments regarding this study are appropriate at this stage. Some insights gained in completing this work are also shared. Recommendations are made concerning further work that might be required in the final paragraph of this chapter.

6.2 Perspective on this study

A great amount of development and modelling has been done on transient compressible flow in pipe networks for commercial software. A large part of this work has not been published, sometimes to maintain a competitive edge. There is, however, still a need in the industry to effectively model more complex thermal-fluid networks.

The NNR requires the use of benchmarks to verify and validate the overall behaviour of a code. To accomplish this, an explicit method was implemented and a commercial code obtained as part of this study.

RELAP5 was chosen as a benchmark. It has been developed for best-estimate transient simulations of light water reactor coolant systems. For many of the benchmark test cases, RELAP5 gave acceptable results. Some anomalies with analytical solutions were, however, found. Learning how to use RELAP5 was no trivial task. The author acknowledges that some of these anomalies could have been caused by incorrect use of the code.

The Lax-Wendroff method was chosen to develop an explicit pipe network simulation code. Winterbone et al. (2000:8) used quasi-steady flow to model boundary conditions. A transient formulation of the continuity equation was used to model boundaries as part of this study. This was extended to enable the implicit treatment of junctions. These models and other models were integrated into a code to enable the modelling of arbitrary structured networks.

6.3 Validation of individual models and components

To isolate the cause of anomalies, individual models or components in Flownet were benchmarked. These individual components or models include pipes, boundary conditions, heat transfer, tanks and non-inertial elements.

Flownet compared very well with analytical results for steady-state flow. An anomaly was, however, identified for isothermal flow at high Mach numbers. This was deemed unimportant, as isothermal conditions are not used in modelling the PBMR. No significant differences were found between the Lax-Wendroff method and the analytical solution. RELAP5 results differed with analytical results at high Mach numbers. An energy conservation problem was also identified when modelling flow through an orifice. These anomalies prevailed whenever flow at high Mach numbers or flow through an orifice was modelled. For transient flow, results compared very well between Lax-Wendroff and Flownet. If one of the anomalies mentioned in RELAP5 did not influence the results, it also compared favourably.

An anomaly in determining the total temperature at some boundaries was found between Flownet and the Lax-Wendroff method. From the results it seemed only to occur at boundaries with a combination of no or little flow, as well as fast pressure transients. In all probability this anomaly is due to the difference in boundary modelling between Flownet and Lax-Wendroff. This localized effect was considered to have a small or no impact on the rest of the solution.

With these benchmark test cases completed, one can conclude that the implementation of these components in Flownet is valid.

6.4 Validation of model and component integration

In pipe networks, junctions are used to integrate individual elements, models and components. A good correlation was found between Flownet, RELAP5, Lax-Wendroff and steady-state analytical solutions for junctions. Differences with RELAP5 were ascribed to the stated anomaly found at high Mach numbers. For transient flow, results obtained using RELAP did not seem accurate. The reason for this could not be identified. Results between Flownet and Lax-Wendroff correlated very well.

With the implementation of junctions validated, an arbitrarily structured network was simulated. Steady flow results compared well between Flownet, RELAP5 and Lax-Wendroff. Some differences found with RELAP5 for steady-state and transient flow can again be explained in the light of previously stated anomalies. Transient results between Lax-Wendroff and Flownet compared very well. The only noteworthy differences found were attributed to the total temperature anomaly at boundaries with little or no flow and fast pressure transients.

Considering the benchmark cases done and the results obtained, one can come to the following conclusion. The implementation of individual components considered in this study as well as integration of these components to model pipe networks using Flownet has been validated.

6.5 Recommendations for further work

During the course of this study, certain anomalies were identified. The NRC (USA) should be contacted concerning the anomalies identified in RELAP5. The anomaly in Flownet when modelling isothermal flow at high Mach numbers must be resolved. The difference in total temperature between Flownet and Lax-Wendroff when solving transient flow at certain boundaries must also be resolved.

With the completion of this study, various individual components and their integration in Flownet were validated. This study did not cover the verification and validation of specific element models in Flownet. Validating, for instance, one of the valve models in Flownet, might require comparison with experimental data. Junctions were implemented without including loss factors. The validation of, for example, a specific junction geometry with experimental data, will still be required. This study only forms part of the verification and validation process, and further validation will be required on models and components such as:

- Convective Heat Transfer (CHT) elements
- Junction loss models
- Valve models
- Distributed heat exchanger modelling
- Turbo machine modelling

REFERENCES

BENSON, R.S., GARG, R.D. & WOOLLATT, D. 1964. A numerical solution of unsteady flow problems. *Int. J. Mech. Sci.*, (6):117-144.

BOTHA, D (F). November 2001. Section 3, Chapter 4: Thermo-Hydraulic Analysis. (*In* PBMR Safety Analysis Report, Revision 1. Centurion, South Africa.) 34p.

COETZEE, R.V. VAN DER MERVE, J. AND VAN RAVENSWAAY, J.P. 2003 Flownex version 6.41 user manual. M-Tech Industrial, Potchefstroom.

COHEN, H., ROGERS, G.F.C., SARAVANAMUTTOO, H.I.H. 1999. Gas turbine theory. Great Britain: Biddles Ltd. 442 p.

DU TOIT, C.G. GREYVENSTEIN AND G.P. ROUSSEAU, P.G. 2003. A comprehensive reactor model for the integrated network simulation of the PBMR power plant. (*In* International Congress on Advances in Nuclear Power Plants, Cordoba, Spain. 7p).

F-CHART SOFTWARE. 2003. EES - Engineering Equation Solver. [Web:] http://www.fchart.com/. [Date of access: 1 December 2003].

FERZIGER, J.H., PERIC, M. 1999. Computational Methods for Fluid Dynamics. Germany: Springer. 389.

GREYVENSTEIN, G.P. LAURIE, D.P. 1994. A segregated CFD approach to pipe network analysis. *International journal for numerical methods in engineering*, (37):6385-3705, Feb. 18.

GREYVENSTEIN, G.P. 2001. An implicit method for the analysis of transient flows in pipe networks. *International journal for numerical methods in engineering*, (53):1127-1143, Jan. 29.

GREYVENSTEIN, G.P. AND ROUSSEAU, P.G. 2002. Design of a physical model of the PBMR with the aid of Flownet. (*In* HTR-TN, High Temperature Reactor Technology, Petten, The Netherlands: European Nuclear Society. p.318-322.)

GREYVENSTEIN, G.P. AND ROUSSEAU, P.G. NICHOLLS, DAVE. 2003. Design and successful testing of a physical model of the pebble bed modular reactor. *International journal for nuclear power,* G01386(2):105-110, Feb.

HARTREE, D.R. 1953. Some practical methods of using characteristics in the calculation of non-steady compressible flow. US Atomic Energy commission Report AECU-2713.

HIRSCH, C. 1990. Numerical computation of internal and external flows. England : John Wiley & Sons Ltd. 691p.

KIUCHI, T. 1994. An implicit method for transient gas flows in pipe networks. *International Journal of heat and fluid flow*, 15(5):378-383, October.

KREYSZIG, E. 1993. Advanced Engineering Mathematics. 7th ed. Singapore : John Wiley & Sons Inc. 1271.

LANDMAN, W.A. VAN HEERDEN, E. VAN RAVENSWAAY, J.P. AND GREYVENSTEIN, G.P. 2003. Flownet nuclear architecture, implementation, and verification & validation. (*In* International Congress on Advances in Nuclear Power Plants, Cordoba, Spain. 10p.)

LERAT, A. 1979. Une Classe de Schemas aux Differences Implicites pour les Systemes Hyperboliques de Lois de Conservation. *Comptes Rendus Academie des Sciences*. (A288):1033-1036, Paris.

LERAT, A. 1983. Implicit methods of second order accuracy for the Euler equations. AIAA Paper 83-1925, AIAA 6th Computational Fluid Dynamics Conference; also *AIAA journal*, (23):33-40.

LISKA. R. & WENDROFF. B. Comparison of several difference schemes on 1d and 2d test problems for the Euler equations. Czech Technical University, 2002. [Web:] Available with animations at
http://www-troja.fjfi.cvut.cz/~liska/CompareEuler/compare8.
[Date of access: 14 Feb. 03].

NATIONAL NUCLEAR REGULATOR. 2001. Licensing guide – Requirements for licensing submission involving computer codes and evaluation models for safety calculations. LG-1038. South Africa. 11p.

NUCLEAR SAFETY ANALYSIS DIVISION. May 2001. RELAP5/MOD3.3Beta Code Manual. NUREG/CR-5535/Rev 1-Vol I. Idaho National Engineering Laboratory.

PATANKAR, S.V. 1980. Numerical heat transfer and fluid flow. New York : McGraw-Hill.

RANSOM, V.H. May 1989. Course A--Numerical Modelling of Two-Phase Flows for Presentation at Ecole d'Ete d'Analyse Numerique. EGG-EAST-8546. Idaho National Engineering Laboratory.

ROUSSEAU, P.G. AND GREYVENSTEIN, G.P. 2002. Modelling of the HTTR in Flownet. (*In* HTR-TN, High Temperature Reactor Technology, Petten, The Netherlands : European Nuclear Society. p.141-147.)

ROUSSEAU, P.G. AND VAN RAVENSWAAY, J.P. 2003. Thermal-fluid comparison of three- and single-shaft closed loop Brayton cycle configuration for

HTGR power conversion. (*In* International Congress on Advances in Nuclear Power Plants, Cordoba, Spain. 9p.)

SAAD, M.A. 1985. Compressible fluid flow. New Jersey : Prentice-Hall. 560 p.

SHAMES, I.H. 1992. Mechanics of fluids. Singapore : McGraw-Hill. 858 p.

SOD, G.A. 1978. A survey of several finite difference methods for systems of nonliniear hyperbolic conservation laws. *Journal of computational physics,*(27):1-31.

VAN NIEKERK, W.M.K. ROUSSEAU, P.G. AND GREYVENSTEIN, G.P. 2003. Operation and simulation of a three-shaft, closed-loop, Brayton cycle model of the PBMR power plant. (*In* International Congress on Advances in Nuclear Power Plants, Cordoba, Spain. 7p.)

VAN RAVENSWAAY, J.P. 1998. An implicit method for transient pipe network analysis. Potchefstroom: PU for CHE. (Thesis – M.Eng.) 131p.

VERSTEEG, H.K., MALALASEKERA, W. 1998. An introduction to Computational Fluid Dynamics. Malaysia : Longham Group Ltd. 257.

WINTERBONE, D.E.& PEARSON, R.J. 2000. Theory of engine manifold design. London : Professional Engineering Publishing Limited. 476p.

APPENDIX A: DERIVATION OF DIFFERENTIAL EQUATIONS

A.1 Introduction

The conservation of mass, momentum and energy can be described using partial differential equations. Such a form of these laws can be formulated by applying these laws over an infinitesimal control volume. Figure A.1 shows such a control volume for an infinitesimal length of pipe.

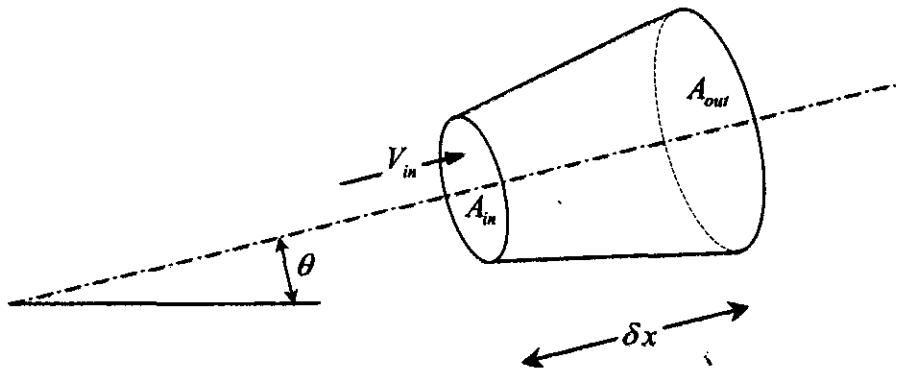


Figure A.1: *Variable area, Infinitesimal length of pipe.*

Allowing for variable area between the inlet and outlet, each of the conservation laws will now be considered.

A.2 Continuity

For a Control Volume (CV), conservation of mass is given by (Shames, 1992:150)

$$\oiint_{CS}(\rho \boldsymbol{V}.\boldsymbol{dA}) = -\frac{\partial}{\partial t}\iiint_{CV}\rho dv \qquad \text{(A.1)}$$

Here ρ is the density, $\boldsymbol{V}$ is the outward facing velocity vector on the Control Surface (CS) and $\boldsymbol{dA}$ the incremental outward facing area vector. This first surface integral gives the net efflux of mass trough the control surface. On the right side of Equation (A.1), the negative time derivative of the volume integral gives the rate at which mass decreases in the CV.

Consider now the CV given in Figure A.1. In deriving the differential form, the CV is shrunk and each term is evaluated as $\delta x \to 0$. For a pipe, the velocity is perpendicular to the inlet and outlet areas. With a one-dimensional approach, the velocity and density are taken as constant over a cross-section of the pipe. As a result

$$\oiint_{CS}(\rho \boldsymbol{V}.\boldsymbol{dA}) = (\rho VA)_{outlet} - (\rho VA)_{inlet} \tag{A.2}$$

For a very small length of pipe we can assume a constant value for the density throughout the CV. A good approximation of the density – volume integral is to use the average area of the CV. This approximation approaches the exact solution as $\delta x \to 0$.

$$\iiint_{CV}\rho dv = \lim_{\delta x \to 0}\left\{0.5\left(A_{inlet} + A_{outlet}\right)\rho\delta x\right\} \tag{A.3}$$

Substitution of (A.2) and (A.3) into (A.1) leads to

$$\lim_{\delta x \to 0}\left\{(\rho VA)_{outlet} - (\rho VA)_{inlet}\right\} = -\frac{\partial}{\partial t}\lim_{\delta x \to 0}\left\{0.5\left(A_{inlet} + A_{outlet}\right)\rho\delta x\right\} \tag{A.4}$$

The CV geometry is time independent, so Equation (A.4) can be divided by δx.

$$\lim_{\delta x \to 0}\left\{\frac{(\rho VA)_{outlet} - (\rho VA)_{inlet}}{\delta x}\right\} = -\frac{\partial}{\partial t}\lim_{\delta x \to 0}\left\{0.5\left(A_{inlet} + A_{outlet}\right)\rho\right\} \tag{A.5}$$

As $\delta x \to 0$ we have that

$$A_{inlet} = A_{outlet} = A \tag{A.6}$$

and

$$\lim_{\delta x \to 0}\left\{\frac{(\rho VA)_{outlet} - (\rho VA)_{inlet}}{\delta x}\right\} = \frac{\partial(\rho VA)}{\partial x} \tag{A.7}$$

Substitution into (A.5) gives

$$\frac{\partial(\rho VA)}{\partial x} = -\frac{\partial}{\partial t}(A\rho) \tag{A.8}$$

Here the area A is also independent of time and can be manipulated as such.

$$\frac{\partial\rho}{\partial t} + \frac{\partial(\rho VA)}{A\partial x} = 0 \tag{A.9}$$

Equation (A.9) is then the partial differential equation describing conservation of mass.

A.3 Momentum conservation

For a CV, conservation of momentum is given by (Shames, 1992:155)

$$\oiint_{CS} \boldsymbol{T}dA + \iiint_{CV} \boldsymbol{B}\rho dv = \oiint_{CS} \boldsymbol{V}(\rho \boldsymbol{V}.\boldsymbol{dA}) + \frac{\partial}{\partial t}\iiint_{CV} \boldsymbol{V}(\rho dv) \qquad \text{(A.10)}$$

This formulation is derived from Newton's second law with terms on the left accounting for the total force, and terms on the right for the total rate of momentum change. Here $\boldsymbol{T}$ is the force vector per unit area acting on the CS and $\boldsymbol{B}$ is the body force vector per unit mass acting on mass inside the CV. On the left we therefore have the net force acting on the CV.

The surface integral on the right represents the rate of momentum efflux out of the CV. Here the velocity vector $\boldsymbol{V}$ in the CV is multiplied by $(\rho \boldsymbol{V}.\boldsymbol{dA})$ the mass flux component parallel to the area vector $\boldsymbol{dA}$. The volume integral term on the right represents the rate at which momentum increases in the CV. Differentiating the total mass – velocity product partially in time gives this rate of change. Consider again the CV given in Figure A.1. In deriving the differential form, the control volume is shrunk and each term is evaluated as $\delta x \to 0$.

Surface forces acting on the CV surface are included in $\oiint_{CS} \boldsymbol{T}dA$. Two types are found to have an impact and will now be considered. Firstly, shear forces F_{shear} due to friction are found on the walls of the pipe in the CV. Shear stresses τ on the walls of a pipe are proportional to the square of the fluid velocity in that pipe (Streeter & Wylie, 1979:227).

$$\tau = \lambda \tfrac{1}{2} \rho V^2 \qquad \text{(A.11)}$$

Here λ is a dimensionless coefficient. For the Darcy Weisbach formulation of friction in pipes, this coefficient is $\lambda = \frac{f}{4}$. The friction factor f is determined from experimental data for various Reynolds numbers. Because the shear stress acts at the wall of the pipe, the shear force is given by

$$\begin{aligned} F_{shear} &= \tau P \delta x \\ &= \lambda \tfrac{1}{2} \rho V^2 \pi D \delta x \\ &= \frac{f}{4}\frac{\rho V^2}{2}\pi D \delta x \end{aligned} \qquad \text{(A.12)}$$

with $p = \pi D$ the perimeter of the pipe. With the area A of the pipe section given as $\frac{\pi D^2}{4}$, the expression for shear force can be rewritten as

$$\begin{aligned} F_{shear} &= \frac{4\tau_w A \delta x}{D} \\ &= f \frac{\rho V^2}{2} \frac{A \delta x}{D} \end{aligned} \tag{A.13}$$

It should be remembered that the force term is a vector quantity. Equation (A.13) in its current form will always give a positive value. The shear force is, however, always directed to oppose the flow. A sensible way to implement this is by changing the form of (A.13) so that the flow direction determines the force direction.

$$F_{shear} = -f \frac{\rho V |V|}{2} \frac{A \delta x}{D} \tag{A.14}$$

The second type of force exerted on the CV is due to the difference in pressure between the CV inlet and outlet. This net pressure force $F_{pressure}$ is exerted on the CV is given by

$$F_{pressure} = A_{in} p_{in} + \left(\frac{p_{out} + p_{in}}{2} \right) \left(A_{out} - A_{in} \right) - A_{out} p_{out} \tag{A.15}$$

The second term on the left represents the force exerted by the walls of the pipe. Here the direction of pressure force at the inlet is in the positive x direction, and the outlet in the negative direction. In this way the sign of the force designates its direction. This can be rewritten in the following manner.

$$\begin{aligned} F_{pressure} &= A_{in} p_{in} + \left(\frac{p_{out} + p_{in}}{2} \right) \left(A_{out} - A_{in} \right) - A_{out} p_{out} \\ &= A_{in} p_{in} + \frac{p_{in}}{2} \left(A_{out} - A_{in} \right) + \frac{p_{out}}{2} \left(A_{out} - A_{in} \right) - A_{out} p_{out} \\ &= \frac{p_{in}}{2} A_{in} + \frac{p_{in}}{2} A_{out} - \frac{p_{out}}{2} A_{in} - \frac{p_{out}}{2} A_{out} \\ &= p_{in} \left(\frac{A_{in} + A_{out}}{2} \right) - p_{out} \left(\frac{A_{in} + A_{out}}{2} \right) \\ &= p_{in} A_{average} - p_{out} A_{average} \end{aligned} \tag{A.16}$$

As $\delta x \to 0$ we have that $A_{average} = A$.

Body forces acting on the fluid in the CV are included in $\iiint_{CV} \boldsymbol{B}\rho dv$. Gravity is the only body force that will be considered in this study. In the CV shown in Figure A.1 the total body force $F_{gravity}$ is given by

$$F_{gravity} = m_{cv}g \tag{A.17}$$

where m_{cv} is the mass inside the CV and g the gravitational acceleration. At any point in time the mass inside the CV is given by the density multiplied by the volume of the CV. When $\delta x \to 0$, the volume of the CV approaches $(A\delta x)$. Therefore

$$F_{gravity} = \rho A(\delta x)g \tag{A.18}$$

This force consists of a component perpendicular as well as parallel to the direction of flow. Only the component parallel to the flow direction will have an effect on momentum in CV. If the pipe centroid runs with an angle θ relative to the horizontal plane (refer to Figure A.1), the component of the gravitational in the direction of flow is given as

$$F_{x-gravity} = -\rho A(\delta x)g\cos\theta \tag{A.19}$$

This relation is derived using simple geometry shown in Figure A.1.

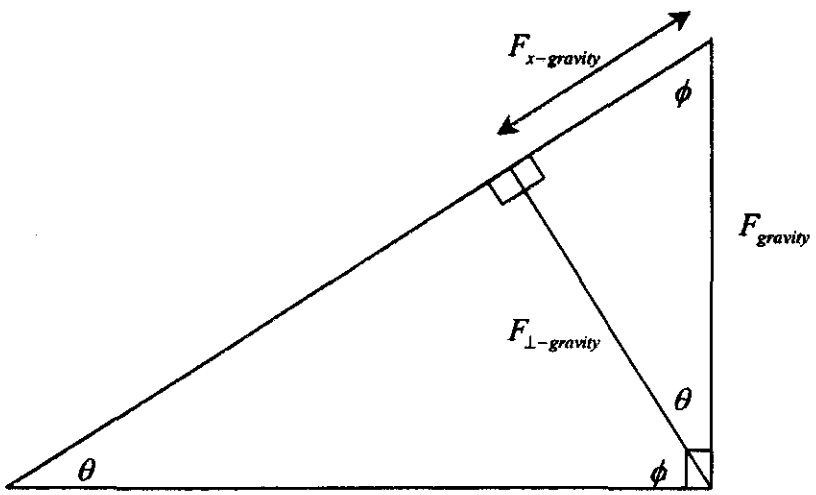


Figure A.2: *Deriving the tangential component of gravitational force.*

The tempo at which momentum is leaving the CV through the control surface is represented by the term $\oiint_{CS} V(\rho V.dA)$. Again assuming one-dimensional flow, the area and velocity vectors are taken co-linear. Further, the velocity and

density are assumed to be constant over the inlet and outlet areas. This surface integral is then evaluated as

$$\oiint_{CS} V(\rho V.dA) = (\rho V^2 A)_{out} - (\rho V^2 A)_{in} \tag{A.20}$$

The rate at which momentum increases in the CV is given by the term $\frac{\partial}{\partial t}\iiint_{CV} V(\rho dv)$. As $\delta x \to 0$, the velocity and density approach a constant value throughout the CV. Again we can then take the volume of the CV as $A\delta x$. The result of this is that

$$\frac{\partial}{\partial t}\iiint_{CV} V(\rho dv) = \frac{\partial}{\partial t}(\rho V A \delta x) \tag{A.21}$$

For the CV under discussion, the geometry does not change with time and

$$\frac{\partial}{\partial t}\iiint_{CV} V(\rho dv) = \frac{\partial \rho V}{\partial t} A\delta x \tag{A.22}$$

By using new form for each of the terms in Equations (A.14), (A.15), (A.19), (A.20) and (A.22) in Equation (A.10), we get that

$$\begin{aligned} &-f\frac{\rho V|V|}{2}\frac{A\delta x}{D} + A(p_{in} - p_{uit}) - \rho A(\delta x) g\cos\theta \\ &= \left\{(\rho V^2 A)_{out} - (\rho V^2 A)_{in}\right\} + \frac{\partial \rho V}{\partial t} A\delta x \end{aligned} \tag{A.23}$$

Dividing (A.23) by $A\delta x$ and rearranging the pressure results in

$$-f\frac{\rho V|V|}{2D} - \frac{(p_{uit} - p_{in})}{\delta x} - \rho g\cos\theta = \frac{(\rho V^2 A)_{out} - (\rho V^2 A)_{in}}{A\delta x} + \frac{\partial \rho V}{\partial t} \tag{A.24}$$

With $\delta x \to 0$, partial derivatives in the direction of flow are formed. By rearranging the terms we get the partial differential equation describing momentum conservation.

$$\frac{\partial(\rho V)}{\partial t} + \frac{\partial(\rho V^2 A)}{A\partial x} + \frac{\partial P}{\partial x} + \rho g\cos\theta + \frac{f\rho V|V|}{2D} = 0 \tag{A.25}$$

A.4 Energy conservation

For the CV under consideration, no energy crosses the boundary in the form of shaft work. Further, no other body force except gravity is exerted on the fluid. For this CV conservation of energy (Shames, 1992:229) is written as

$$\frac{dQ}{dt} = \oiint_{CS}\left(\frac{V^2}{2} + h + gz\right)(\rho V.dA) + \frac{\partial}{\partial t}\iiint_{CV}\rho\left(\frac{V^2}{2} + gz + u\right)dv \qquad \text{(A.26)}$$

Here the time derivative on the left represents the rate at which heat is transferred to the CV through the CS. The surface integral on the right represents the total energy that leaves the CV due to mass crossing the CS. This term consists of the kinetic energy $\left(\frac{V^2}{2}\right)$, the enthalpy (h) and the potential energy (gz). Mass crossing the CS has internal energy (u) and contributes to flow work due to the pressure of the fluid. Both these components are included in the enthalpy $(h = u + pv)$. Due to heat transfer and mass leaving the CV, the total energy in the CV changes. This is given by the time derivative of the volume integral on the right. No flow work inside the CV has an effect on the total energy content of the CV. As a result, only the internal, kinetic and potential energy is taken into account in the volume integral.

Consider the total energy leaving the CV due to mass flowing across the CS in Figure A.1. Again, for a one-dimensional approach, we can assume constant properties across the flow and a flow direction perpendicular to the cross-sectional area. This surface integral can then be written as

$$\oiint_{CS}\left(\frac{V^2}{2} + h + gz\right)(\rho V.dA) = \left\{\left(\frac{V^2}{2} + h + gz\right)\rho VA\right\}_{out} - \left\{\left(\frac{V^2}{2} + h + gz\right)\rho VA\right\}_{in} \qquad \text{(A.27)}$$

Total properties of a fluid are defined as the properties of the fluid when the flow is isentropically retarded until it reaches zero velocity. As the flow is retarded, all kinetic energy is transferred to internal and pressure energy. Using an energy balance, the total enthalpy h_0 is given by

$$h_0 = h + \frac{1}{2}V^2 \qquad \text{(A.28)}$$

And the total internal energy u_0 is defined as

$$u_0 = u + \frac{1}{2}V^2 \tag{A.29}$$

Equation (A.27) can then be rewritten as

$$\oiint_{CS}(h_0 + gz)(\rho V.dA) = \{(h_0 + gz)\rho VA\}_{out} - \{(h_0 + gz)\rho VA\}_{in} \tag{A.30}$$

For the volume integral we assume constant values throughout the CV as $\delta x \to 0$. With this same assumption the volume of the CV approaches $A\delta x$. We can then write the rate at which energy is increasing in the CV as

$$\frac{\partial}{\partial t}\iiint_{CV}\rho(gz + u_0)dv = \frac{\partial}{\partial t}\{(gz + u_0)\rho A\delta x\} \tag{A.31}$$

Using (A.30) and (A.31) we can write (A.26) as

$$\frac{dQ}{dt} = \{(h_0 + gz)\rho VA\}_{out} - \{(h_0 + gz)\rho VA\}_{in} + \frac{\partial}{\partial t}\{(gz + u_0)\rho A\delta x\} \tag{A.32}$$

Knowing that the CV's volume $(A\delta x)$ and the potential energy gz inside the CV are independent of time results in

$$\frac{dQ}{dt}\frac{1}{A\delta x} = \frac{\{(h_0 + gz)\rho VA\}_{out} - \{(h_0 + gz)\rho VA\}_{in}}{A\delta x} + \frac{\partial}{\partial t}(\rho u_0) \tag{A.33}$$

As $\delta x \to 0$ we get the partial differential equation for conservation of energy.

$$\dot{q} = \frac{\partial\{(h_0 + gz)\rho VA\}}{A\partial x} + \frac{\partial}{\partial t}(\rho u_0) \tag{A.34}$$

In the above equation, $\dot{q}$ is the rate of heat transfer per unit volume.

A.5 Proof of theorem for compressible gas flow

In this paragraph it will be shown that

$$\rho V\frac{\partial V}{\partial x} + \frac{\partial p}{\partial x} = \frac{p}{p_0}\frac{\partial p_0}{\partial x} + \frac{\rho V^2}{2T_0}\frac{\partial T_0}{\partial x} \tag{A.35}$$

An important relation for the constant pressure specific heat of an ideal gas is used in this theorem. It can be written as a function of the specific heat ratio and the gas constant of the substance.

$$c_p = \frac{\gamma}{\gamma - 1}R \tag{A.36}$$

The relation is proven by rewriting the terms on the left side of the equation. Consider the static pressure partial derivative to x.

$$\begin{aligned}\frac{\partial p}{\partial x} &= \frac{\partial}{\partial x}\left\{p_0 \frac{p}{p_0}\right\} \\ &= \frac{p}{p_0}\frac{\partial p_0}{\partial x} + p_0 \frac{\partial}{\partial x}\left\{\frac{p}{p_0}\right\}\end{aligned} \tag{A.37}$$

For the momentum term, the first law of thermodynamics is used.

$$c_p T_0 = \frac{V^2}{2} + c_p T \tag{A.38}$$

Taking the partial derivative of the kinetic energy term

$$\begin{aligned}\frac{1}{2}\frac{\partial V^2}{\partial x} &= V\frac{\partial V}{\partial x} \\ &= c_p \frac{\partial T_0}{\partial x} - c_p \frac{\partial T}{\partial x} \\ &= c_p \frac{\partial T_0}{\partial x} - c_p \frac{\partial}{\partial x}\left(T_0 \frac{T}{T_0}\right) \\ &= c_p \frac{\partial T_0}{\partial x} - c_p \frac{T}{T_0}\frac{\partial T_0}{\partial x} - c_p T_0 \frac{\partial}{\partial x}\left(\frac{T}{T_0}\right)\end{aligned} \tag{A.39}$$

Consider the coefficients of the total temperature's partial derivative

$$\begin{aligned}c_p - c_p \frac{T}{T_0} &= \frac{1}{T_0}\left(c_p T_0 - c_p T\right) \\ &= \frac{V^2}{2T_0}\end{aligned} \tag{A.40}$$

Therefore the partial derivative of the kinetic energy can be written as

$$V\frac{\partial V}{\partial x} = \frac{V^2}{2T_0}\frac{\partial T_0}{\partial x} + c_p T_0 \frac{\partial}{\partial x}\left(\frac{T}{T_0}\right) \tag{A.41}$$

Equation (A.35) can now be written as

$$\rho V\frac{\partial V}{\partial x} + \frac{\partial p}{\partial x} = \frac{\rho V^2}{2T_0}\frac{\partial T_0}{\partial x} + \frac{p}{p_0}\frac{\partial p_0}{\partial x} + K \tag{A.42}$$

With

$$
\begin{aligned}
K &= p_0 \frac{\partial}{\partial x}\left(\frac{p}{p_0}\right) - \rho c_p T_0 \frac{\partial}{\partial x}\left(\frac{T}{T_0}\right) \\
&= p_0 \frac{\partial}{\partial x}\left(\frac{p}{p_0}\right) - \rho c_p T_0 \frac{\partial}{\partial x}\left(\frac{p}{p_0}\right)^{(\gamma-1)/\gamma} \\
&= p_0 \frac{\partial}{\partial x}\left(\frac{p}{p_0}\right) - \rho c_p T_0 \left[(\gamma-1)/\gamma\right]\left(\frac{p}{p_0}\right)^{\left[(\gamma-1)/\gamma\right]-1} \frac{\partial}{\partial x}\left(\frac{p}{p_0}\right) \\
&= p_0 \frac{\partial}{\partial x}\left(\frac{p}{p_0}\right) - \rho \frac{\gamma}{\gamma-1} R T_0 \left[(\gamma-1)/\gamma\right]\left(\frac{T}{T_0}\right)\left(\frac{p_0}{p}\right)\frac{\partial}{\partial x}\left(\frac{p}{p_0}\right) \\
&= p_0 \frac{\partial}{\partial x}\left(\frac{p}{p_0}\right) - \rho R T \left(\frac{p_0}{p}\right)\frac{\partial}{\partial x}\left(\frac{p}{p_0}\right) \\
&= 0
\end{aligned}
\tag{A.43}
$$

APPENDIX B: COMMERCIAL CODE QUESTIONNAIRE

B.1 Introduction

Each of the software vendors or companies listed in paragraph 2.5 was contacted to obtain more information on the specific commercial code. The following questions were asked as part of a standard questionnaire.

a. Name of software:
b. Name of company who developed (a):
c. Web site for (a):
d. History of software (Short description from initiation to current status):
e. Method used to solve flow (For example finite difference or finite volume, explicit – (MOC) or implicit – Euler, LaGrange):
f. Language used to develop (a) (C++, Fortran etc.):
g. General capabilities (or models) (Can it simulate; two phase flow, transient flow, heat transfer, isothermal flow, real time, non-Newtonian fluids, pipe elasticity, flow in branches, gravitational effects, etc.?):
h. Specific models and capabilities (Can it model; compressors, turbines, heat exchangers, controllers, user defined models?):
i. Are heat exchangers modelled as lumped or distributed systems? (In a distributed approach the heat exchanger is subdivided. Thermal capacitance is included. Temperature and heat transfer are solved for the fluid and the metal in each subdivision.)
j. Can boundary conditions and model parameters be changed during a transient simulation?
k. Applications (What is it used for?) (For example, simulation, design, plant training simulator etc.):
l. Industries that use this tool (For example oil, HVAC, natural gas, nuclear, motor vehicle industry etc.):
m. Price of a commercial licence for (a) (Per year?):

n. Approximate number of commercial users (Please indicate whether we can publish this number. If not, we will only use it to estimate the industry's market size):

o. Details of contact person in this regard:

B.2 Information obtained from web sites and questionnaires

Unfortunately, less than a third of the companies responded. Some of the information for companies that did not respond was obtained from their web sites. For all the codes the information obtained is now presented. If a particular company replied, it will be indicated by a 'responded' written in brackets.

AFT Arrow (Responded)

(b) Applied Flow Technology

(c) www.aft.com

(d) First released in 1995, AFT Arrow has become known as the most capable compressible flow pipe network analysis and modelling software available at anywhere near its cost level and offering this level of ease-of-use. Current version is 2.0 with 3.0 scheduled for release in first quarter 2002. A related product, AFT Titan, will be released in the same time period, offering all of the flow analysis and system modelling tools of AFT Arrow, but also incorporating an optimization engine. AFT Titan will automatically size piping and components in the system to minimize cost.

(e) Newton-Raphson matrix iteration plus many proprietary methods developed by AFT.

(f) Visual Basic.

(g) AFT Arrow simulates single phase, stead-state flow. Systems may be simple or complex network, closed or open loop and any combination of parallel and series flow. Adiabatic, isothermal or generalized heat transfer across pipe boundaries and heat exchangers is supported, using both ideal and real gas modelling. Capabilities include Mach number up to and including sonic choking. With available Chempak Property Database, approximately

600 gases are available, static pre-mixtures may be defined and dynamic mixing of flowstreams are modelled.

(h) Built-in modelling tools include; fans/compressors, heat exchangers, flow and pressure control valves, fixed pressure and flow boundaries, tanks, tee/wyes using the Idelchik relationships, stop valves, check valves, relief valves and a wide variety of piping fittings.

(i) Heat exchangers are modelled as 'lumped', and may be specified as a fixed heat flux or selected from one of several different configurations (counter flow, etc.) and specified with heat transfer area, heat transfer coefficient, secondary fluid flow, specific heat and temperature.

(j) Not applicable.

(k) AFT Arrow applications range from new system design, modifications of existing systems to simulating operations.

(l) Power, chemical, petro-chemical, natural gas, semi-conductor, aerospace, building systems, marine, nuclear, heating/ventilation and air conditioning, pharmaceutical.

(m) $3 500.

(n) 300 – NOT FOR PUBLICATION

(o) Thomas Glassen
Director of Operations & Business Development
Tel: 719-686-1000, Fax: 719-686-1001, email; tomglassen@aft.com

BOS Fluids

(b) Paulin Research

(c) www.paulin.com

(g) steady and transient flow

(m) $4 500.00 purchase, $1 000.00 annually

C-MAX

(b) UNICADE Inc.

(c) www.unicade.com

(m) $1 990 purchase cost, yearly cost 20% of purchase price

Delta-Q

(b) Helix Technologies Pty Ltd

(c) www.helixtech.com.au

(k) Design and optimize pipe networks for compressible and incompressible fluids

(m) Price of a commercial licence for (a): AU$2 035 (Per year?)

DESIGN II

(b) ChemShare Corporation

(c) www.winsim.com

(m) $1 995 per year

DFS DesignNet

(b) ABZ, Incorporated

(c) www.abzinc.com

(d) In 1989, ABZ saw the need to provide an efficient and reliable method for calculating fluid flow in complex systems, not only in power plants, but in the chemical and other process industries. ABZ completed the development of the award winning 'Crane Companion' in 1992. Since then, ABZ has improved the program and now offers a complete fluid flow analysis program called Design Flow Solutions.

(m) $950 (Per year?)

EASY5

(b) Boeing

(c) www.boeing.com

EDI Software

(b) Name of company who developed (a): Engineering Dynamics Incorporated

(c) Web site for (a): www.engdyn.com

(g) Reciprocating Compressors & Pumps, cavitation model, Centrifugal Compressors & Pumps, transient flow

(k) Digital Piping Pulsation Simulation, Acoustic Filter & Silencer Design

Flow Net

(b) Engineering Design System

(c) www.edstech.com

(g) Flow in branches, incompressible and compressible flow, two-phase flow, isothermal flow

(k) Simulation, design

FLOWMASTER (Responded)

(b) Flowmaster international Ltd

(c) www.flowmaster.com

(d) Developed as a commercial tool right from the start in mid-1980s, in collaboration with the British Hydromechanics Research Association. Brought to the market in 1987, and it should be noted that the first customer is still a customer and recently purchased more copies.

(e) Mainly Method of Characteristics.

(f) C++ and Fortran.

(g) Single Phase Incompressible or Compressible flow for both Steady-state and Transient. Includes Heat Transfer options. Single Line, Branched, Looped, Multi-looped systems. Newtonian flow in pipes or ducts for pumped or gravity fed systems. Large range of components supplied with performance data.

(k) Systems design analysis

(l) Aerospace, Automotive, Process,
Mining, Ships, Petrochemical, Power Generation, Water/Gas Utilities

(m) Range from £5K to £50K.

(n) Approx. 700 (do not publish).

(o) Jonathan Levy,
Waterflow Systems Software,
PO Box 12153
Mill Street
Cape Town 8010
South Africa
Tel +27 (21) 461 2397

jonlev@iafrica.com

Distributor for FLOWMASTER in South Africa.

FlowTran

(b) William J Turner Pty Ltd

(c) www.users.bigpond.com/wjturner

(g) Steady and transient flow

(k) Tracking the behaviour of an operating pipeline in real time; prediction of future behaviour of an operating pipeline. Checking the consistency of measurements with simulation of the pipeline; modelling the behaviour of new or modified pipelines; and Leak Detection in operating pipelines.

FluidFlow

(b) Flite Software Ltd

(c) www.fluidflowinfo.com

(l) Electronic Chip Manufacturing Industry, Oil & Gas Industry, Chemical Process Industry, Engineering Consultancy Firms, Food and Beverage Processing, General Industrial, Heating, Ventilation and Air-conditioning (HVAC) Industry, Mining Industry, Power Industry, Education, Shipbuilding

GASWorkS

(b) Accutech 2000 Pty Ltd

(c) www.accutech2000.com.au

GENNET

(b) Fluid Flow Consultants

(c) www.fluidflow.tulsa.net

(g) Two phase flow, gas & liquid flow

OLGA 2000 (Responded)

(a) Scandpower AS

(b) www.olga2000.com

(c) The initial development of the transient multiphase simulator OLGA goes back to two Norwegian research institutes in the early eighties. IFE started the development of the simulator in 1980. SINTEF has from 1983 operated a field scale high-pressure loop, essential for development and support and verification of the model. Thanks to technical and financial support from the Norwegian and International petroleum companies, OLGA has been under continuous development through the years

(d) Combination of Euler and Lagrange for slug tracking model.

(e) C++ and Fortran.

(f) All aspects, except for pipe elasticity. Transient Multiphase flow in pipelines.

(g) Simulation, design, plant training simulator.

(h) Separators, compressors, controllers, leak, plug, pig, heat exchange, check valve, pumps, valves.

(i) A heat exchanger can be used alone or be included in an anti-surge recirculation loop around a compressor, either as a part of the pipeline section where the compressor is situated, or as a part of the recirculation loop which is external to the pipeline. The heat exchanger is an idealized heat sink, and no description of the real heat transfer process is included. It is rather a way of specifying a temperature at the heat exchanger outlet, consistent with the energy equation in OLGA. A heat source/sink is estimated that will give the specified fluid temperature for a particular section. An upper limit of the heat source is also specified.

(j) Yes.

(k) Oil and gas, Oil companies, engineering.

(m) All major oil companies and engineering companies in the world. (200 to300 users).

(n) Arnfinn Amundsen
Marketing Executive
aam@scandpower.com
Phone : + 47 64 84 44 00
Fax : + 47 64 84 45 00

PIPE-FLO

(b) Engineered Software

(c) www.eng-software.com

PIPE2000 (Responded)

(b) University of Kentucky

(c) www.kypipe.com

(d) Developed in 1982 for gas distribution networks.

(e) Simultaneous solution of non-linear energy/momentum equations using Newton-Raphson approach.

(f) Fortran (engine), Delphi (graphical interface).

(g) Simulate real gas flow in any network configuration.

(h) Handles compressors, regulators.

(j) Lumped.

(k) Not applicable.

(l) Natural gas distribution systems – air distribution networks – landfill gas collection.

(m) Utilities, consultants.

(n) $2 995 One-time cost free-technical support.

(o) 300.

(p) Dr Don J. Wood, djwood@engr.uky.edu 859 257 3436 Director of Civil Eng. Software centre.

PIPEFLO

(b) Neotechnology Consultants Ltd.

(c) www.neotec.com

Pipeline Studio

(b) Name of company who developed (a): Energy Solutions International

(c) Web site for (a): www.energy-solutions.com

(g) Steady and transient flow.

PIPENET™

(b) Sunrise Systems Limited

(c) www.sunrise-sys.com

PIPESIM suite/2000

(b) Baker Jardine.

(c) www.bakerjardine.com

(k) Design - Operate – Optimize.

PULS & PlantFLOW

(b) Rebis.

(c) www.rebis.com

RELAP5

(c) www.nrc.gov/RES/RELAP5

SIMONE

(b) LIWACOM

(c) www.liwacom.de

SIMOTTO

(b) Jodocy & Schmitz AG

(c) www.euregio.net/simotto

(n) Renting leasing and buying options. EURO 25.500 to buy product.

SINDA/FLUINT (Responded)

Both nongeometric/sketchpad (SinapsPlus) and CAD/geometric
(Thermal Desktop/FloCAD) graphical interfaces available.

(b) C&R Technologies, Inc.

(c) www.crtech.com

(d) Thermal (structural heat transfer) portions date back to 1960 as the aerospace standard thermal management software. Fluid analysis capabilities date back to 1985, initially based on nuclear thermo-hydraulic modelling methods, but allowing more assumptions (for faster executions) and user expansibility.

(e) Finite difference/Control Volume (Eulerian). Staggered momentum control volumes available, but other assumptions may be made as well. Implicit flow solution with autonomous time step control for transients.

(f) Fortran and C.

(g) Radiation, conduction, convection, steady and transient flow, single and two-phase flow, homogenous/slip/nonequilibrium two-phase flow, dissolution/evolution of gas phases. Pure fluid substances, or mixtures of gases, liquids, or both.

(h) Any component can be built using network-style building blocks and user logic or spreadsheet expressions, and common components are 'built-in'. Also features parametrics/sensitivities, statistical design (reliability assessments), optimization, automated correlation/calibration to test data, goal-seeking, worst-case scenario searching.

(i) Both are available.

(j) Yes. ANYTHING can be changed at any time using concurrent user logic and/or spreadsheet-like expressions.

(k) Both simulation and design mode are available. Has been applied to trouble shooting as well.

(l) Eerospace, electronics, HVAC, furnace, petrochemical, biomedical, and automotive industries

(m) US$6 000 for a single fixed licence of SINDA/FLUINT on PC. Licence is perpetual, including the first year of update and unlimited usage support. Additional supporting products are available, as well as Unix (HP, Sun) licenses and floating licenses. Discounts for multiple purchases, site licenses, educational sites, etc. Graphical user interfaces are also available for use with SINDA/FLUINT.

(n) Approximately 4 000 users worldwide. (Can publish.)

(o) Cindy Beer, cindy.beer@crtech.com, 303 567 5414, Director of Sales.)

SINDA/G

(b) Network Analysis, Inc.

(c) www.sinda.com

Engineer's Aide SINET (Responded)

(b) EPCON International

(c) www.epcon.com

(d) Developed over the past 20 years – received a US Chemical Industry Award recipient in 1999 based on significant impact to optimize plant utility systems (Chemical Processing Magazine – article is on web site at www.epcon.com)

(e) Advanced Proprietary Method.

(f) C++, Visual Basic.

(g) Simulates two phase flow, heat transfer, isothermal flow, non-Newtonian fluids, flow in branches, gravitational effects, with rigorous thermodynamics for mixture and flash calculations.

(h) Models compressors, turbines, heat exchangers, controllers, and user-defined models for pressure and temperature drop.

(i) Either lumped (simplified) or distributed (fully rigorous exchanger computation for flow and temperature drop) can be specified.

(j) Steady-state simulation only.

(k) Simulation, design, troubleshooting, and general productivity tool for process/chemical/mechanical engineers in the field.

(l) Chemical, Pharmaceutical, petrochemical, oil, HVAC, natural gas, nuclear, pulp and paper, and food.

(m) From $1 200 p.a.

(n) 10 000+ users worldwide - used corporate wide by leading chemical and petrochemical companies including 3M, BASF, Chevron, Dow Chemical, Dow Corning, Eastman, Equistar, Lyondell, Shell, and Sunoco. (OK to publish.)

(o) Todd J. Willman, Director of Software Development, 281-398-9400, ext 811, tjw@epcon.com

SNAP (Responded)

(b) Advantica

(c) www.advanticatech.com

(d) Developed in the 1980s to meet the needs of British Gas, the state monopoly integrated gas industry. British Gas has since broken up into separate infrastructure and trading companies. The software is used within Transco, the gas transport company, and by some companies outside of the group.

(e) Hardy-Cross

(f) FORTRAN, with a command-line interface. No graphics.

(g) Steady-state flow in networks, including branches and loops. Includes the effect of altitude on pressures. Includes a heuristic algorithm for the optimal selection of pipe diameters for design of new networks and extensions. The demand model can include diversity effects (a statistical phenomenon where the design load per connected customer decreases as the total number of customers increases).

(h) Design of small networks and extensions, for instance new housing developments.

(l) Natural gas.

(m) £5 000 for a five-year licence.

(n) Many users within the Lattice group (a successor company to British Gas, and owners of Transco. About 12 commercial licensees outside of the Lattice group.

(o) Martin Thorne, Advantica Technologies Ltd, Ashby Rd, Loughborough, LE11 3LX, United Kingdom. Phone +44 1509 282340.

D-SPICE™

(b) Fantoft Process Technologies AS

(c) www.fantoft.com

(k) Model predictive control system, training simulator, plant management systems?, Human Machine Interface (HMI), optimization of process plants.

The Stoner Pipeline Simulator (SPS) (Responded)

(b) Stoner Associates, Inc.

(c) www.stoner.com

(d) Developed in 1969

Initially a Mainframe application

- Migrated to VMS & OpenVMS (early 1980s)
- Migrated to UNIX (early 1980s)
- Migrated to Windows (mid-1990s)
- Currently available for Windows and UNIX and OpenVMS

(e) The SPS family uses a proprietary implicit technique for solving the equations governing fluid dynamics.

(f) C++

(g) The following list highlights some of the capabilities of SPS, it is not intended as comprehensive.

- Gas or liquid transient simulation
- Single-phase flow
- Isothermal and transient thermal simulation capabilities
- Real-time simulation (when integrated with a SCADA system)
- Leak detection (when integrated with a SCADA system)
- Non-Newtonian flow
- Slack line flow
- Gas composition tracking
- Idealized or detailed regulator modelling
- Idealized or detailed compressor modelling
- Control system modelling
- Single path, looped and branched analysis
- Batch tracking
- Gas composition tracking

(h) SPS can model the equipment typically found in gas transmission systems. The list below is a subset of the equipment that can be modelled.

- Compressors (centrifugal and reciprocating)
- Valves
- Regulators
- Control systems (Actuators, Sensors, Relays, Controllers, etc.)
- Heat Exchangers

(i) Heat Exchangers are modelled as shell and tube heat exchangers.

(j) Yes

(k) Off-line – design, planning (what-if scenarios), operator training (can also be integrated with SCADA).

On-line – pipeline observation, leak detection.

(l) Pipeline transmission companies (gas & oil), engineering consultancies to the gas and oil transmission industry.

(n) 75 Companies.

(o) Beth Edmonds
Business Development Manager
Stoner Associates
Tel: 44 121 717 7772
Email: beth.edmonds@stoner.com

TOPAZ

(b) Engineering Sciences Centre

(c) www.esc.sandia.gov

TRAC-P

(c) www.nrc.gov/RES/TRAC-P

WAVE

(b) Ricardo Plc

(c) www.ricardo.com

(a) Engine performance and turbocharger matching, Design of intake and exhaust system for noise reduction, Coupled engine control and driveline simulation, Advanced diesel and SI combustion: knock, NOx emissions, Hybrid 1D/3D flow simulations, Thermal Analysis of combustion chamber components and exhaust system warm-up.

(b) Motor sport, automotive, motorcycle, truck, agricultural, locomotive, marine and power generation.

APPENDIX C: RELATIONS FOR TOTAL PRESSURE BOUNDARIES

C.1 Introduction

Flow at total pressure boundaries is solved using the iterative Newton Raphson method. It is therefore preferable to describe the boundary total pressure as a function of the boundary mass flow per unit area – $p_0 = f(\rho V)_i$. An analytical derivative for this function is obtained for use in the Newton Raphson method – $\frac{\partial f(\rho V)_i}{\partial (\rho V)_i}$.

C.2 Total pressure as a function of ρV

Before deriving the function, a few relations and definitions used in the process are presented.

$(\rho V)_i = (\rho V)'_i$ therefore no distinction is made between the boundary mass flow per unit area for the intermediate and new time levels. For the rest of this paragraph, derivatives to $(\rho V)_i$ are indicated by $''$. In paragraph 3.5.1, it was established that at the boundary

$$\rho_i = \rho_i^0 - 2S\Delta t \frac{(\rho VA)'_{i+S\frac{1}{2}} - (\rho V)_i A_i}{A_i \Delta x} \tag{C.1}$$

$$(T_0)_i = (T_0)'_{i+S} - S\frac{\dot{q}'_i \Delta x}{c_p (\rho V)_i} \tag{C.2}$$

The variable $S = \pm 1$ was introduced here to extend these equations to boundaries at the upstream end of a pipe. S is positive for upstream boundaries and negative for downstream boundaries. The derivatives of each of these functions to $(\rho V)_i$ are then

$$\rho''_i = \frac{2S\Delta t}{\Delta x} \tag{C.3}$$

$$(T_0)_i'' = S\frac{\dot{q}_i'\Delta x}{c_p(\rho V)_i^2} \tag{C.4}$$

Using the definition of T_0, static temperature is given by $T = T_0 - V^2/2c_p$. Rewriting in terms of ρ and ρV gives

$$T = T_0 - (\rho V)^2/(2c_p\rho^2) \tag{C.5}$$

Using the ideal gas law, the static pressure can also be written as a function of ρ and ρV

$$\begin{aligned} p &= \rho RT \\ &= R\left\{\rho T_0 - (\rho V)^2/(2c_p\rho)\right\} \end{aligned} \tag{C.6}$$

The following isentropic relation for stagnation and static quantities is then used to write p_0 as a function of ρ, ρV and T_0.

$$\begin{aligned} \frac{p}{p_0} &= \left(\frac{T}{T_0}\right)^{\gamma/(\gamma-1)} \\ \rho R\frac{T_0 - (\rho V)^2/(2c_p\rho^2)}{p_0} &= \left\{\frac{T_0 - (\rho V)^2/(2c_p\rho^2)}{T_0}\right\}^{\gamma/(\gamma-1)} \\ p_0 &= \rho R\left\{1 - \frac{(\rho V)^2}{2c_p\rho^2 T_0}\right\}^{\gamma/(1-\gamma)}\left\{T_0 - \frac{(\rho V)^2}{2c_p\rho^2}\right\} \\ &= \frac{\rho R}{T_0}\left\{1 - \frac{(\rho V)^2}{2c_p\rho^2 T_0}\right\}^{1/(1-\gamma)} \end{aligned} \tag{C.7}$$

For the next time step, $(p_0)_i$ is then written as a function of $(\rho V)_i$

$$(p_0)_i = f(\rho V)_i = \frac{\rho_i R}{(T_0)_i}\left\{1 - \frac{(\rho V)_i^2}{2c_p\rho_i^2(T_0)_i}\right\}^{1/(1-\gamma)} \tag{C.8}$$

with ρ_i and $(T_0)_i$ as given by Equations (C.1) and (C.2).

The derivative of Equation (C.8) is then

$$\frac{\partial f(\rho V)_i}{\partial(\rho V)_i} = R\frac{\rho_i''(T_0)_i - \rho_i(T_0)_i''}{(T_0)_i^2}\left\{1-\frac{(\rho V)_i^2}{2c_p\rho_i^2(T_0)_i}\right\}^{1/(1-\gamma)}$$
$$-\frac{\rho_i R}{(1-\gamma)(T_0)_i}\left\{1-\frac{(\rho V)_i^2}{2c_p\rho_i^2(T_0)_i}\right\}^{\gamma/(1-\gamma)} \qquad \text{(C.9)}$$
$$\times\frac{2(\rho V)_i\left\{2c_p\rho_i^2(T_0)_i\right\} - 2c_p(\rho V)_i^2\left\{2\rho_i\rho_i''(T_0)_i + \rho_i^2(T_0)_i''\right\}}{\left\{2c_p\rho_i^2(T_0)_i\right\}^2}$$

This derivative can be written in a slightly simpler form.

$$\frac{\partial f(\rho V)_i}{\partial(\rho V)_i} = R\frac{\rho_i''(T_0)_i - \rho_i(T_0)_i''}{(T_0)_i^2}\left\{1-\frac{(\rho V)_i^2}{2c_p\rho_i^2(T_0)_i}\right\}^{1/(1-\gamma)}$$
$$+\frac{2\rho_i(T_0)_i(\rho V)_i - (\rho V)_i^2\left\{2\rho_i''(T_0)_i + \rho_i(T_0)_i''\right\}}{2k\rho_i^2(T_0)_i^3}\left\{1-\frac{(\rho V)_i^2}{2c_p\rho_i^2(T_0)_i}\right\}^{\gamma/(1-\gamma)} \qquad \text{(C.10)}$$

With Equations (C.8) and (C.10) implemented in a Newton Raphson procedure, the mass flow at a total pressure boundary can now be determined as described in paragraph 3.5.

APPENDIX D: ANALYTICAL METHOD FOR STEADY-STATE FLOW IN PIPES

D.1 Introduction

In this appendix, the analytical solution methodology for fluid flow in a pipe is described. This method is capable of solving adiabatic flow, flow with heat transfer as well as isothermal flow.

D.2 Solution methodology of the analytical method

To solve adiabatic flow, flow with heat transfer and isothermal flow, the following equations in differential form were used (Saad, 1985:281).

$$\frac{dM^2}{M^2} = \frac{dT_0}{T_0}\left[\frac{\left(1+\gamma M^2\right)\left(1+\frac{\gamma-1}{2}M^2\right)}{1-M^2}\right] + \left(f\frac{dx}{D}+k\frac{dx}{L}\right)\left[\frac{\gamma M^2\left(1+\frac{\gamma-1}{2}M^2\right)}{1-M^2}\right] \quad \text{(D.1)}$$

$$\frac{dp_0}{p_0} = -\frac{dT_0}{T_0}\left(\frac{\gamma M^2}{2}\right) - \left(f\frac{dx}{D}+k\frac{dx}{L}\right)\left(\frac{\gamma M^2}{2}\right) \quad \text{(D.2)}$$

These equations were integrated numerically using the trapezoidal rule (Kreyszig, 1993:958). This method is therefore not analytical in the strictest sense. It does, however, not use partial derivatives, and serves as a very accurate alternative calculation.

For adiabatic flow and flow with heat transfer, the total temperature variation in a pipe is given by

$$Q = mc_p\Delta T_0 \quad \text{(D.3)}$$

Mass flow is calculated using Equation (3.45). With appropriate boundary conditions, the flow in a pipe can be determined by simultaneously solving the trapezoidal rule equations together with Equation. (D.3). The inlet total pressure and temperature as well as the outlet Mach number were specified as boundary conditions.

For isothermal flow, the static temperature throughout the pipe remains constant. The total temperature at each point in the pipe is then calculated from

$$\frac{T}{T_0} = \frac{1}{1+(\gamma-1)M^2/2} \tag{D.4}$$

This equation then replaces Equation (D.3) when solving isothermal flow.

D.3 EES implementation of the analytical method

EES was used to solve the equations mentioned in the previous paragraph (F-Chart Software, 2003). The equations as used in EES are given here.

```
"This EES program solves steady state differential equations for a constant area pipe. Adiabatic flow, isothermal flow or flow with heat transfer is considered (Saad, 1985:281)."


FUNCTION term(Mach|2 ,gamma)
    term = (1+(gamma-1)/2*Mach|2) / (1-Mach|2)      "This function is used repeatedly in the trapezoidal rule equations"
END


FUNCTION friction(Rey , edD)                    "Calculation of friction factor"
      IF (Rey>5000) THEN
            friction = 0.25 / ( LOG10(edD/3.7 + 5.74/Rey^0.9) )^2     "Turbulent friction factor"
      ELSE
            IF (Rey<2300) THEN
                  friction = 64/Rey                    "Laminar friction factor"
            ELSE
                  friction = (Rey/1000-2.3)/2.7 * 0.25 / ( LOG10(edD/3.7 + 5.74/Rey^0.9) )^2 + (5-Rey/1000)/2.7 * 64/Rey   "linear interpolation between friction factors"
            ENDIF
      ENDIF
END
```

```
"Gas properties"
R = 2080                "[J/kg·K]"
cp = 5200               "[J/kg·K]"
cv = cp - R             "[J/kg·K]"
gamma = cp/cv "Specific heat ratio"
mu = 0.00002            "[kg/m·s]"


"Geometry & subdivisions"
L = 10                  "[m] Length"
D = 0.01                "[m] Diameter"
A = PI*D^2/4            "[m.2] Area"
inc = 50                "Increments"
fact = (1/200)^(1/inc)  "Factor such that last increment is 1/200 of first increment - due to larger gradients in last section of pipe"


"Friction and loss factors"
e = 0.000030            "Wall roughness"
k = 0.0         "k-loss, to be proportionally divided for each sub-increment"
Rey = m_dot[1]/A*D/mu"Reynolds number"
f = friction (Rey,e/D)  "Friction factor"


"Boundary conditions. '0' is inlet and 'inc' is outlet"
M_out = 0.95            "Outlet Mach no."
M|2[inc] = M_out^2      "Outlet Mach no. squared"
T_0[0] = 273.15+15      "Specify inlet static temperature for isothermal flow / Specify inlet total temperature for non-isothermal flow"
T[0] = T_0[0]  /  ( 1+(gamma-1)/2*M|2[0] )      "Inlet total & static temperature ratio"
p_0[0] = 900            "[kPa] Inlet total pressure"
T_0_out = -85 +273.15                   "[°C] Only for non-isothermal flow"
```

```
"Equations for each sub-increment"
duplicate i=1,inc
        dxx[i] = dxx[i-1]*fact                                  "Increment length ratio - factor smaller than previous increment"
                                                                "Numerical integration of differential equation for change in Mach number squared"
        dM1|2[i] = 0.5*(  M|2[i]*(1+gamma*M|2[i]) * term(M|2[i],gamma)/T_0[i] + M|2[i-1]*(1+gamma*M|2[i-1]) * term(M|2[i-1],gamma)/T_0[i-1]  ) *
(T_0[i]-T_0[i-1])
        dM2|2[i] = 0.5*(  gamma*M|2[i]^2 * term(M|2[i],gamma) + gamma*M|2[i-1]^2 * term(M|2[i-1],gamma)  )  *  (f*dxx[i]/D + k*dxx[i]/L)
        M|2[i] = (dM1|2[i] + dM2|2[i]) +  M|2[i-1]
                                                                "Numerical integration of differential equation for change in total pressure"
        dp_0[i] = 0.5*(  p_0[i]*(-gamma*M|2[i]/2 )/T_0[i] + p_0[i-1]*(-gamma*M|2[i-1]/2 )/T_0[i-1]  ) * (T_0[i]-T_0[i-1]) + 0.5*
(  p_0[i]*(-gamma*M|2[i]/2 ) + p_0[i-1]*(-gamma*M|2[i-1]/2 )  ) *(f*dxx[i]/D + k*dxx[i]/L)
        p_0[i] = p_0[i-1] + dp_0[i]
        T[i] = T_0[i]  /  ( 1+(gamma-1)/2*M|2[i] )  "Total & static temperature ratio"
        Q_sub[i] = m_dot[i]*cp*(T_0[i]-T_0[i-1])                "Heat transfer for each sub-increment"
        "T[i] = T[0]                                            For isothermal flow static temperature remains constant"
        T_0[i] = T_0[i-1] + DeltaT_0 * dxx[i]/L     "Change in total temperature - only for non-isothermal flow"
        m_dot[i] = A * sqrt(gamma*M|2[i]/R/T_0[i]) * 1000 * p_0[i] / (1 + (gamma-1)*M|2[i]/2)^((gamma+1)/2/(gamma-1))    "Used to check if grid is
fine enough - mass conservation"
end

Q = SUM(Q_sub[i], i=1,inc)              "Calculation of total heat transfer"
L = SUM(dxx[i], i=1,inc)          "Ensure sum of all sub-increment lengths = total length"
DELTAp_0 = p_0[0] - p_0[inc]   "Change in total pressure across pipe"
DELTAT_0 = T_0_out - T_0[0]  "Change in total temperature across pipe - only for non-isothermal flow"
m_dot_error = (m_dot[inc] - m_dot[1])/m_dot[1]  "Used to check if grid is fine enough - mass conservation"
```